TECHNICAL REPORT STANDARD TITLE PAGE

1. Report No.	2. Government Accession No.	3. Recipient's Catalog No.
FHWA/TX-90+472-4		

4. Title and Subtitle DEVELOPMENT OF PROCEDURES FOR A STATEWIDE DIAGNOSTIC SURVEY ON CONTINUOUSLY REINFORCED CONCRETE PAVEMENTS	5. Report Date November 1989
	6. Performing Organization Code
7. Author(s) Angela Jannini Weissmann and Kenneth Hankins	8. Performing Organization Report No. Research Report 472-4
9. Performing Organization Name and Address Center for Transportation Research The University of Texas at Austin Austin, Texas 78712-1075	10. Work Unit No.
	11. Contract or Grant No. Research Study 3-8-86-472
12. Sponsoring Agency Name and Address Texas State Department of Highways and Public Transportation; Transportation Planning Division P. O. Box 5051 Austin, Texas 78763-5051	13. Type of Report and Period Covered Interim
	14. Sponsoring Agency Code

15. Supplementary Notes

Study conducted in cooperation with the U. S. Department of Transportation, Federal Highway Administration

Research Study Title: "Rigid Pavement Data Base"

16. Abstract

This report documents the work undertaken in 1987 to develop procedures for a statewide diagnostic survey on continuously reinforced concrete pavements (CRCP), which included the following data: (1) deflections, (2) pavement temperatures, and (3) crack width. This data was used to calibrate a performance prediction model for CRCP in Texas.

Since the data needs were quite specific, no appropriate procedure for their collection was found in the literature, and studies were conducted to develop collection procedures for the required data. These studies are documented in this report, and the findings are summarized in Chapter 6 in the form of a manual for field crews. A preliminary analysis made as a basis for planning these studies is also documented. In the study related to crack width, operator ability to repeat and reproduce data for the crack width measurements was checked; the minimum number of readings per crack was determined; and a literature survey was taken and documented. The development of a procedure to measurement pavement temperature included checking the influences of aggregate type and insulation conditions on temperature estimates, and calibrating models to give temperature and temperature gradient estimates. The phenomenon of heat transfer in solids is briefly discussed, thermocouple principles are explained, and the data acquisition and storage systems are described. A literature survey of Falling Weight Deflectometer measurements is summarized. The concepts underlying the field procedure for measuring deflections are described. The findings described in this document should provide valuable guidance for any agency needing to conduct a similar survey.

17. Key Words	18. Distribution Statement
Falling Weight Deflectometer, deflections, continuously reinforced concrete pavement (CRCP), crack width, temperature gradient, evaluation, nondestructive, thermocouple, operator	No restrictions. This document is available to the public through the National Technical Information Service, Springfield, Virginia 22161.

19. Security Classif. (of this report)	20. Security Classif. (of this page)	21. No. of Pages	22. Price
Unclassified	Unclassified	82	

Form DOT F 1700.7 (8-69)

DEVELOPMENT OF PROCEDURES FOR A STATEWIDE DIAGNOSTIC SURVEY ON CONTINUOUSLY REINFORCED CONCRETE PAVEMENTS

by

Angela Jannini Weissmann
Kenneth Hankins

Research Report Number 472-4

Research Project 3-8-86-472

Rigid Pavement Data Base

conducted for

Texas State Department of Highways and Public Transportation

in cooperation with the

U.S. Department of Transportation Federal Highway Administration

by the

CENTER FOR TRANSPORTATION RESEARCH

Bureau of Engineering Research

THE UNIVERSITY OF TEXAS AT AUSTIN

November 1989

The contents of this report reflect the views of the authors, who are responsible for the facts and the accuracy of the data presented herein. The contents do not necessarily reflect the official views or policies of the Federal Highway Administration. This report does not constitute a standard, specification, or regulation.

PREFACE

This report documents a part of the work conducted in 1987 under Research Study 3-8-86-472, "Rigid Pavement Data Base." The main objectives of this research study are to develop a data base and to calibrate a performance prediction model for Texas continuously reinforced concrete pavements (CRCP). In order to implement these objectives, a statewide diagnostic survey on CRCP was made in 1988. The survey consisted of collecting the following types of data: crack width, deflection, and pavement temperatures. This report documents the development of the procedures to obtain the data.

LIST OF REPORTS

Report No. 472-1, "Evaluation of Proposed Texas SDHPT Design Standards for CRCP," by Mooncheol Won, B. Frank McCullough, and W. R. Hudson, presents the results of an evaluation of the proposed CRCP Design Standard for various coarse aggregates used, describes the theoretical models used in the study, and discusses several important design parameters in CRCP.

Report No. 472-2, "Development of a Long-Term Monitoring System for Texas CRC Pavement Network," by Chia-pei J. Chou, B. Frank McCullough, W. R. Hudson, and C. L. Saraf, presents the application of experimental design method to develop a long-term monitoring system in Texas. Development of a distress index and a decision criteria index for determining the present and terminal conditions of pavements is also discussed.

Research Report 472-3, "A Twenty-Four-Year Performance Review of Concrete Pavement Sections Using Silicious and Lightweight Coarse Aggregates," by Mooncheol Won, Kenneth Hankins, and B. Frank McCullough, presents the results of statistical analyses over a twenty-four-year performance period of Continuously Reinforced Concrete Pavements made with lightweight and conventional/standard aggregates. The performance variables include pavement deflections and visual condition survey data. Recommendations and directions for future research emanating from the study are also presented for consideration by CRCP designers.

Research Report 472-4, "Development of Procedures for a CRCP Diagnostic Survey," by Angela Jannini Weissmann and Kenneth Hankins, describes and discusses the work involved in developing the procedures used for collecting the desired diagnostic data.

ABSTRACT

This report documents the work undertaken in 1987 to develop procedures for a statewide diagnostic survey on continuously reinforced concrete pavements (CRCP), which included collecting the following data:

- deflections,
- pavement temperatures, and
- crack width.

These data were used to calibrate a performance prediction model for CRCP in Texas.

Since the data needs were quite specific, no appropriate procedure for their collection was found in the literature, and studies were conducted to develop collection procedures for the required data. These studies are documented in this report, and the findings are summarized in Chapter 6 in the form of a manual for field crews. A preliminary analysis made as a basis for planning these studies is also documented.

In the study related to crack width, operator ability to repeat and reproduce data for the crack width measurements was checked; the minimum number of readings per crack was determined; and a literature survey was taken and documented.

The development of a procedure to measure pavement temperature included checking the influences of aggregate type and insulation conditions on temperature estimates, and calibrating models to give temperature and temperature gradient estimates. The phenomenon of heat transfer in solids is briefly discussed, thermocouple principles are explained, and the data acquisition and storage systems are described.

A literature survey of Falling Weight Deflectometer measurements is summarized. The concepts underlying the field procedure for measuring deflections are described.

The findings described in this document should provide valuable guidance for any agency needing to conduct a similar survey.

KEY WORDS: Falling Weight Deflectometer, deflections, continuously reinforced concrete pavement, rigid pavement evaluation, nondestructive testing, nondestructive evaluation, crack width, temperature gradient, diagnostic survey, field evaluation, operator reproducibility, operator repeatability, thermocouple.

SUMMARY

The main objectives of this project are to develop a data base and to study CRCP performance in Texas. In order to fulfill these objectives, a statewide diagnostic survey was conducted in 1988 to collect the following data:

(a) deflections,
(b) crack width, and
(c) pavement temperature.

Network-level surveys such as the one conducted under this project require collection of a considerable amount of data. The feasibility of these large scale studies depends on the availability of expeditious and cheap procedures to collect the data. However, if speed and cheapness are obtained entirely at the expense of accuracy, the data become useless.

A considerable part of the work conducted under this study consisted of developing procedures for collecting the data listed above that are expeditious enough for a network level survey, and at the same time providing sufficient accuracy. This report documents the work undertaken to arrive at such procedures.

Chapter 1 presents the objectives of this work and describes the test sites. Chapter 2 describes a preliminary study undertaken to design the experiments for the crack with and pavement temperature procedures. Chapter 3 describes the development of a procedure to measure crack width. Chapter 4 describes the work that led to a procedure for measuring pavement temperatures and pavement temperature gradients. Chapter 5 describes the procedure for measuring deflections, and Chapter 6 consists of a manual of instructions to field crews that summarizes all the findings.

IMPLEMENTATION STATEMENT

The procedures described in this report were implemented in the summer of 1988, when they were used in a statewide CRCP diagnostic survey undertaken in this project. The next report in this series describes the field survey and its preparations.

The field procedures developed in this project can also be valuable for future surveys of the same kind.

TABLE OF CONTENTS

CHAPTER 1. INTRODUCTION

BACKGROUND

Research that seeks to identify the main causes of pavement deterioration, a very complex process, remains both controversial and problematic. The difficulties in accurately predicting explicative variables (such as traffic composition), the problems associated with reliably obtaining elasticity moduli of the pavement layers, plus the high costs involved in gathering data — all of these factors may be initially discouraging when attempting to research the precise causes of pavement deterioration. Yet when considering the high costs of building and maintaining a road, an investment in research on design and rehabilitation strategies will almost always yield a return. Project 472, which is now investigating continuously reinforced concrete pavement (CRCP) performance in Texas, is part of such a research effort.

A large-scale study on pavement deterioration was pioneered by the AASHO road test, which studied pavement behavior and generated a performance prediction model (Ref 1) that is still used worldwide, sometimes blindly, sometimes with awareness of the limitations inherent in extrapolation of empirical models. But because of excellent routine maintenance, it has been observed that the AASHO's PSI (present serviceability index) (Ref 1) is not a reliable indicator of pavement performance in the Texas CRCP network (Ref 6). Thus, a better way to evaluate the CRCP terminal condition is required. Earlier in this project, an experiment (Ref 6) determined the variables that affect CRCP performance. One of the interesting results of this study was the finding that punch-outs and patches were the most significant indicators of CRCP performance. The availability of a condition survey data base (Ref 52) permitted the development of a new decision-aid tool, termed the Z-index (Ref 6), for the CRCP in Texas. This distress index, which is a function of punch-outs and patches in the pavement, was developed to provide the Texas State Department of Highways and Public Transportation (SDHPT) with guidelines for evaluating the present pavement conditions and for scheduling rehabilitation (Ref 6). However, the need for a more adequate performance prediction model for Texas CRCP still remains. In essence, such a model would predict pavement deterioration resulting from the combination of traffic and environmental effects. The calibration of this model would require appropriate data for the explicative variables, and past experience (Refs 1 and 6) indicates that the following variables are good candidates for inclusion in the model:

D = slab thickness,
E_c = elasticity modulus of the PC concrete,
f_f = flexure strength of the PC concrete,
K = modulus of reaction on top of subbase,
J = load transfer coefficient,
C_d = drainage coefficient, and
W_{eq} = equivalent single axle loads.

In the same broad area—that of modeling CRCP behavior—Project 422 is now developing a computer program to predict cracking characteristics (spacing and width) of CRCP, taking into consideration the random variability in the material properties. And while historical condition survey data enables the calibration of models that are part of this computer program, data relating to materials stiffness (E_c, f_f, and K), load transfer (J), and crack width were not available in the data base. Therefore, as part of this project's efforts, a field survey (termed a "diagnostic survey") was undertaken to obtain all data required for calibrating the models.

In the diagnostic survey, deflection measurements were taken to back-calculate E_c, f_f, J, and K. The basic idea underlying the process of back-calculating those data from deflections is that, since elasticity moduli, load, geometric characteristics, and deflections are related, the former can be estimated from the rest. There are some programs that can take deflection basins, geometric characteristics, and loading as inputs, and, using equations from layered theory, interactively select a combination of elasticity moduli that satisfies the specific combination of inputs. Programs RPEDD and FPEDD (Ref 47), examples of those programs, were developed at The University of Texas at Austin and are available in the mainframe. In addition, deflection values measured at both sides of discontinuities can provide an estimate of the load transfer, and thus deflections at those positions were also taken during the diagnostic survey.

Crack width measurements, as well as deflection measurements, can be affected by the pavement temperature. For example, crack widths at a given spot can be significantly different when taken at low temperatures than when taken at high temperatures (Refs 63, 42, and 25). Effects of slab warping due to vertical temperature differentials can significantly affect deflections (Ref 49, 25, 31, and 43). Reference 31 showed that changes in the pavement shape and supporting conditions can be the result of changes in the temperature gradient along the slab thickness, thus suggesting that corrections for the temperature effects are necessary for better use of deflection data for back-calculating stiffness.

OBJECTIVES

The objective of this report is to document the development of the procedures for reliably obtaining the data mentioned above. The work included:

(1) an experiment leading to the crack width measurement procedure;
(2) an experiment leading to a reliable way for estimating temperatures along pavement thickness; and
(3) a literature review and technical discussions leading to the procedure for taking the deflection measurements.

DESCRIPTION OF THE TEST FACILITIES

Two test sites located at Balcones Research Center were used in the experiments. The test site used for the crack width experiment was constructed under Inter-Agency Contract 1530, with the Texas SDHPT, to study the problem of the operation of overweighted vehicles on Texas roadways (Refs 17, 18, and 19). One of the tasks outlined in that contract was the construction of test sections that would represent the most common pavement types in Texas. The test sections were to be subjected to overload failure to provide evidence in pending court cases (Refs 18 and 19). Those test sections consisted of three paved tracks of different characteristics and were cracked by the traffic loads imposed during testing. The concrete pavements were used for the crack width experiment in this project. Figure 1.1 depicts a layout of the test facility.

The pavement temperature experiment and the preliminary study to plan the two experiments utilized data taken at the test site constructed under Project 3-8-83-355, "Construction of a Multipurpose Rigid Pavement Research Test Facility." It consists of a long and a short slab separated by a doweled joint. The shorter slab can be moved in such a manner that known joint widths can be established for the purpose of load transfer studies. The pavement is supported by a series of layers of known thickness and structural capacity (Ref 62). The layers are, from bottom to top:

(1) a 7-foot embankment;
(2) 6 inches of crushed stone;
(3) 3 inches of asphaltic concrete cement; and
(4) 10 inches of P.C. concrete reinforced at every 36 inches in both the transverse and longitudinal directions with bars #4.

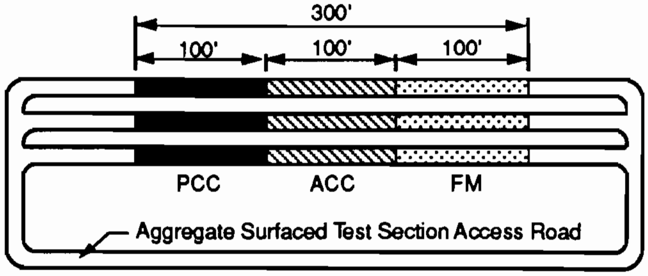

Fig 1.1. Layout of test sections used in the crack width experiment (Ref 17).

The concrete utilized for the slabs was a class A concrete, which has a minimum of 5 sacks of cement per cubic yard, a minimum compressive strength of 3000 psi at 28 days, maximum water/cement ratio of 0.5, slump ranging from 1 to 3, and fine aggregate number one. The coarse aggregate type was crushed limestone. The long slab has four sets of thermocouples, each set consisting of one thermocouple one inch below the surface, one at mid-depth, and another one inch above the bottom of the slab. Three of the four sets of thermocouples are permanently monitored, and temperature measurements are stored in a micro-computer located in an adjacent instrumentation building. Ambient temperature is also permanently monitored and stored in the same computer. Figure 1.2 depicts a layout of the test site for experiment 2 and shows the locations of the monitored thermocouples.

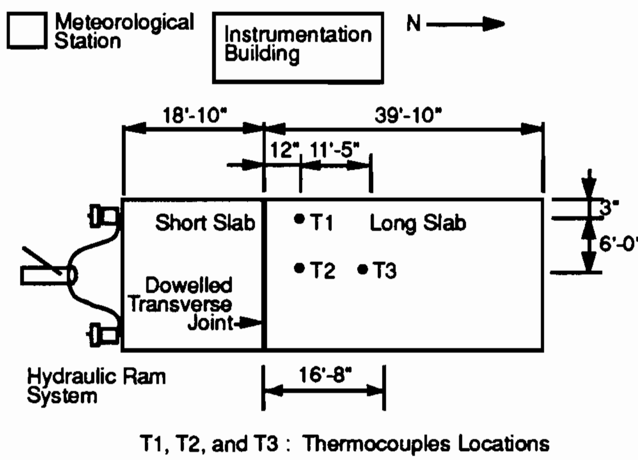

Fig 1.2. Layout of the BRC testing facility used for the temperature experiment (Ref 62).

CHAPTER 2. PRELIMINARY STUDY FOR DESIGNING THE EXPERIMENTS

OBJECTIVES

In order to plan the two experiments described in this document, a preliminary analysis of slab temperature data was performed (Ref 56). The purposes of this preliminary analysis were

(1) to determine the required procedures to ensure that results from the crack width experiments were not affected by any temperature variation; and
(2) to check the temperature variation pattern in order to select the most appropriate statistical application for modeling the pavement temperature, and then design the pavement temperature experiment.

DATA USED IN THE ANALYSIS

The data consisted of slab and ambient temperature measurements taken at the test slab at Balcones Research Center (BRC) described in Chapter 1 and depicted in Fig 1.2. The data acquisition system is described in detail in Chapter 4.

By the time this study was initiated, one day of temperature data was available in The University of Texas' computers, which was used for this preliminary analysis. Table 2.1 shows the raw data.

ANALYSIS OF THE DATA

Figures 2.1 through 2.3 show slab temperature variation by horizontal locations and by time of day, while Figs 2.4 through 2.6 show the temperature variation by vertical locations.

Figures 2.1 through 2.6 show that temperatures vary cyclically throughout the day. Furthermore, phase shifts and different wave lengths are encountered among the three vertical measurement locations for all three sets of thermocouples. In other words, there is a temperature gradient in the vertical direction of the pavement due to different conditions for heat dissipation at surface, mid-depth, and bottom of the pavement.

Examination of Figs 2.1 through 2.6 reveals that a factorial design using analysis of variance, or regression using least-squares fit, may not be strictly valid for the statistical analysis of temperature data. Those procedures are valid only for data sampled from normal populations in which every individual observation is independent from previous observations, and the error term is a random variable, normally distributed around zero. In the case of temperature data, this assumption cannot be made. Temperature data constitute an auto-correlated time series, where each observation is not independent from the previous observation; on the contrary, pavement temperature at a given instant t is, for instance, 70° F, because, among other factors, its temperature at instant t-1 was, say, 69° F. This concept is fully discussed in Chapter 4.

It can also be seen in Figs 2.1 through 2.6 that slab temperature changes during time intervals of up to one hour are practically nil. Since crack width changes due to temperature cannot affect the measurements in the crack width experiment to any extent, this result is very important in establishing the possible sample sizes to be taken at each crack during the experiment and the field survey.

It is expected that temperatures at horizontal location 1 (Fig 1.2) be the closest to ambient temperature, followed by locations 2 and 3, respectively. Location 1, in a corner, is near two free edges, through which heat can be exchanged at a rate faster than that at location 2, which is near one free edge only, and thus dissipates heat faster than location 3, which is in the interior of the slab. This tendency is confirmed by Figs 2.4, 2.5, and 2.6.

Heat dissipation phenomenon would also lead one to expect phase shifts encountered among different depths to be much higher than the shifts due to different horizontal distances to free edges. Figures 2.1 through 2.6 show that the data corroborated this. Phase shifts due to difference in plain view location are nil as compared to the ones due to difference in depths.

The small phase shift among horizontal locations, as well as the strong auto-correlation of the temperature data, can be better illustrated by interpreting the results of the following least-squares fitted models:

Model 1:

$$TC3_t = a + b*TC1_{t-1}$$

and Model 2:

$$TC3_t = a + b*TC1_{t-1} + c*TC1_t$$

where

TC1 and TC3 = temperature at slab locations 1 and 3,
t = time at which the temperature was measured, and
a, b, and c = regression parameters.

Table 2.2 summarizes the results of regression Models 1 and 2. Figure 2.7 shows the residual plot for Model 2.

The results for regression Model 1 show that, although some of the temperatures at a given instant at location 3 can be explained as a linear function of temperature at the previous instant in location 1 (significant t and

TABLE 2.1. RAW DATA FOR PRELIMINARY ANALYSIS

Surface 1	Mid-Depth 1	Bottom 1	Surface 2	Mid-Depth 2	Bottom 2	Surface 3	Mid-Depth 3	Bottom 3
44.70	39.21	35.34	42.68	37.55	33.75	41.71	34.37	32.71
44.87	39.91	35.92	42.61	38.18	34.20	41.73	35.00	33.25
44.89	40.46	36.48	42.67	38.64	34.62	41.68	35.51	33.72
45.85	40.92	36.94	43.71	39.13	35.01	42.78	35.93	34.14
46.41	41.58	37.39	43.78	39.71	35.39	42.99	36.43	34.54
46.61	42.03	37.83	43.56	40.12	35.76	43.01	36.89	34.96
44.94	42.16	38.26	41.90	40.16	36.12	41.13	37.18	35.32
43.85	41.88	38.56	40.90	39.90	36.43	39.99	37.18	35.63
42.29	41.41	38.72	39.38	39.47	36.68	38.33	37.04	35.79
40.88	40.76	38.77	38.21	38.89	36.83	36.85	36.69	35.86
39.87	40.13	38.70	37.48	38.33	36.87	36.00	36.29	35.79
39.12	39.54	38.56	36.91	37.85	36.87	35.41	35.29	35.64
38.42	39.03	38.37	36.28	37.43	36.82	34.79	35.57	35.50
37.69	38.55	38.18	35.62	37.01	36.73	34.06	35.27	35.31
36.95	38.05	37.96	34.93	36.55	36.62	33.43	34.93	35.11
36.43	37.53	37.72	34.35	36.19	36.48	32.88	34.59	34.90
35.66	37.05	37.45	33.68	35.69	36.32	32.32	34.25	34.67
35.03	36.56	37.22	33.09	35.24	36.16	31.85	33.92	34.44
34.49	36.10	36.95	32.67	34.80	35.96	31.41	33.57	34.19
33.98	35.66	36.65	32.13	34.41	35.75	30.96	33.25	33.94
33.92	35.24	36.38	31.71	34.01	35.55	30.57	32.95	33.66
33.88	34.84	36.09	31.37	33.65	35.36	30.25	32.66	33.42
32.65	34.47	35.79	30.98	33.31	35.11	29.88	32.36	33.17
32.30	34.13	35.52	30.68	32.96	34.91	29.58	32.11	32.94
31.98	33.76	35.02	30.17	32.39	34.48	29.31	31.81	32.72
31.68	33.46	35.02	30.17	32.39	34.48	29.05	31.53	32.49
31.43	33.17	34.75	29.97	32.14	34.26	28.78	31.31	32.26
31.18	32.92	34.50	29.75	31.89	34.05	28.53	31.08	32.04
30.98	32.67	34.28	29.50	31.67	33.86	28.08	30.66	31.64
30.73	32.43	34.04	29.25	31.43	33.66	28.08	30.66	31.64
30.51	32.20	33.84	29.08	31.20	33.48	27.90	30.46	31.46
30.31	31.95	33.62	28.87	30.98	33.31	27.70	30.24	31.26
30.15	31.74	33.43	28.71	30.79	33.12	27.60	30.07	31.08
29.90	31.54	33.23	28.48	30.61	32.92	27.43	29.90	30.90
29.75	31.35	33.04	28.38	30.42	32.78	27.35	29.73	30.75
29.65	31.18	32.84	28.31	30.25	32.60	27.37	29.58	30.58
29.85	31.07	32.71	28.68	30.16	32.47	27.69	29.47	30.45
30.35	31.04	32.56	29.32	30.20	32.30	28.36	29.41	30.32
31.25	31.28	32.47	30.35	30.40	32.18	29.42	29.49	30.25
32.68	31.70	32.44	31.87	30.87	32.10	30.58	29.72	30.25
34.05	32.30	32.46	33.18	31.42	32.06	31.25	29.94	30.27
35.41	33.07	32.64	34.58	32.12	32.12	31.97	30.21	30.38
36.81	33.86	32.91	35.71	32.89	32.23	33.60	30.58	30.56
38.00	34.61	33.19	37.18	33.57	32.38	34.99	31.05	30.76
39.20	35.54	33.53	38.67	34.46	32.59	35.83	31.54	31.01
41.30	36.57	33.98	40.13	35.42	32.86	37.35	32.12	31.31
42.93	37.59	34.45	41.42	36.26	33.17	38.81	32.72	31.68
44.18	38.62	34.97	42.49	37.28	33.55	40.35	33.46	32.11

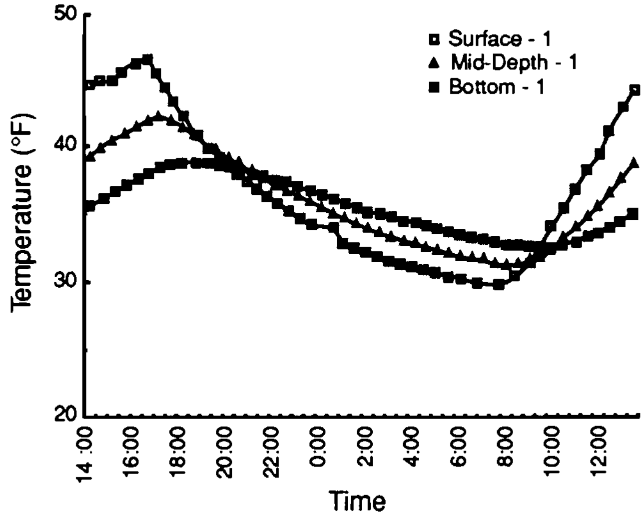

Fig 2.1. Temperatures at Location 1.

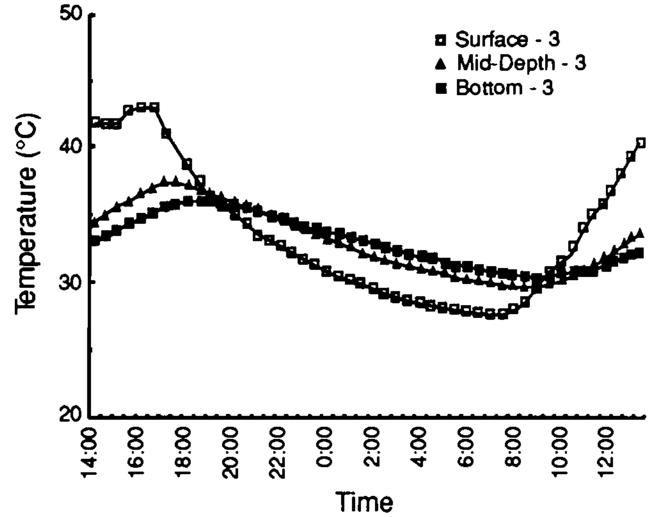

Fig 2.3. Temperatures at Location 3.

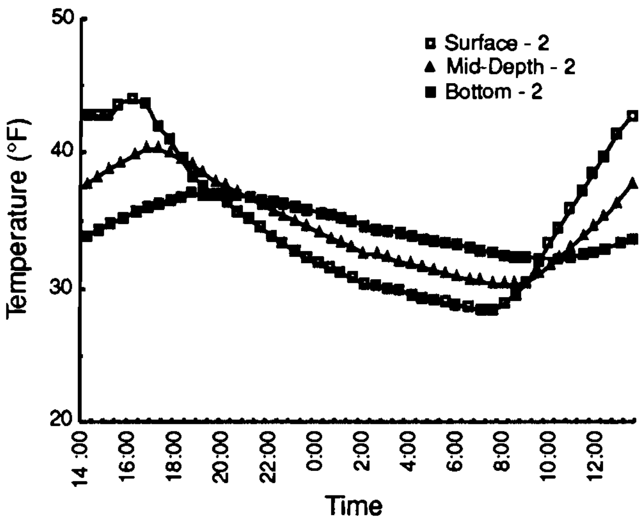

Fig 2.2. Temperatures at Location 2.

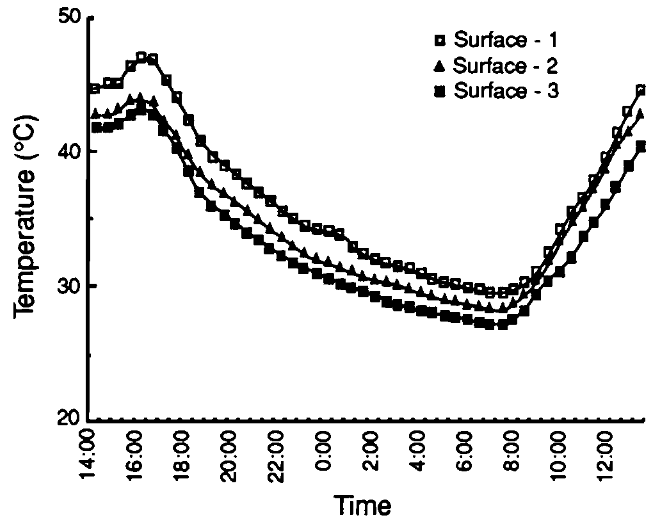

Fig 2.4. Temperatures at the surface.

F ratios for the regression), the amount of variation that remains unexplained is unacceptable (low value of R^2).

An attempt to explain the previously described unexplained variation by the temperature at TC1 on the same instant (regression Model 2) reveals that, although terms with and without time lag both have significant coefficients, the term without time lag is far more significant than the one with time lag (t-ratios for the regression parameters). Furthermore, the amount of the variation that was unexplained by the first regression becomes almost entirely and highly significantly explained by the addition of the new term in the model.

These results reinforce the observation that no significant time lag is evident among different horizontal locations. It does not, however, permit one to say that Model 2 is an acceptable explanation of the phenomenon for the following reasons:

(1) The equation is strictly valid for that particular day (temperature distribution) and that particular slab.

(2) Even for that particular day and slab, further analysis would be necessary before using the equation fitted to Model 2 for prediction purposes, because there are three points having large influence on the curve. More importantly, Fig 2.7 depicts a residual plot with a non-random pattern, which indicates that the unexplained portion of the phenomenon is due not purely to random error but also to some systematic factor.

(3) The cyclical variation of the residual plot is due to the auto-regressive properties of the temperature time series, which cannot be taken into account by the least-squares fitting (Refs 5, 37, 32, and 10). The bias in the results due to lack of consideration of the auto-regressive part of the temperature variable would affect mostly the error and, thus, the significance tests of the regression parameters (Ref 37). In this case, since the values of the statistics of significance tests were extremely high, this bias was not expected to affect the conclusion itself. Therefore, further regression of the temperature was not done for this preliminary analysis purposes.

When attempting to correlate slab temperatures to ambient temperature (available, but not shown in Table 2.1), very poor results were obtained. These poor results were already expected, because it is known that ambient temperature alone does not sufficiently explain the pavement temperature. Many other factors, such as solar radiation, surface reflectivity, and wind speed, also affect pavement temperature (Refs 25 and 24).

SUMMARY OF THE CONCLUSIONS

The importance of temperature gradient along slab depth, the evidence of small time-lag among different horizontal locations, the lack of good correlation between ambient and slab temperature, and the strong auto-regressive property of the data are concluded from the analysis. Due to the auto-correlation, statistical procedures other than usual least-squares linear fitting and analysis of variance are necessary to analyze data from the temperature experiment without bias.

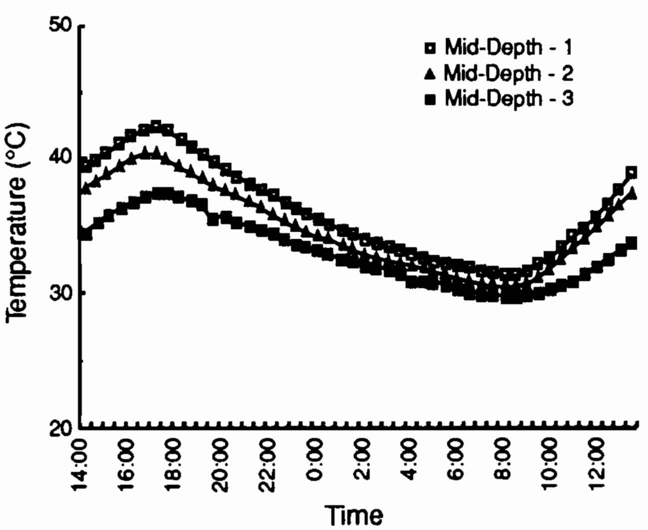

Fig 2.5. Temperatures at mid-depth.

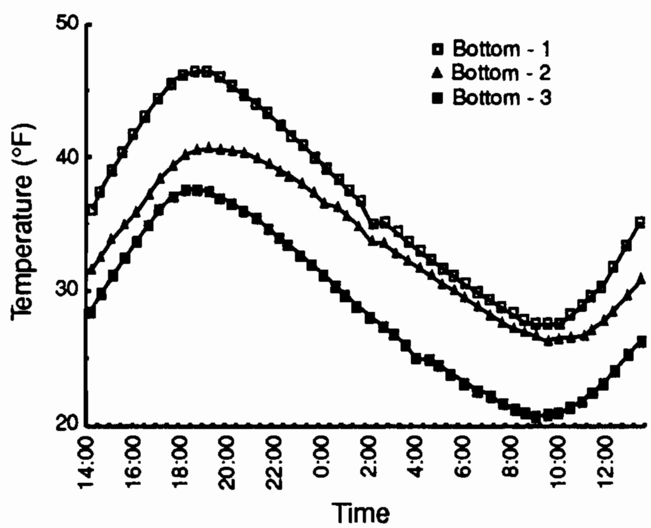

Fig 2.6. Temperatures at bottom.

TABLE 2.2. REGRESSION RESULTS FOR MODELS 1 AND 2 (REF 56)

Model	d.f.	R^2	F-Ratio	Model Coefficient	t-Ratio
Model 1					
$16.9 + 0467\ x_{t-1}$	38	26.1	14.75	16.900	3.96
				0.476	3.84
Model 2					
$0.7 - 0.131\ x_{t-1} + 0.75\ x_t$	37	99.3	2,728.4	10.700	24.59
				-0.131	-8.59
				0.750	62.64

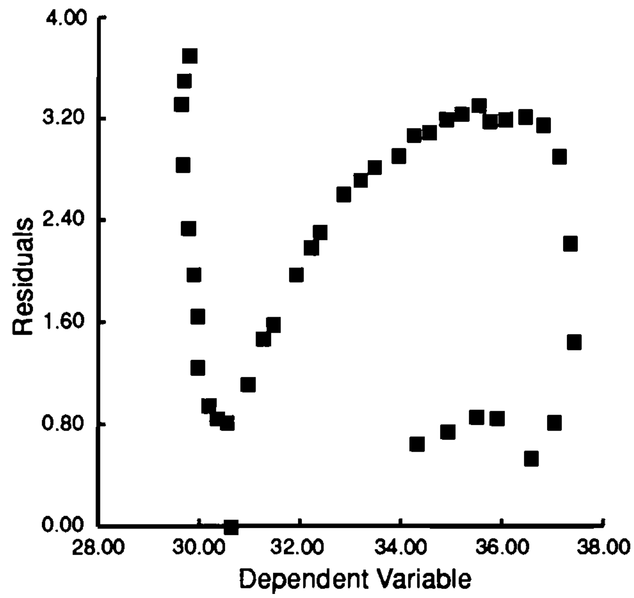

Note: Due to software capabilities, the residuals scale had to be changed to make all the residuals positive.

Fig 2.7. Residual plot of the regression of TCI.

CHAPTER 3. DEVELOPMENT OF A PROCEDURE FOR MEASURING CRACK WIDTH ON CONCRETE PAVEMENTS

PRELIMINARY CONSIDERATIONS

Continuously reinforced concrete pavements (CRCP) consist of long portland cement concrete pavement slabs with continuous longitudinal steel reinforcement. Intermediate transverse joints, which could permit slab movement, are not included in CRCP. The pavement is allowed to crack, and the cracks are held tightly closed by the steel reinforcement, thereby retaining aggregate interlock to assure load transfer across the cracks and to prevent the intrusion of water and incompressibles that cause pavement distress (Ref 12). The importance of crack width for pavement performance is crucial; if the cracks are too wide, poor load transfer and, thus, higher stresses are to be expected (in addition to pumping and its consequences).

In seeking a procedure to measure crack width, it is useful to first consider that crack movements due to temperature changes cannot affect the crack width measurements to any extent. It is arguable whether changes in slab temperature affect crack opening in any detectable way; if they do, it would be impossible to distinguish variance due to this fact, from variance due to the factors that are intended to be examined in the experiment. The preliminary analysis of slab temperature data, described in Chapter 2, permitted determination of the time interval during which the slab temperature would remain approximately constant, thus ensuring that crack width changes due to temperature changes would not affect the experiment results.

An important finding of Ref 26 with respect to crack width measurements procedures was used to design the experiment described herein and to recommend the field procedure to measure crack width. Reference 26 describes an analysis of variance showing that the differences between the means of width measurements taken at different transverse locations in the same crack were not significant, i.e., no trend of increasing or decreasing width across the crack was found. This finding suggests that replicated measurements on the same crack can be reduced to the minimum necessary to achieve a reasonable standard error. It also permits the factor "transverse location" to be left out of the experiment, because of the previous evidence of its non-significance.

OBJECTIVES

Two separate experiments were conducted at the Balcones Research Center (BRC) road test facility, depicted in Fig 1.1. They consisted of two separate sets of measurements used for different purposes. The device used for taking the readings was a microscope precise to 0.001 inch.

The objective of the first experiment was to verify the importance of assisting the field crews with previous training lessons in the crack width measurement task.

The objective of the second experiment was threefold: to investigate the influence on the accuracy of crack width measurements of the crack characteristics, to determine the between-operator variance (reproducibility), and to estimate the sample size necessary to achieve an acceptable measurement error.

EXPERIMENT 1 - ANALYSIS OF THE IMPORTANCE OF OPERATOR TRAINING

Since the main purpose of this experiment was to verify the importance of operator training on the accuracy of the crack width measurements, the following were chosen as operators to take the necessary data:

(1) an expert engineer highly skilled in field data collection,
(2) an engineer with some experience in this subject, and
(3) an undergraduate student with no experience.

These operators will be referred to as 1, 2, and 3, throughout this report. In order to ensure that Operator 3 (the trainee) would truly represent a trainee with no experience, the nature of the crack width measurement and the problems to be expected were not discussed with Operator 3 before taking data for the first experiment. His only instructions were on how to use the microscope.

In order to avoid bias on the data due to progressive training Operator 3 might eventually acquire during the test, and at the same time obtain enough replications, it was decided to take at least six readings, and at most ten, at each crack. Table 3.1 presents the raw data and their statistical summary.

Since the main purpose of experiment 1 was to verify the importance of operator training on the accuracy of the results, the variances were analyzed first. Levene's test of homogeneity of variances (Ref 39) was applied to Table 3.1 data. The full output of this test is depicted in Table 3.2.

The result of Levene's test was highly significant, and it shows that at least one of the variances differ from the rest. Although visual inspection of the data

TABLE 3.1. CRACK WIDTH DATA FOR EXPERIMENT 1

Operator	Width Readings (0.001-in.)	Mean	Standard Deviation
1	12	12.17	1.72
	11		
	15		
	10		
	13		
	12		
2	11	11.67	1.37
	14		
	11		
	12		
	10		
	12		
3	13	20.33	8.36
	16		
	20		
	30		
	12		
	31		

immediately indicates variance of Operator 3 is the one that differs, pairwise F-tests (Ref 39) were done among the three possible combinations in order to provide more a accurate conclusion. The following F-ratios were obtained (Ref 54):

$$F_1 = S^2_{\text{Operator 3}} / S^2_{\text{Operator 2}} = 37.24$$

$$F_2 = S^2_{\text{Operator 3}} / S^2_{\text{Operator 1}} = 23.62$$

$$F_3 = S^2_{\text{Operator 1}} / S^2_{\text{Operator 2}} = 1.58$$

The F-ratio for 5 degrees of freedom in the numerator and 5 degrees of freedom in the denominator is 14.94 for 0.5 percent significance (Ref 39). Therefore, no evidence was found that variances of Operator 2 and Operator 1 do differ; but Operator 3 variance is significantly different than both of the others. The overall significance level for the three pairwise comparisons is approximately 1.5 percent, which is usually acceptable as a significance level for statistical tests (Refs 39 and 3).

The conclusion is that, at an overall confidence level of 98.5 percent, measurements taken by an untrained operator presented higher variance than the others. Moreover, no significant difference was found between measurements taken by a very highly skilled engineer and by another with limited experience in concrete pavement surveys.

The coefficients of variation also show evidence of the importance of previous training. They are:

Untrained student (Operator 3)	41.1 percent
Limited trained engineer (Operator 2)	11.7 percent
Highly skilled engineer (Operator 1)	14.1 percent

TABLE 3.2. RESULTS OF LEVENE'S TEST (REF 54) ON EXPERIMENT 1 DATA

Analysis of Variance

Due To	Degrees of Freedom	Sum of Squares	ms = ss/df	F-Ratio
Factor	2	128.59	64.29	11.63
Error	15	82.91	5.53	
Total	17	211.50		

Pooled Standard Deviation = 2.35

Level	Sample Size	Mean	Standard Deviation	95% Confidence Interval for Means
Operator 1	6	1.22	1.08	[– 0.8, 3.2]
Operator 2	6	1.00	0.82	[– 1.0, 3.0]
Operator 3	6	6.78	3.84	[4.8, 6.8]

Since the variances of the three samples are not homogeneous, the analysis of variance method cannot be applied to check homogeneity of means (Refs 39, 5, and 3). Three sets of pairwise comparisons (Ref 54) were performed among the means. The results are depicted at Table 3.3.

TABLE 3.3 RESULTS OF PAIRWISE COMPARISONS OF MEANS ON DATA OF EXPERIMENT 1 (REF 54)

Comparison Performed	T-Value	95% Confidence Interval for Mean Differences	Significance Level of Test
Operators 1 vs 2	– 0.557	[– 2.53, 1.53]	0.5911
Operators 2 vs 3	2.506	[– 0.22, 17.56]	0.0541
Operators 3 vs 1	2.344	[– 0.79, 17.13]	0.0661

Table 3.3 shows that one can safely consider the means of Operator 2 and Operator 1 to be equal. As for Operator 3, the individual t-tests were significant at 5.4 percent in one case and at 6.6 percent in the other. Since three pairwise comparisons were done, the individual tests have to be significant at no more than about 2 percent to provide an overall significance level of about 5 percent. Therefore, no highly significant statistical evidence was found that the mean of Operator 3 is different from the others. However, the highly significant difference between variances, discussed previously, already renders it evident that operators responsible for crack width readings must be previously trained.

Figures 3.1, 3.2, and 3.3 depict the normal plots (Ref 54) of the measurements obtained by the three operators. It can be seen that both Operator 2 and Operator 1 plots (Figs 3.1 and 3.2) are fairly normal, whereas Operator 3 (Fig 3.3) presents deviation from normality. It

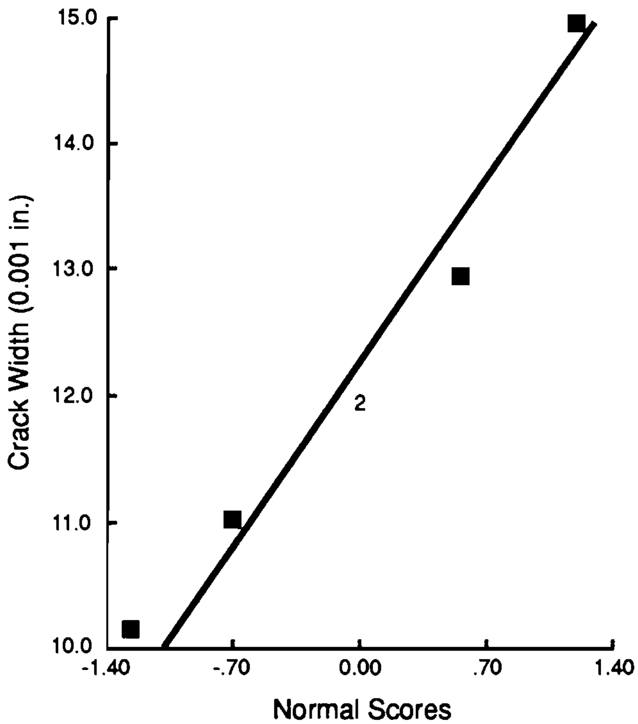

Fig 3.1. Normal plot of data taken by Operator 1 (Ref 54).

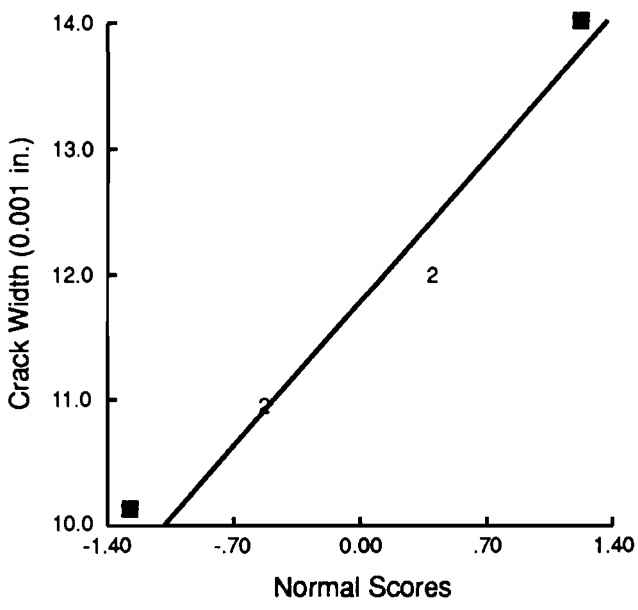

Fig 3.2. Normal plot of data taken by Operator 2 (Ref 54).

is important to remark that a good plot would show normality, i.e., measurements affected only by a random error symmetrically distributed around zero. Therefore, Operator 3 (untrained) was providing results affected by some systematic error, whereas Operators 1 and 2 were not.

It is thus concluded that field crews used to measure crack width must have a training lesson. It is also concluded that limited training on this task (e.g., Operator 2) results in virtually the same accuracy as several years of experience in data collection on rigid pavements (Operator 3).

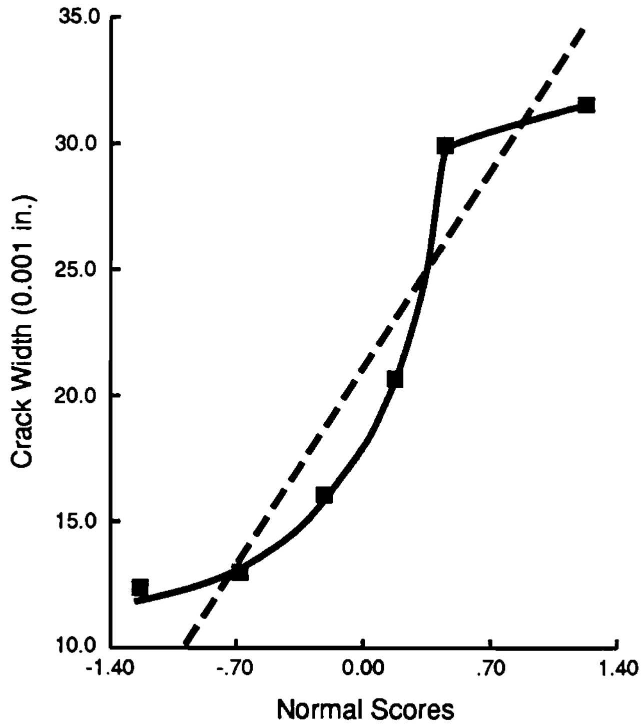

Fig 3.3. Normal plot of data taken by Operator 3 (Ref 54).

EXPERIMENT 2 - ANALYSIS OF THE DATA FOR ASCERTAINING THE CRACK WIDTH MEASUREMENT PROCEDURE

The specific purpose of this analysis was to check whether or not some cracks can be considered more difficult to measure than others. Also, a second check was intended on between-operators variance, although, due to the results of experiment 1, no significant difference was expected to be found among the three at this stage of the study.

Since no other criterion could be set forth to characterize what a difficult crack could be, it was decided to select a narrow, a medium, and a large crack and check whether or not the accuracy of the measurements was different for the three cases. Table 3.4 shows the raw data and the statistical summary.

Operator 3 could no longer be considered untrained, due to his previous participation in the same kind of experiment and to discussions with him and information given to him before the second experiment. Furthermore, results of the analysis previously described indicated that

TABLE 3.4. RAW DATA FOR THE EXPERIMENT 2

	Wide Crack			Medium Crack			Narrow Crack		
	Op 1	Op 2	Op 3	Op 1	Op 2	Op 3	Op 1	Op 2	Op 3
	62	60	56	32	27	31	6	10	12
	53	61	60	38	40	28	8	8	11
	53	49	60	25	20	28	7	10	10
	48	60	58	30	35	36	7	11	11
	50	59	59	24	21	30	10	9	10
	51	64	58	30	23	36	8	8	8
	62	58	55	18	40	33	7	8	10
	58	52	58	22	27	25	6	8	11
	51	49	62	25	19	35	8	10	9
	54	51	58	19	30	30	7	9	11
Mean	54.2	56.3	58.4	26.3	28.2	31.2	7.4	9.1	10.3
Standard Deviation	4.89	5.5	2.0	6.2	7.9	3.7	1.2	1.1	1.2
Sample Size		30			30			30	
Mean		56.3			28.6			8.9	
Standard Deviation		4.6			6.3			1.6	

no difference existed among trained operators, regardless of the amount of training. Statistical analysis was thus also performed on the aggregated samples, i.e., all three operators' readings of the narrow, the medium, and the large crack, and those were used to estimate the sample size to recommend for the field procedure.

Table 3.5 shows the results of Levene's test of homogeneity of variances for each Operator at each crack and for all measurements taken at each crack, i.e., on data aggregated by crack type. It can be seen from these results that the variances cannot be considered homogeneous in any case. Figures 3.4, 3.5, and 3.6 show the normal plots of each operator's readings at each crack.

Although some of the plots indicate some systematic deviation from normality, most of them are fairly normal. Figures 3.7 through 3.9 depict the normal plots for the aggregated samples of the narrow, the large, and the medium cracks. It can be seen from those Figures that the homogeneity of results among operators cannot be expected to hold strictly, especially for cracks that present more difficulties in reading. The narrow crack, which was the easiest to read, is the one that presents a fairly normal plot. The description of a "difficult" crack is given in the conclusions and recommendations.

Since Levene's test indicated that the variances are not homogeneous, and since the samples cannot all be considered normal, analysis of variance cannot be applied to compare the means. In the case of nine samples, performing all possible 36 pairwise comparisons is not statistically acceptable, because to obtain an overall significance level of 5 percent the individual significance levels of each test ought to be so low that the null hypothesis would be accepted for almost all tests. Therefore, no more statistical tests can be performed that would give reliable information.

The sample sizes recommended for the crack width measurements are shown in Table 3.6. Estimates were done for a 5 percent probability that the error will not exceed the listed values, and they were obtained through a procedure described in Ref 39.

The results depicted in Table 3.6 show that, depending on the difficulties in obtaining the readings, the expected precision will vary widely for the same sample size. It was clearly realized during the experiment that it is not possible to reduce the variances just by being more careful or by taking some other controllable action; the only safe way of avoiding poor results is by avoiding difficult cracks (defined later in this Chapter).

CONCLUSIONS

The following conclusions and comments can be drawn from the experiments described and analyzed above.

(1) Previous training of the operators is very important to ensure not only good individual reliability, but also good reproducibility of data taken by different operators.

(2) Sample sizes can be estimated from the experiment. However, care must be taken with the difficult cracks; it is not possible, from a practical standpoint, to take enough readings to ensure a low expected error.

(3) Crack width is a very difficult and imprecise parameter by its own nature; actually, what the experiment shows, in agreement with the literature (Refs 26, 12, 66, 15, 48, 45, and 53), is that no strict and precise width exists for a single crack; however, Ref 26 findings on non-significance of crack width variations across the crack support the validity of assigning an average representative number to a given crack at a given pavement temperature.

TABLE 3.5. RESULTS OF LEVENE'S TEST OF HOMOGENEITY OF VARIANCES (REF 54)

Source of Data	Levels	F-Ratio	Degrees of Freedom: Numerator	Degrees of Freedom: Denominator
Wide Crack	Operators	1,887.20	2	27
Medium Crack	Operators	2.80	2	27
Narrow Crack	Operators	0.01	2	27
All Cracks	Crack Type	19.10	2	87

$F_{2,\,27} = 2.96$ for 1% significance

(4) The available microscope has a source of light, but sunlight is necessary to obtain good visibility, i.e., the available microscope does not permit one to work at night.

(5) Spalled cracks should be avoided because no good reproducibility or repeatability can be obtained. It is important to note that the spalling does not need to be visible without a microscope.

(6) Faulted (stepped) cracks should be avoided. A microscope is an instrument that can be focused on only one level at a time. If a crack has unlevel sides, even at a microscopic magnitude, the operator will always see one side focused and the other side fuzzy. The only way to overcome this problem is to focus the microscope on one of the sides, write up or memorize the reading, focus it on the other side, take another reading, and obtain the final width by subtraction. Other possible sources of error in this case are

- (a) that the focusing error will accumulate twice;
- (b) that there are gross errors in subtracting the two readings;
- (c) that the gross errors in recording the readings are increased;
- (d) that the time to take one single reading is more than doubled, which may cause the time constraint to be overlooked; and
- (e) that the operator may inadvertently move the microscope between the two focusings, causing a non-existent width to be recorded for that particular spot.

(7) The measurements taken at each crack in the field are to be averaged in order to get some reliable typical value for the width of that particular crack at a given temperature. False results may be obtained if the temperature changes significantly during the time the readings are being taken. It is arguable whether or not the crack opening due to small temperature changes can be detected by usual microscopes; thus, it is safer to avoid that possible influence on the results.

(8) The differences among variances of the three types of cracks were not due to the difference in relative widths but, instead, were due to different frequencies of spalling and faulting. Those factors do not depend directly and strictly on width; if they did, the large crack would have the largest variance. Presence or absence of spalling and faulting was felt to be the most important factor that influences the precision of the crack width readings taken by trained operators.

TABLE 3.6. SAMPLE SIZES (REF 54)

Error (0.001 in.)	Narrow (S = 1.13)	Medium (S = 6.19)	Large (S = 4.41)
0.5	20	613	311
1.0	5	153	78
1.5	2	68	35
2.0	–	38	19
2.5	–	25	12
3.0	–	17	9

RECOMMENDED FIELD PROCEDURE FOR MEASURING CRACK WIDTH

Once the crack to be measured is selected, the operator should take at least six readings of it in a time interval preferably no longer than one hour. The time constraint is important in order to make absolutely certain that crack opening and closing due to temperature differentials does not affect the results of the experiment to any extent. However, a time interval of up to two hours can be acceptable if some delay occurs.

Each reading should be taken at a different location along the crack. At each location, the operator, using his or her best judgment, should attempt to put the microscope in what appears to be a non-spalled, non-faulted area. The operator should then focus the microscope, carefully sliding it back and forth until he/she is confident that what is being seen is actual width and not microscopic spalling or the distance between the crack wall and a piece of pulled-off aggregate: the former case gives falsely large widths, whereas the latter can yield falsely narrow readings. Once the reading is taken, the operator should pack the microscope, seek another location, and repeat the procedure described above. If time permits, more than six readings are desirable; on the other hand, a few careful readings yield a more reliable result than a large number affected by some wrong

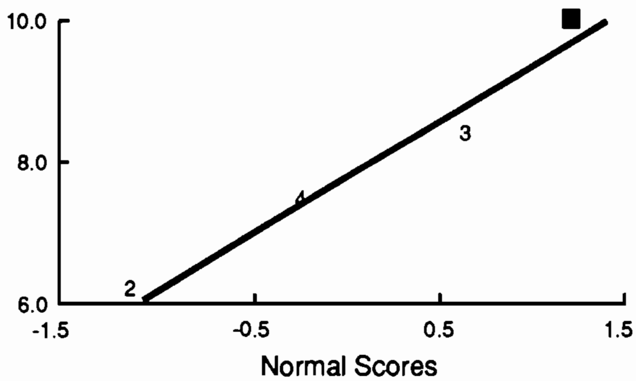

(a) Measurements taken by Operator 1.

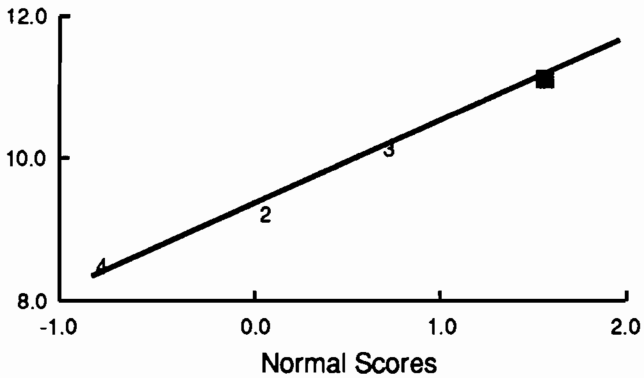

(b) Measurements taken by Operator 2.

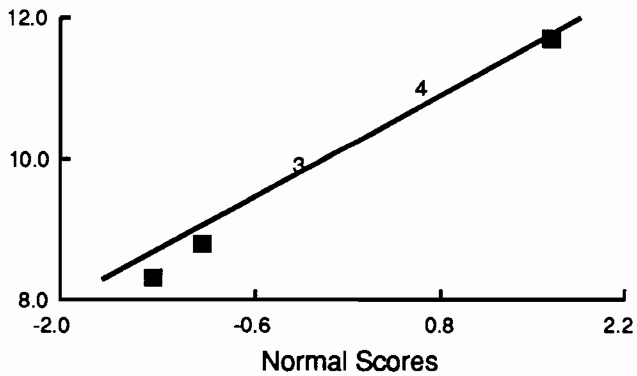

(c) Measurements taken by Operator 3.

Fig 3.4. Normal plots of data from narrow crack (Ref 54).

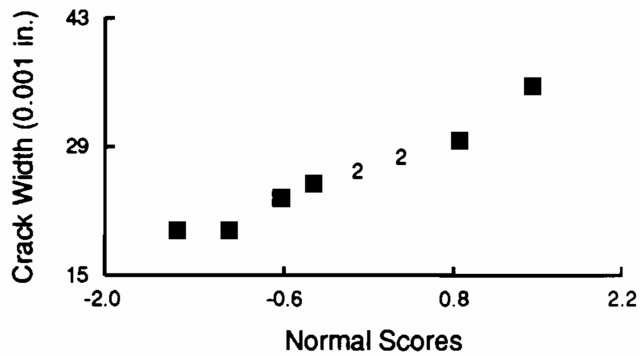

(a) Measurements taken by Operator 1.

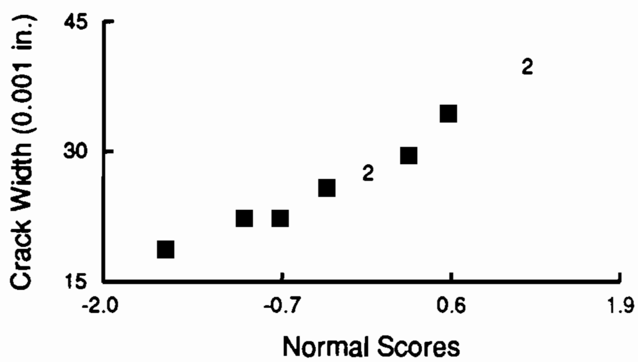

(b) Measurements taken by Operator 2.

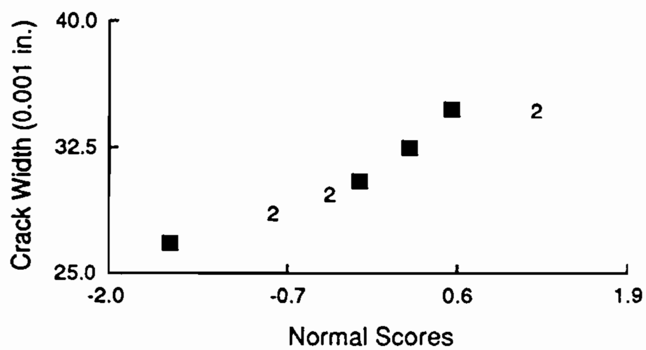

(c) Measurements taken by Operator 3.

Fig 3.5. Normal plots of data from medium crack (Ref 54).

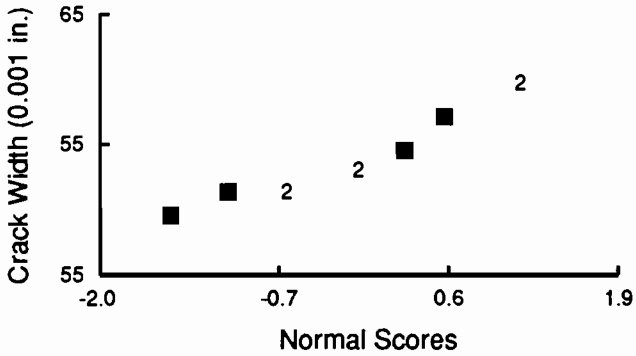

(a) Measurements taken by Operator 1.

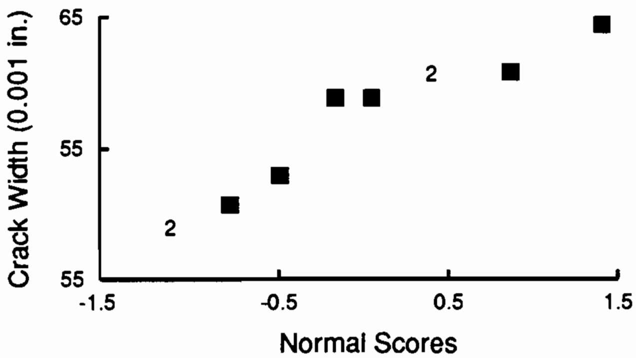

(b) Measurements taken by Operator 2.

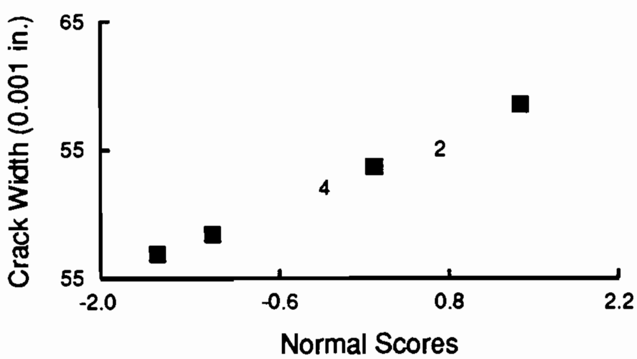

(c) Measurements taken by Operator 3.

Fig 3.6. Normal plots of data from wide crack (Ref 54).

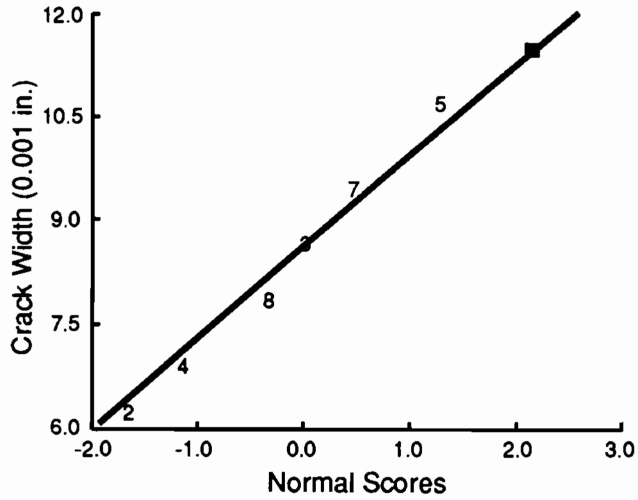

Fig 3.7. Normal plot of the aggregated data for the narrow crack (Ref 54).

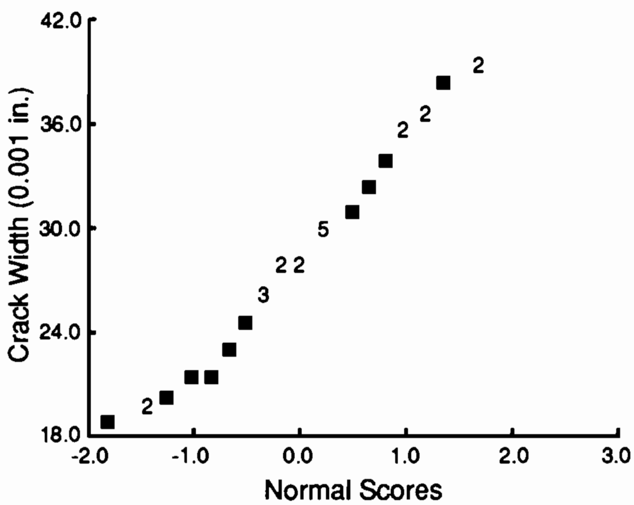

Fig 3.8. Normal plot of the aggregated data for the medium crack (Ref 54).

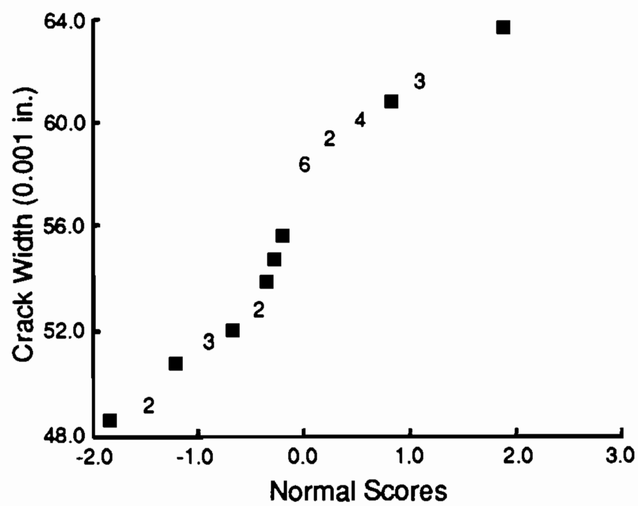

Fig 3.9. Normal plot of the aggregated data for the wide crack (Ref 54).

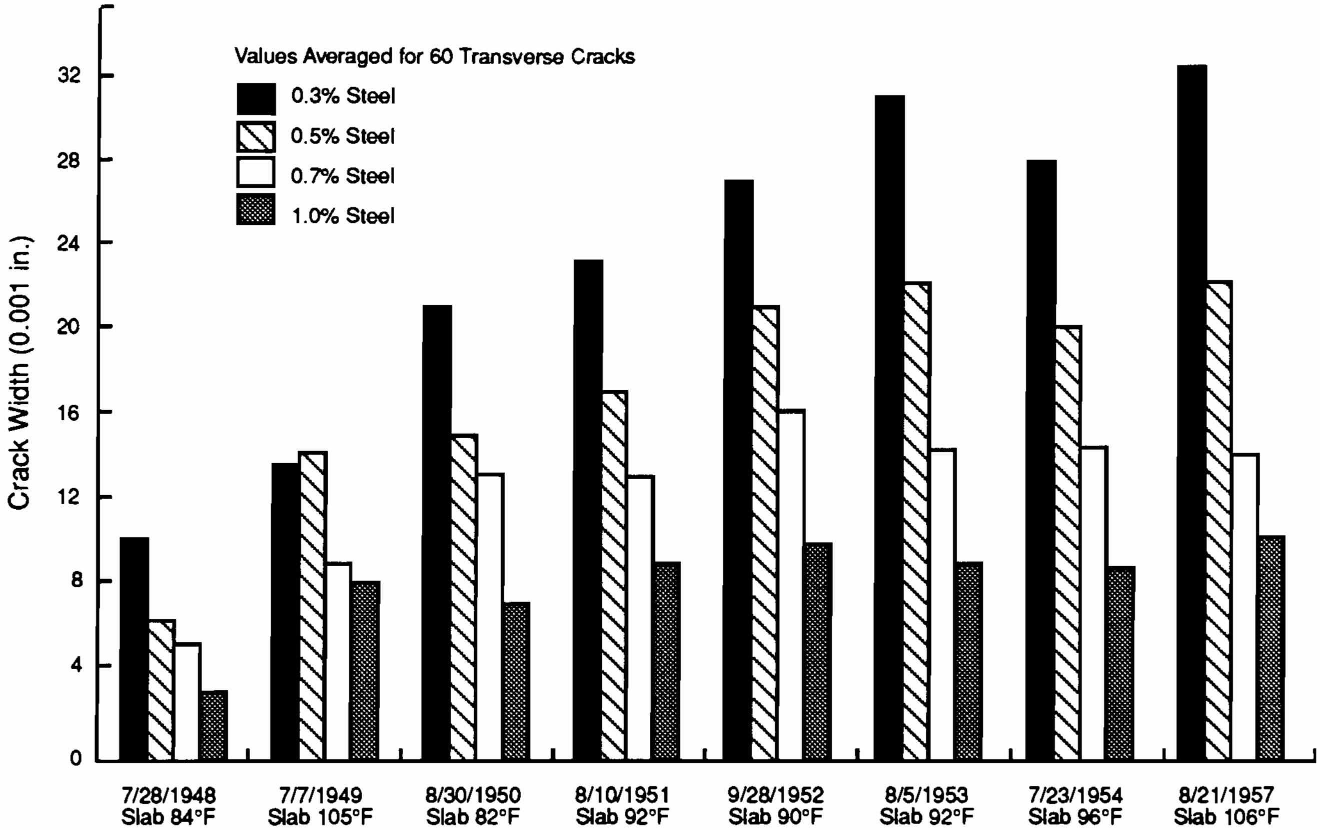

Fig 3.10. Effect of amount of longitudinal reinforcing steel on width of representative cracks, 7-inch sections (Ref 15).

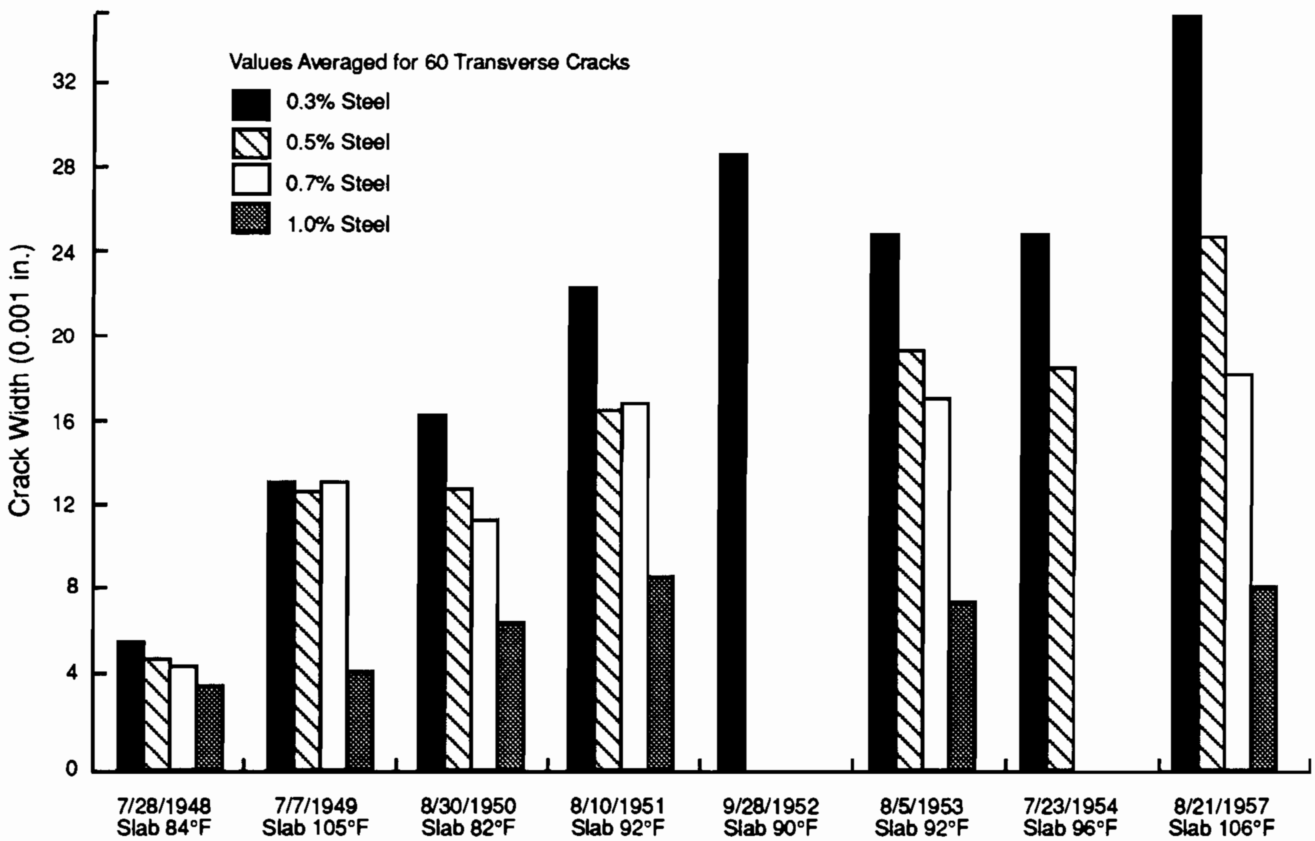

Fig 3.11. Effect of amount of longitudinal reinforcing steel on width of representative cracks, 8-inch sections (Ref 15).

readings. If the selected crack turns out to be spalled or stepped or both, it is recommended that another selection be made to avoid results such as the ones obtained for the medium crack of the experiment above.

The procedure for sampling the cracks depends on the objectives of the crack width measurements in the field. For example, if one of the objectives is to analyze the influence of crack spacing on crack width, the sampling cannot be random; instead, it has to be done according to the desired crack spacing. Recommendations on sampling, therefore, have to be made on a case-by-case basis after the sections for diagnostic study are selected and every particular objective of the crack width measurement is ascertained.

Reference 26 found that, on a statewide basis, only one set of data failed to support the hypothesis of uniformity of crack widths in continuous pavement segments. This isolated exception to uniformity was considered due to construction practices, environmental conditions, and/or material properties. This finding indicates that there is no need for concern about the consequences of systematic sampling, such as the one necessary for checking the influence of crack spacing on crack width. In the case of the diagnostic survey conducted in this project, this particular finding was useful because practical constraints on available personnel in the field were governing the number of cracks to be surveyed in each test section.

COMMENTS AND FURTHER CONSIDERATIONS

Prior to undertaking the experiment described above, a bibliographical search on the subject of crack width measurements on pavements was conducted, seeking some already tested or standardized procedure in the literature. And while such a procedure was not found (thus requiring the above described experiments to be undertaken), the search did yield other interesting findings worth summarizing.

Zuk (Ref 66) describes laboratory studies in which crack width was measured by means of a microscope. He also describes a comprehensive formulation for determining variation of CRCP crack width with depth. Zuk seems to be mainly concerned with variation of crack width with load repetitions and with type and amount of reinforcement. Figures 3.10 and 3.11 summarize the findings about crack width of an experimental CRCP in Illinois, which was observed for ten years (Ref 15). The measurement of crack width was considered difficult (Ref 15). At the time of construction, a series of brass plugs was installed along the edge of the central 30 feet of each test section for the purpose of measuring the widths of cracks that might subsequently form in these areas. Since enough cracks did not form between the plugs to give reliable data, crack width was measured by

TABLE 3.7. CRACK WIDTH DATA FOR 8-INCH SECTION FROM REF 48

Location and Incidental Data		July 1948	Aug 1948	Oct 1950	Dec 1950	July 1951	Nov-Dec 1951	June 1952	Mar 1953	Sept 1954	Jan 1956	Mar 1957	June 1957
847 + 50 to 847 + 95	Slab Temp	—	—	75°	31°	102°	48°	95°	38°	—	—	43°	101°
Inside Lane	No. Cracks	—	—	7	7	7	7	7	7	—	—	7	7
49 Spaces @ 10"	Avg Spacing	—	—	5.8'	5.8'	5.8'	5.8'	5.8'	5.8'	—	—	5.8'	5.8'
Const - Oct 16, 1947	Avg Width	—	—	.009"	.009"	.010"	.013"	.011"	.011"	—	—	.010"	.010"
	Max. Width	—	—	.011"	.011"	.011"	.015"	.013"	.014"	—	—	.012"	.012"
820 + 52 to 820 + 84	Slab Temp	90°	—	69°	31°	87°	48°	95°	—	—	—	43°	106°
Outside Lane	No. Cracks	7	—	9	9	9	9	9	—	—	—	9	9
38 Spaces @ 10"	Avg Spacing	4.5'	—	3.5'	3.5'	3.5'	3.5'	3.5'	—	—	—	3.5'	3.5'
Const - Oct 9, 1947	Avg Width	.002"	—	.007"	.007"	.007"	.008"	.007"	—	—	—	.006"	.006"
	Max. Width	.004"	—	.014"	.012"	.012"	.013"	.012"	—	—	—	.011"	.011"
831 + 40 to 831 + 80	Slab Temp	—	—	69°	31°	86°	48°	94°	38°	—	—	43°	105°
Outside Lane	No. Cracks	—	—	4	4	4	4	4	4	—	—	4	4
49 Spaces @ 10"	Avg Spacing	—	—	10.2'	10.2'	10.2'	10.2'	10.2'	10.2'	—	—	10.2'	10.2'
Const - Oct 8, 1947	Avg Width	—	—	.014"	.016"	.015"	.016"	.015"	.015"	—	—	.015"	.015"
	Max. Width	—	—	.018"	.020"	.019"	.020"	.019"	.019"	—	—	.020"	.020"
835 + 00 to 835 + 20	Slab Temp	90°	—	75°	31°	84°	54°	94°	—	—	—	42°	105°
Outside Lane	No. Cracks	7	—	6	7	7	7	7	—	—	—	7	7
23 Spaces @ 10"	Avg Spacing	4.8'	—	3.2'	2.7'	2.7'	2.7'	2.7'	—	—	—	2.7'	2.7'
Const - Oct 7, 1949	Avg Width	.006"	—	.010"	.012"	.010"	.011"	.010"	—	—	—	.010"	.010"
	Max. Width	.008"	—	.017"	.020"	.019"	.020"	.019"	—	—	—	.019"	.020"
848 + 00 to 848 + 50	Slab Temp	—	101°	75°	31°	102°	54°	94°	—	82°	42°	43°	100°
Outside Lane	No. Cracks	—	17	21	21	21	21	21	—	21	21	21	21
60 Spaces @ 10"	Avg Spacing	—	2.9'	2.4'	2.4'	2.4'	2.4'	2.4'	—	2.4'	2.4'	2.4'	2.4'
Const - Oct 6, 1947	Avg Width	—	.001"	.006"	.007"	.006"	.008"	.007"	—	.006"	.006"	.006"	.005"
	Max. Width	—	.003"	.011"	.012"	.011"	.012"	.012"	—	.011"	.011"	.011"	.010"

TABLE 3.8. CRACK WIDTH DATA FOR 10-INCH SECTION FROM REF 48

Location and Incidental Data		Nov 1947	Oct-Nov 1950	Dec 1950	July 1951	Nov-Dec 1951	Mar 1952	June 10, 1952	June 27, 1952	Mar 1953	Sept 1954	Mar 1957	June 1957
894 + 78 to 895 + 00 Inside Lane 26 Spaces @ 10" Const - Sept 29, 1947	Slab Temp	—	72°	32°	94°	48°	—	93°	100°	—	—	43°	95°
	No. Cracks	—	5	5	5	5	—	5	5	—	—	5	5
	Avg Spacing	—	4.3'	4.3'	4.3'	4.3'	—	4.3'	4.3'	—	—	4.3'	4.3'
	Avg Width	—	.013"	.013"	.011"	.013"	—	.011"	.010"	—	—	.012"	.012"
	Max. Width	—	.022"	.022"	.019"	.022"	—	.020"	.020"	—	—	.020"	.020"
910 + 00 to 910 + 50 Outside Lane 60 Spaces @ 10" Const - Sept 26, 1947	Slab Temp	52°	76°	30°	92°	47°	—	93°	—	38°	—	43°	94°
	No. Cracks	5	8	9	9	9	—	9	—	9	—	9	9
	Avg Spacing	10.0'	6.2'	5.6"	5.6'	5.6'	—	5.6'	—	5.6'	—	5.6'	5.6'
	Avg Width	.008"	.010"	.013"	.010"	.012"	—	.010"	—	.011"	—	.011"	.010"
	Max. Width	.012"	.017"	.023"	.021"	.022"	—	.019"	—	.020"	—	.021"	.021"
921 + 11 to 921 +61 Outside Lane 60 Spaces @ 10" Const - Sept 24, 1947	Slab Temp	52°	69°	—	94°	55°	—	88°	100°	—	—	43°	92°
	No. Cracks	4	10	—	10	10	—	10	10	—	—	10	10
	Avg Spacing	12.5'	5.0'	—	5.0'	5.0'	—	5.0'	5.0'	—	—	5.0"	5.0"
	Avg Width	.005"	.007"	—	.008"	.010"	—	.008"	.008"	—	—	.008"	.010"
	Max. Width	.008"	.015"	—	.016"	.021"	—	.018"	.017"	—	—	.018"	.021"
886 + 62 to 886 + 92 Outside Lane 43 Spaces @ 10" Const - Sept 16, 1947	Slab Temp	—	73°	—	94°	34°	—	93°	100°	—	—	43°	96°
	No. Cracks	—	8	—	78	8	—	6	8	—	—	8	8
	Avg Spacing	—	4.5'	—	4.5'	4.5'	—	4.5'	4.5'	—	—	4.5'	4.5'
	Avg Width	—	.013"	—	.014"	.018"	—	.014"	.014"	—	—	.016"	.016"
	Max. Width	—	.019"	—	.019"	.022"	—	.018"	.018"	—	—	.020"	.019"
910 + 25 to 910 + 50 Outside Lane 30 Spaces @ 10" Const - Sept 11, 1947	Slab Temp	52°	70°	30°	—	47°	38°	93°	—	—	—	41°	94°
	No. Cracks	4	6	6	—	6	6	6	—	—	—	6	6
	Avg Spacing	6.2'	4.2'	4.2'	—	4.2'	4.2'	4.2'	—	—	—	4.2'	4.2"
	Avg Width	.015"	.016"	.020"	—	.020"	.021"	.018"	—	—	—	.022"	.023"
	Max. Width	.020"	.025"	.029"	—	.027"	.028"	.027"	—	—	—	.029"	.030"
921 + 25 to 921 + 50 Outside Lane 30 Spaces @ 10" Const - Sept 10, 1947	Slab Temp	52°	77°	32°	—	55°	—	88°	—	—	84°	43°	94°
	No. Cracks	4	8	8	—	8	—	8	—	—	8	9	9
	Avg Spacing	6.2'	3.1'	3.1'	—	3.1'	—	3.1'	—	—	3.1'	2.8'	2.8'
	Avg Width	.008"	.008"	.012"	—	.010"	—	.009"	—	—	.011"	.010"	.010"
	Max. Width	.011"	.015"	.018"	—	.018"	—	.016"	—	—	.017"	.017"	.017"
925 + 34 to 925 + 50 Outside Lane 19 Spaces @ 10" Const - Sept 9, 1947	Slab Temp	70°	77°	30°	95°	40°	—	88°	—	—	82°	43°	94°
	No. Cracks	2	4	4	4	4	—	4	—	—	4	4	4
	Avg Spacing	7.9'	3.9'	3.9'	3.9'	3.9'	—	3.9'	—	—	3.9'	3.9'	3.9'
	Avg Width	.008"	.013"	.013"	.010"	.013"	—	.010"	—	—	.013"	.012"	.014"
	Max. Width	.013"	.017"	.017"	.014"	.018"	—	.015"	—	—	.018"	.017"	.017"

TABLE 3.9. VARIATION OF CRACK WIDTH DATA WITH DEPTH (REF 6)

				Distance Below Surface							
				Crack-Width Measurement (in.)[a]						Steel	
Core Number	Section (in.)	Lane	Engineers Stations	0	1	3	5	7	9	Upper	Lower
1	10	Outside	927+81	-	-	-	-	0.008	0.001	6.0	8.5
2	10	Outside	894+92	0.060	0.020	0.016	0.008	0.004	M	3.0	7.2
3	10	Outside	910+49	0.050	0.018	0.014	0.010	0.004	M	2.4	7.7
10	10	Outside	886+82	0.020	M	M	M	M	M	2.5	7.0
21	10	Outside	905+22	0.020	0.020	0.016	0.012	0.008	0.008	1.7	7.3
9	10	Inside	894+88	0.025	0.012	M	M	M	M	2.6	7.2
5	8	Outside	835+14	0.025	0.020	0.008	0.004	M	-	3.2	5.4
6	8	Outside	831+70	0.020	0.016	0.004	M	M	-	3.2	5.4
7	8	Outside	831+70	0.020	0.018	0.016	0.006	M	-	3.0	5.2
19	8	Outside	823+08	0.030	0.016	0.010	0.004	M	-	3.2	6.2
22	8	Outside	820+63	0.010	0.004	0.004	0.003	M	-	2.2	5.0
23	8	Outside	831+94	0.010	0.001	M	M	M	-	3.2	5.1

[a]M = Crack of microscopic width

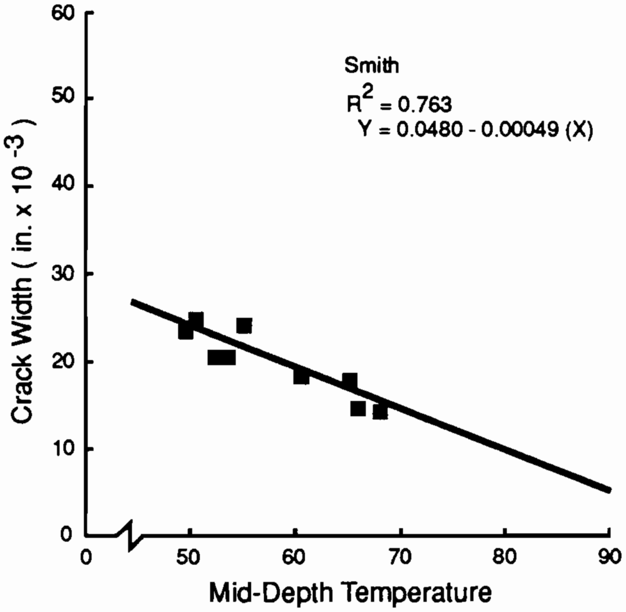

Fig 3.12. Crack width versus mid-depth slab temperature – Smith.

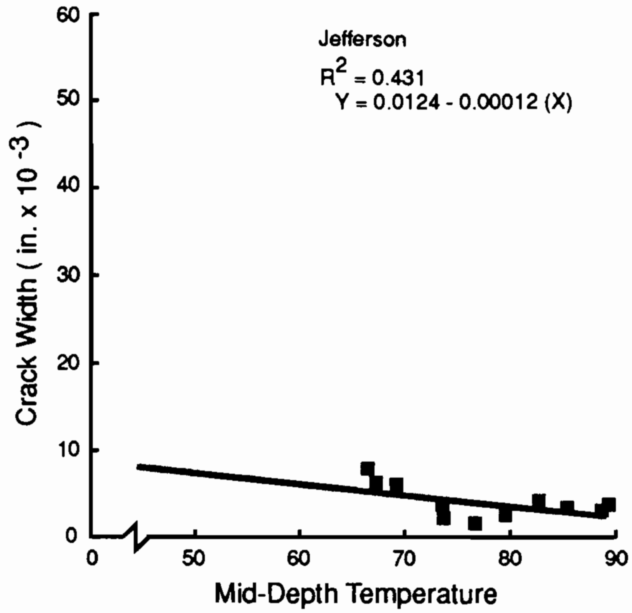

Fig 3.14. Crack width versus mid-depth slab temperature – Jefferson.

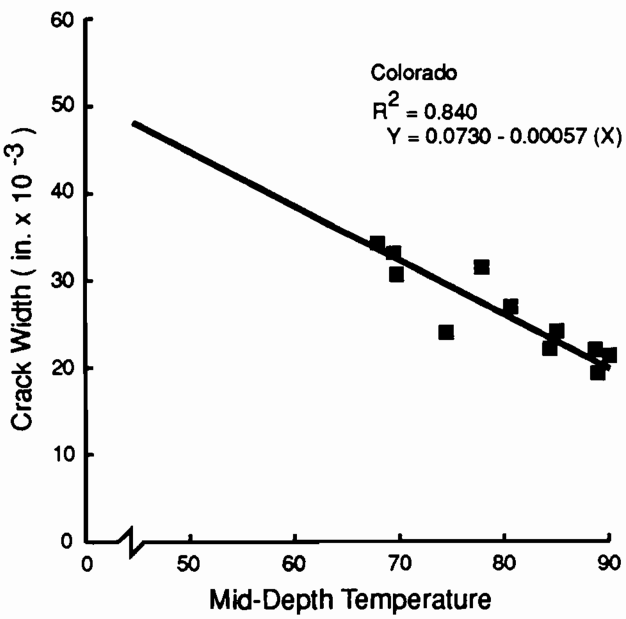

Fig 3.13. Crack width versus mid-depth slab temperature – Colorado.

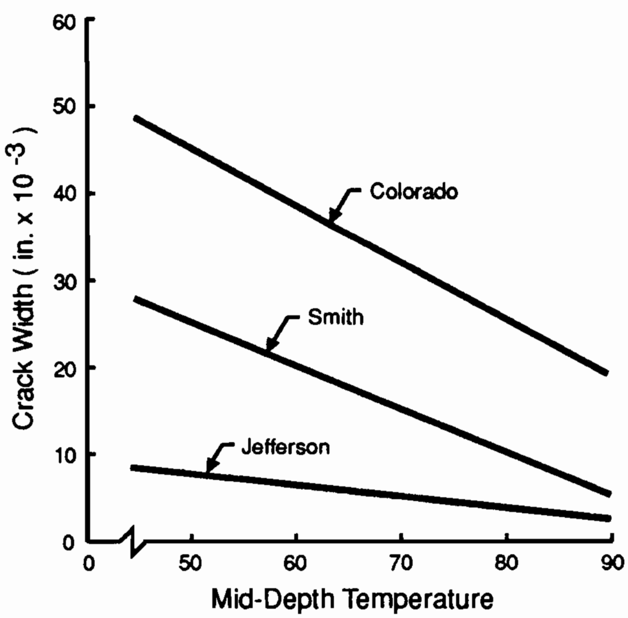

Fig 3.15. Comparison of regression lines (crack width versus mid-depth temperature) for three projects.

means of a microscope precise to 0.001 inch. Unexpectedly, Figs 3.10 and 3.11 do not show any systematic change in crack width with changes in temperature. The author (Ref 15) is also concerned with the variation of crack width with crack depth. After discussing other previous findings and presenting some laboratory data, he concludes that a reasonable approximation of the real width would be half the surface width (Ref 15).

Van Breemen (Ref 48) also found little influence of slab temperature on crack width, and, like Lindsay (Ref 15), he was concerned with the variation of crack width with depth. Tables 3.7 and 3.8 show data obtained by means of gauge plugs installed within the plastic concrete. The crack widths shown are based on the increased distance between the plugs. Because the concrete is subject to shrinkage—a fact not taken into account by Van Breemen (Ref 48)—the actual crack widths are likely to be higher than those recorded.

It is interesting to note that measurements taken at the cracks in March 1957 and June 1957 showed that the decrease in crack width in the period was practically nil, despite an increase in pavement temperature of more than 50° F. With respect to the differences observed between July and December (60° F temperature drop), measurements showed that

(1) the cracks in the 8-inch section had undergone an average opening of only 0.001 inch, and
(2) the cracks in the 10-inch section had undergone an average opening of only 0.0015 inch.

Table 3.9 summarizes the observed variation of crack width with depth. It can be seen that all cracks were much narrower in the lower two-thirds than at the surface and were only of microscopic width at the lower third. Reference 48 presents very interesting pictures of the cores referred to in Table 3.9. The author concludes that, due to the marked difference in crack width from top to bottom, the surface appearance of the pavement, at least in general, is not indicative of its true structural condition (Ref 48).

Reference 45 also has some data on variation of crack width with slab temperature during the year. Conclusions similar to the previous ones can be drawn from Ref 45.

Pennsylvania data (Refs 63 and 42), however, disagree with some of the results summarized previously. In fact, Ref 63 presents data of three-month crack width measurements, and, as the cooler weather approached, the cracks became wider. When the weather was quite warm, the cracks averaged 0.12 to 0.20 inch. With the advent of the cold weather, these cracks assumed widths of 0.25 to 0.35 inch. Reference 42 also presents some results that show the influence of temperature changes on crack width.

References 46 and 25 describe an experiment in which crack width was measured by means of the microscope. It is important to note that Ref 25 found a relationship between slab temperature at mid-depth and crack width. Figures 3.12 to 3.15 show some of the referred correlations.

None of the references (Refs 66, 15, 48, 45, 63, and 42) describes in detail the criteria used to obtain a representative crack width, although all of them refer to the problems of width variation with depth, and some refer to its variation with location across the crack. Nor are there any procedures indicated to take into account eventual crack width variation with temperature changes.

It is interesting to note also that Ref 21 investigated the possibilities and accuracy of detecting cracks by means of the GM profilometer, the Dynaflect, and other equipment. The authors, while finding several promising pavement evaluation methods, conclude that, at present, no method can be as accurate as the traditional visual survey (Ref 21).

The literature suggests that the most widely used device to obtain crack width is the microscope precise to 0.001 inch. There is no consensus regarding exactly where and how many times to measure, vertically and horizontally.

Lindsay's (Ref 15) previous finding that deeper crack width is about one-half of the superficial width seems to be worthy of further study, if crack widths at some depth need to be known. Further research on this subject could yield useful practical results if some correlation between superficial and internal width can be found.

The conflicting findings about influence of temperature on crack width need to be investigated in more detail in order to release the time constraint put into the procedure recommended for the crack width measurements. Also, further investigation of the magnitude of this influence should be very useful for analyzing and comparing crack widths measured at different pavements on different days.

CHAPTER 4. DEVELOPMMENT OF PROCEDURE FOR ESTIMATING PAVEMENT TEMPERATURE

BACKGROUND

The phenomenon of heat conduction is complex and depends on several factors (Ref 9). The simplest description of this phenomenon is the one-dimension second-order heat transfer equation, which describes the change in temperature of a given material with time as a function of its thermal properties and the temperature gradient along the considered dimension (Ref 9). The equation is

$$\frac{dT}{dt} = a\left(\frac{d^2T}{dx^2}\right) \tag{4.1}$$

where

T = temperature,
t = time,
x = dimension in the material, and
a = thermal diffusivity.

Equation 4.1 is a simplified model of heat conduction, but it shows the key characteristic that a model for estimating temperatures in a solid should possess: auto-correlation. In other words, the temperature at a given instant is a function of the temperature at a previous instant, and any formulation for solving Eq 4.1 requires that some boundary conditions, such as subbase temperature and an initial temperature regime, be known. This also means that any temperature model having as dependent variables such factors as thermal properties, air temperature, wind speed, or solar radiation, would also require as inputs an initial temperature regime, which may be represented by surface temperatures, and a lower boundary condition, which can be represented by subbase temperatures (Ref 28).

The literature has some examples (Refs 4, 24, 25, 38, and 56) of models that predict temperatures at the surface of flexible pavements from factors such as thermal properties of the material, air temperature, daily temperature range, wind speed, solar radiation, and time of the day. Reference 38 improved upon the method described in Ref 4 to develop a computer program, entitled TEMPRD, for estimating surface temperatures in the pavement. Reference 28 presents practical tests of these methods, which generated less accurate predictions than those desired for corrections of diagnostic survey data. For the data required for the subject project, however, the most important drawback of those methods is that they predict only the surface temperature, whereas the diagnostic survey requires predictions of the temperature gradient along the pavement depth.

The auto-correlation characteristics of the heat conduction phenomenon can thus be viewed as the main contributor to the problem of predicting pavement temperatures: a model is required to estimate pavement temperatures, but initial temperature estimates are required to permit application of the model.

All those factors suggest that the most reliable method for obtaining pavement temperatures will be as close as possible to direct measurement. From a practical standpoint, this can be attained by measuring the temperatures in a portable slab, which consists of a concrete block that has thermocouples embedded within it at different depths and is tranportable by two people.

Reference 24 is the earliest study found that investigated the feasability of estimating temperature differentials of a highway slab with the portable slab method. The experiment described in Ref 24 was conducted at Interstate Highway 10, near the State Highway 71 overpass in Colorado county. Resistance thermometers were installed within this pavement, near its top and its bottom, during regular paving operations. The resistance thermometers were hooked to a junction box near a guard rail post. Three portable test slabs were cast, using the same concrete and thickness (9.5 inches) as the highway section. Their plain view dimensions in inches were 18 x 16, 16 x 12, and 12 x 12. Resistance thermometers were put inside the portable slabs at the same vertical locations as those in the highway test section. The experiment (Ref 24) was conducted in two phases. In the first phase, the accuracy of the results of the test slab was determined and found to be good. In the second phase, the influence of the conditions of the base material, and the necessity (or non-necessity) of banking earth around the test slab, were investigated. In phase one, all conditions were the same for the test slabs and the pavement; in phase two, the portable slabs were placed on stabilized soil and had earth banked around; next, they were put on non-stabilized soil, to simulate the field condition (on the ground near the road). For each 24-hour cycle, linear regression equations were fit to predict temperature differentials at the pavement as a function of those at the portable slabs. It was found that the regression parameters did not remain constant from day to day but did remain within a narrow band. This result held for both phase one and phase two data. The overall conclusions (Ref 24) were favorable to this method of measuring temperature differentials; recommendations were made to study the influence on the predicted temperatures of other variables, such as coarse aggregate type.

OBJECTIVES

The ultimate objective of the experiment described in this chapter was to arrive at a procedure for estimating pavement temperatures that could be implemented in the diagnostic survey. The recommendations of Ref 24 were used as guidelines for designing the experiment. For the sake of clarity, this broad objective sought

(1) to check the influence of aggregate type on pavement temperature estimates as a function of the portable slab temperatures,
(2) to verify the influence of pavement thickness on the estimates,
(3) to investigate whether or not it is necessary to either bury the portable slab at the test site or to bank earth around it in order to reliably estimate the pavement temperature, and
(4) to check whether different models would have to be calibrated for different seasons, or if one model would be suitable for temperature estimates at any season.

These objectives were accomplished by means of an experiment undertaken from October to December of 1987 in the BRC test site depicted in Fig 1.2 of Chapter 1.

DESIGN OF THE EXPERIMENT AND SUMMARY OF THE DATA

Three pairs of 14-inch x 14-inch slabs, each of them 6, 10, and 14 inches thick, were cast. Each pair consisted of two slabs of the same thickness, one made with limestone aggregate and the other with silicious river gravel aggregate. Those aggregate types were selected because they are prevalent in the test sections studied in this project. Each slab had thermocouples at three different locations: top (one inch below surface), mid-depth, and bottom (one inch above bottom). The slabs had insulation all around. The slabs sizes, and thermocouple locations, are depicted in Fig 4.1. Table 4.1 summarizes the number of portable slabs of each dimension and type.

The experiment consisted of simultaneously taking temperature readings at the portable slabs, sketched in

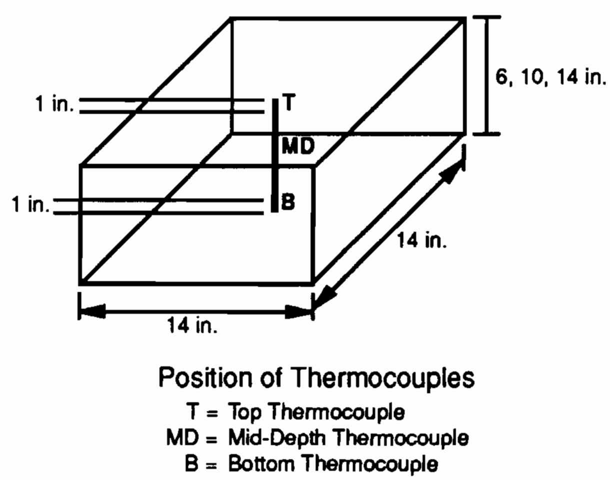

Fig 4.1. Scheme of the portable slabs.

TABLE 4.1. NUMBER OF PORTABLE SLABS OF EACH THICKNESS AND AGGREGATE

Aggregate Type	6 in.	10 in.	14 in.
Limestone	1	1	1
River Gravel	1	1	1

Fig 4.1, and at the test slab, depicted in Fig 1.2. The data were taken every half-hour. Ambient temperature was also recorded.

Four sets of data, representing buried and non-buried portable slabs, cloudy and sunny days, and hot and cold weather, were taken and analyzed. They consisted of

(1) five days of measurements with the portable slabs on the ground;
(2) five days of measurements with buried portable slabs;
(3) four weeks of discontinuous measurements, out of which the data taken on cloudy days were extracted to form the third data set; and
(4) ten days of measurements with mixed weather conditions and no interruptions in the data acquisition process.

Table 4.2 summarizes the data taken and the characteristics of each data set. (These data sets will hereafter be referred to according to the numbers assigned in Table 4.2.) Figures 4.2 to 4.5 present samples of the four sets of data obtained for the top thermocouples in the six-inch portable slabs and in the pavement. The complete plots of all data sets can be found in Appendix A of this report.

TABLE 4.2. SUMMARY OF DATA COLLECTED

Data Set		Dates Collected	
Number	Characteristic	From	To
1	Unburied Slabs	10/05/87	10/09/87
2	Buried Slabs	1022/87	1026/87
3	Cloudy Days Sample	12/18/87	12/24/87
4	Mixed Weather, Continuous Data	12/04/87	12/14/87

Figure 1.2 shows that there are three thermocouple locations at the pavement test slab: interior (location 1), at the joint (location 2), and at the corner (location 3). Therefore, it would be possible to investigate how to estimate pavement temperature at three different pavement locations of interest in the field: at a corner, at a discontinuity (joint or crack), and at the interior of the pavement. Results discussed in Chapter 2, however, indicated that the vertical temperature gradients (along different depths) are larger than the horizontal gradients.

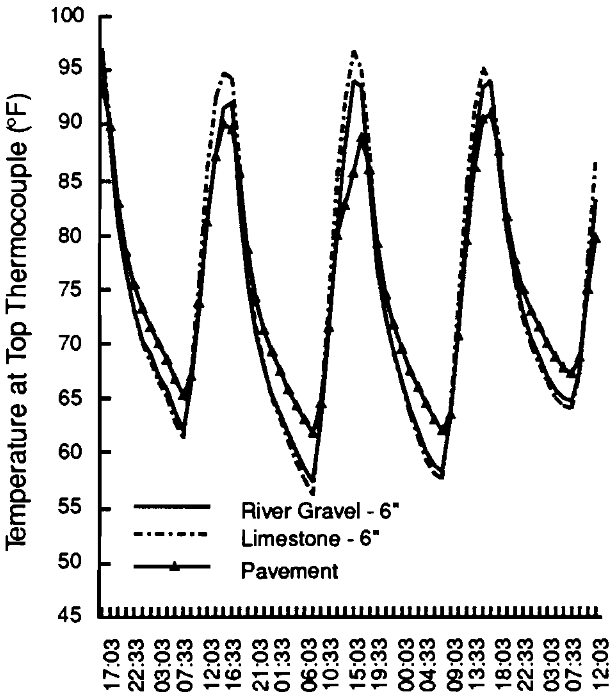

Fig 4.2. Sample of data from data set 1.

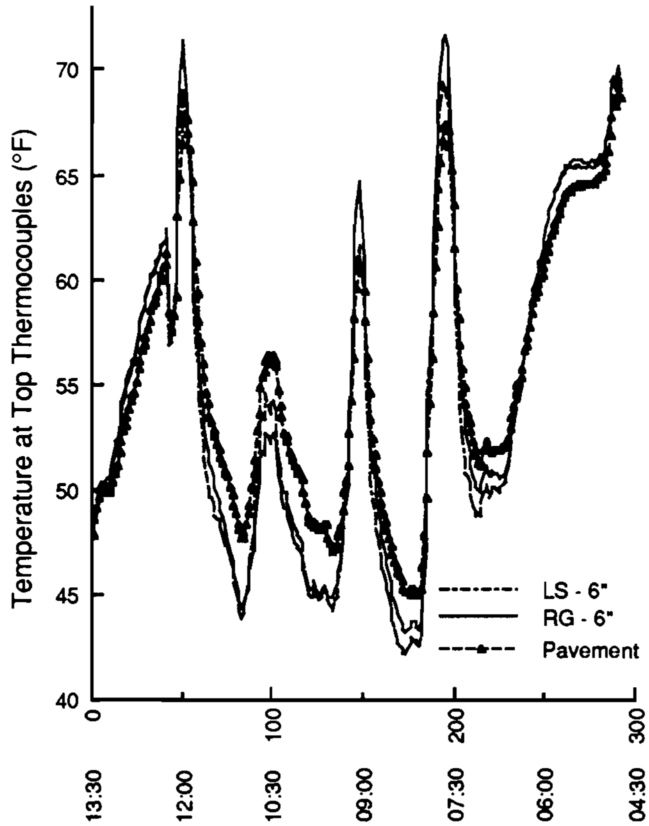

Fig 4.4. Sample of data from data set 3.

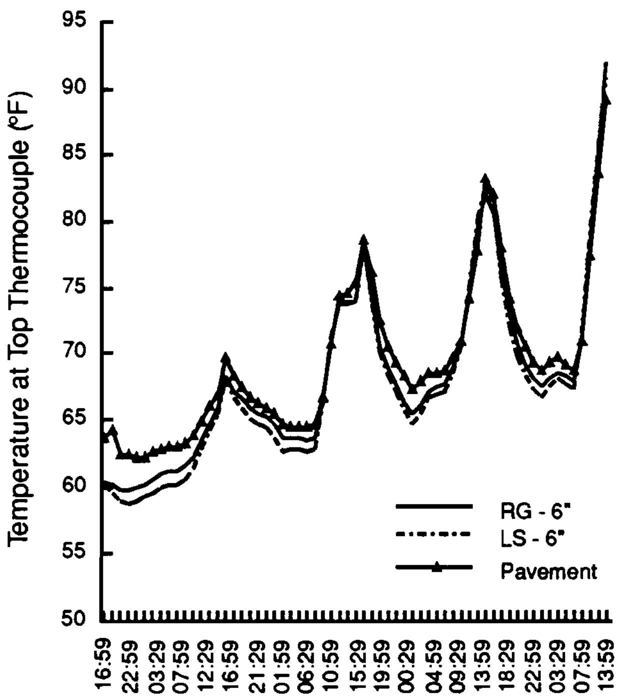

Fig 4.3. Sample of data from data set 2.

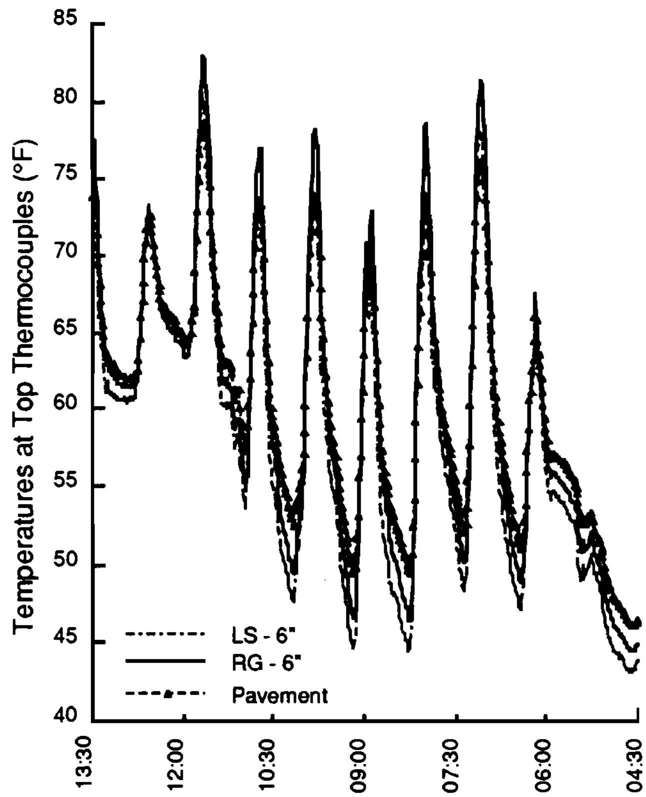

Fig 4.5. Sample of data from data set 4.

Moreover, corrections for temperature effects are important for back-calculation of pavement stiffness parameters from deflections; those calculations should be performed only for interior slab conditions, for reasons explained in Chapter 5. Consequently, this study concentrated primarily on modeling the temperatures at the interior of the slab, and only the data from thermocouples at location 3 were used to represent pavement temperatures.

DATA ACQUISITION AND STORAGE SYSTEM

INTRODUCTION

The temperatures recorded in this experiment were obtained by means of thermocouples embedded within the concrete at the test slab at Balcones Research Center (Fig 1.2) and at the portable slabs (Fig 4.1) described in the previous item. The data acquisition system consisted of the thermocouples and of the automatic recording system. Both are described in this section. In addition, the procedures used to store the data are described.

THE THERMOCOUPLE

Thermocouples consist of wires made of different materials, joined at both ends. When one junction of the thermocouple is heated, a continuous electric current flows in the thermoelectric circuit. If this circuit is broken at the center, the net open circuit voltage is a function of the junction temperature and of the composition of the two metals. This voltage is termed Seebeck voltage (Ref 30). Figure 4.6 depicts a thermoelectric circuit and the Seebeck voltage.

For small changes in voltage, the Seebeck voltage is directly proportional to the absolute temperature:

$$\Delta V = c\,\Delta T \qquad (4.2)$$

where

ΔV = voltage,
ΔT = absolute temperature, and
c = constant of proportionality.

One cannot, however, measure directly the Seebeck voltage, because any connection of a voltmeter to the thermocouple would create at least one new thermoelectric circuit in connection with the first. Figure 4.7 depicts the equivalent circuit of a copper-constantan thermocouple hooked to a voltmeter with copper connecting wires. One is interested only in V_1, but the new copper-constantan junction J_2 will add V_2 to the reading of voltmeter V. Thus, the voltmeter reading will be proportional to the temperature differential between J_1 and J_2. In other words, the temperature at J_2 must be found in order to achieve the ultimate objective of any thermocouple installation, which is to find the temperature at junction J_1.

One way to determine the temperature at J_2 is to place the junction into an ice bath, thus forcing its temperature down to 273.15K (32° F), and establishing J_2 as the reference junction. The temperature T_{J2} is now the reference temperature (T_{ref}). Since the voltmeter reading is

$$V = V_1 - V_2 = c\,(T_{J1} - T_{ref}) \qquad (4.3)$$

it is now possible to calculate the temperature at J_2 and to reference the voltage V to T_{ref} (273.15 K, in this case). Reference 30 claims that this method is very accurate, because ice temperature can be precisely controlled.

Due to the practical difficulties in physically keeping one of the junctions inside an ice bath, an isothermal block must be part of the circuit. The isothermal block is an electrical insulator that is also a good heat conductor, and it serves to keep any two junctions at the same temperature. The ice bath can thus be replaced by an isothermal block, as depicted in Fig 4.8. The output voltage V is still given by Eq 4.3, where now T_{ref} is the reference

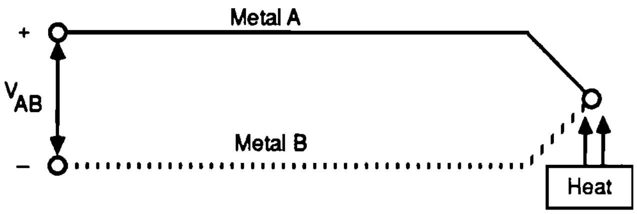

Fig 4.6. The thermocouple.

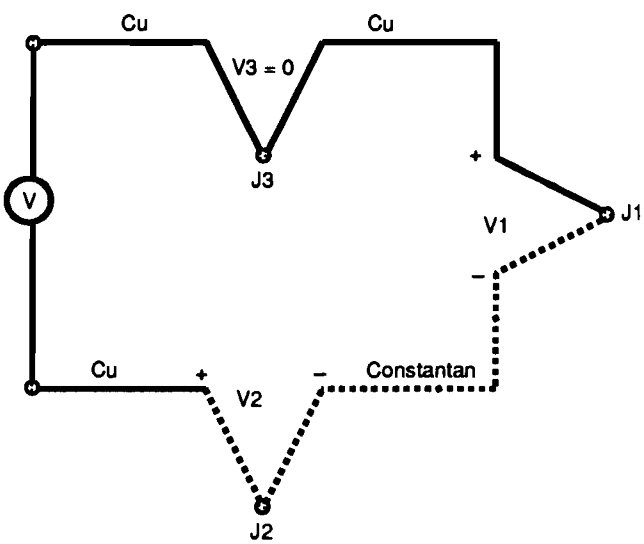

Fig 4.7. Equivalent circuit of a copper-constantan thermocouple with a voltmeter.

temperature of the isothermal block. The temperature at the isothermal block is measured by a thermistor in the isothermal block circuit; a thermistor has electrical resistance proportional to temperature.

The thermistor itself is not directly used as a temperature measurement device, for the following reasons (Ref 30):

(1) thermistors are useful only over a narrow temperature range,
(2) thermocouples are more rigged than thermistors,
(3) thermocouples can be manufactured on the spot,
(4) thermocouple use is as easy as connecting a pair of wires, and
(5) the isothermal junction can be used for more than one thermocouple.

The measurement procedure includes

(1) measuring the resistance at the thermistor (R_t) to find T_{ref},
(2) converting T_{ref} to its equivalent voltage V_{ref}, using previous calibration data,
(3) measuring V and obtain V_1 by subtraction, and
(4) converting V_1 to temperature T_{J1}.

THE DATA RECORDING SYSTEM

At the BRC test site, all calculations used to determine the temperature at the desired junction are performed on a Hewlett Packard computer that is part of the acquisition system to which the thermocouples can be hooked. The software, provided by Hewlett Packard, can be fed with the appropriate constants to perform the above mentioned voltage/temperature conversions for the thermocouple type that is being used. In this experiment, the thermocouples used are copper-constantan, type T, capable of measuring temperatures ranging from –160° C to 400° C, with a precision of ±0.5° C (Ref 30).

The automatic recording system is capable of recording 40 channels simultaneously. Eighteen channels were used to record the portable slab thermocouples, nine were hooked to the test slab thermocouples, and two were used to record two replicates of ambient temperature. A printout of the data is also automatically made. Figure 4.9 depicts a simplified layout of the test site and the data recording system.

APPROACH FOR ANALYZING THE DATA

In this experiment, answers to two basic problems were sought: First, is there any significant difference between temperature data from different treatments, such as buried and unburied portable slabs, or aggregate type? Second, which models can reliably predict pavement temperatures using the portable slab temperatures? These basic objectives were stated as specific questions that were

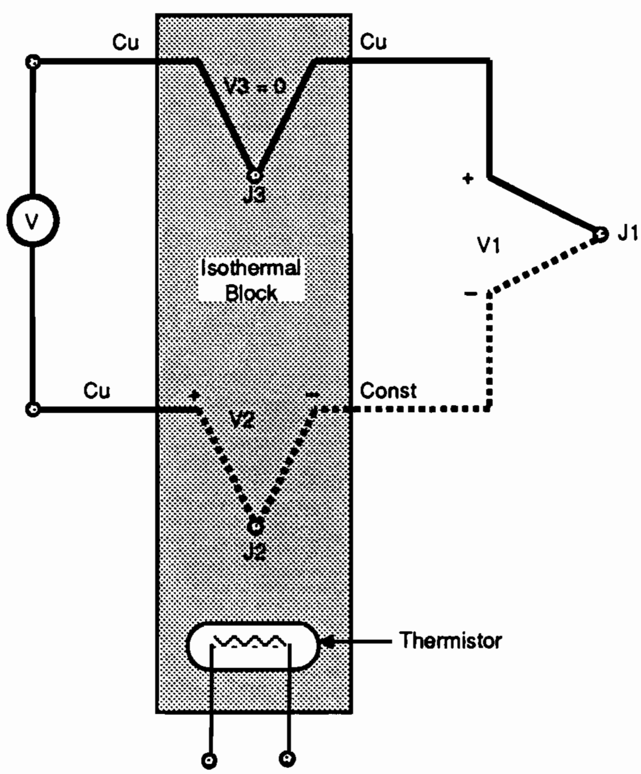

Fig 4.8. Equivalent circuit of a copper-constantan thermocouple with voltmeter and isothermal block.

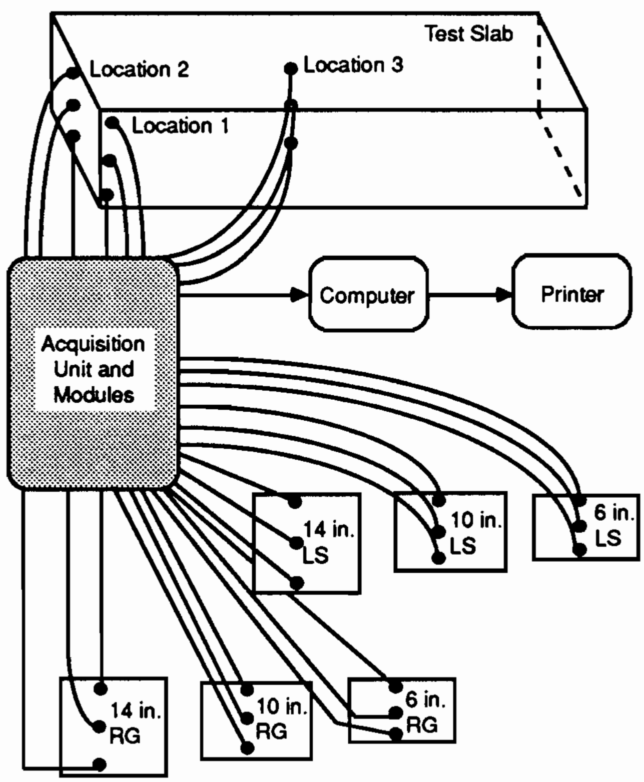

Fig 4.9. Layout of the BRC test site.

divided into studies, each one meant to answer a specific question. The objectives of these studies are detailed below. The results and conclusions are presented later in the chapter.

STUDY 1

This study was done first, using data set #1, and its objective was

(1) to determine whether or not the aggregate type used in the portable slab had a significant influence on the reliability of the temperature estimates, and, if yes,
(2) to determine how this influence manifested itself.

STUDY 2

The practice of either burying the portable slab or banking earth around it is desirable as the best way to simulate the heat dissipation conditions that the actual pavement is subject to. However, the practical inconveniences of this task are evident; therefore, study 2 checked the influence of this practice on the reliability of pavement temperature estimates. This study was the second to be undertaken and used data sets #1 and #2.

STUDY 3

Once the influence of the aggregate type had been determined in study 1, and the effect of banking earth around the slab had been determined in study 2, correlations between temperatures in the pavement and those in the portable were developed. This part of the study consisted of modeling pavement temperatures at a given depth, as shown in Eq 4.4.

$$T_{pvt} = f(D,T_{ps}) \tag{4.4}$$

where

T_{pvt} = pavement temperature,
D = depth, and
T_{ps} = portable slab temperature.

STUDY 4

This study consisted of calibrating models to estimate temperature gradients directly as follows:

$$\Delta T_{pvt} = f(\Delta D,\Delta T_{ps}) \tag{4.5}$$

where

ΔT_{pvt} = pavement temperature gradient or differential,
ΔD = depth differentials, and
ΔT_{ps} = portable slab temperature gradient or differential.

The advantage of obtaining temperature gradients directly from their own models is that error is smaller. Let the variance of any temperature estimate from a model calibrated in study 3 be:

$$V(T_{pvt}) = s^2 \tag{4.6}$$

where

$V(x)$ = variance of x,
T_{pvt} = pavement temperature estimate, and
s^2 = variance of the estimate.

The variance of a temperature gradient estimated by subtracting two point temperature estimates would be twice as large:

$$V(\Delta T_{pvt}) = V(T^{d1}{}_{pvt} - T^{d2}{}_{pvt}) = V(T^{d1}{}_{pvt}) + V(T^{d2}{}_{pvt}) = 2s^2 \tag{4.7}$$

where

$T^{d1}{}_{pvt}$ = temperature estimate at depth d1,
$T^{d2}{}_{pvt}$ = temperature estimate at depth d2, and
All other parameters as in Eqs 4.4, 4.5, and 4.6.

Assuming that the variances of estimates from models from studies 3 and 4 have the same magnitude, a direct estimate of the temperature gradient using a model calibrated exclusively for this purpose would have approximately half the variance of the gradient estimated by subtraction, as shown below:

$$V(\Delta T_{pvt}) = s^2 \tag{4.8}$$

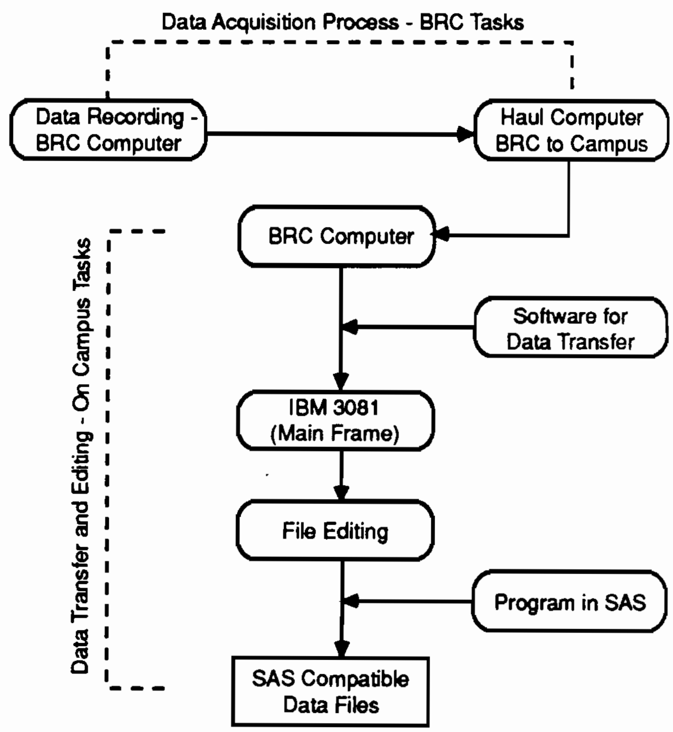

Fig 4.10. Steps for data storage.

All the predictive models in studies 3 and 4 were fitted using data set 4, the largest continuous data set available. Since the influence of weather conditions on heat dissipation in pavements has been widely recognized (Refs 4, 24, 25, 28, 31, and 38), studies 3 and 4 included testing of the models for conditions other than those prevalent for data set 4, which was taken during fairly cold but bright days. Thus, the models were tested with data sets 1 and 2, taken on warm fall days, and data set 3, which was taken exclusively on cloudy days.

STATISTICAL METHODS USED FOR THE ANALYSES

The most widely used procedures to answer the questions formulated above are analysis of variance (ANOVA) and least-squares fitting, both based on general linear model theories. ANOVA is used to test significance of effects of different factors on a given variable. Least-squares is used to fit models that predicted one variable as a function of others. Statistics of tests for both procedures are based on calculations of sums of squares from the samples, which are hypothesized as coming from normal populations with homogeneous variances. The advantages of these procedures include their flexibility and their capability to provide answers to several questions that may arise during data analysis. Unfortunately, though, these methods, for reasons explained below, are not quite appropriate for analysis of the temperature data, especially for testing significance of parameters.

The underlying assumptions of the linear regression by least-squares method are (Ref 39):

(1) for each specific value of the independent variable (X) there is a normal distribution of the dependent variable (Y) from which sample values are drawn at random;

(2) the normal distribution of Y corresponding to a specific value X has a mean $\mu_{Y,X}$, that lies on the population regression line;

(3) the normal distributions of Y for each specific X have the same variance; and

(4) the normal distributions of Y for each specific X are independent.

This mathematical model (Ref 39) can be concisely described by

$$Y = A + B(X - X_m) + e \qquad (4.9)$$

where

X_m = mean value of the independent variable;

$(X-X_m)$ = deviation from the sample mean;

e = error term, assumed to be a random variable drawn from a normal distribution of zero mean and variance s^2; and

A and B = regression parameters.

Comparing the nature of the temperature data with the assumptions above demonstrates that the assumptions are not valid. Assumption 1 seems to be the least problematic; the data acquisition system is always subject to some error that is expected to be randomly distributed around zero. Assumption 2 is difficult to check and is usually assumed. Failures in assumption 3 can sometimes be handled with transformations. Assumption 4, however, is the hardest one to accept in the case of autocorrelated data. In other words, a given temperature measurement may be considered normally distributed around zero, due to error in the data acquisition system; but, regardless of the measurement error, it can never be considered independent of the previous temperatures.

This indicates that the problem would be better tackled by time series analysis. Techniques for efficient time series analysis require the data to have a feature difficult to obtain in this experiment: a continuity, i.e., each data set should be collected without interruptions. Factors such as computer capacity, other experiments being conducted at the same test facility, and the already described data transfer procedure required the data acquisition system to be turned off at specific intervals, causing interruptions in the series. Therefore, data sets 1 and 2 consist of no more than five cycles. Data set 3 (cloudy days), by its own nature, had to have several interruptions and does not consist of a regular, equally spaced, time series. Data set 4 is the largest, but it was entirely collected in the winter, while the diagnostic survey will be conducted in the summer. This fact required further checking, which is described later in this chapter.

Since the observations are auto-correlated, it is also reasonable to expect their errors to be auto-regressive. The error seems to be better described by the following equation (Refs 10, 37, and 29):

$$n_t = e_t + a_1 n_{t-1} + a_2 n_{t-2} \dots + a_p n_{t-p} \qquad (4.10)$$

where

e_t is the error in the least squares model;

subscripts $_{t-1}$, $_{t-2}$, etc., are the particular times when the data was collected;

$a_1, \dots, a_p$, are auto-regressive parameters; and

n is the auto-regressive error.

Equation 4.10 is called an auto-regressive process of order p, meaning that any particular observation of the auto-regressive variable at a given instant t (n_t, in this case) is a function not only of some explicative variable at the same instant (e_t, in this case) but also of the previous values the referred variable assumed in the previous p instants.

One method of regression (Ref 37) that takes into account the auto-regressive error term is based on the Yule-

Walker equations (Refs 10, 13, 29, and 37). The underlying model is

$$y_t = \mathbf{B}\ x_t + n_t \qquad (4.11)$$

where

y_t = estimate of the dependent variable (at instant t),
x_t = vector of independent variables,
$\mathbf{B}$ = vector of regression parameters, and
n_t = error term, which is assumed to be generated by an auto-regressive process of order p (Eq 4.10).

The method starts by forming ordinary least-squares estimates of the regression parameters (vector **B**) and follows by alternating estimation of the regression parameters using generalized least-squares, with estimation of the parameters of the auto-regressive process ($a_1,..., a_p$) using the Yule-Walker equations applied to the sample auto-correlation function of the structural residuals (Ref 37):

$$\mathbf{r} = \mathbf{Y} - \mathbf{X}\ \mathbf{B} \qquad (4.12)$$

where

$\mathbf{Y}$ = vector of the dependent variable values,
$\mathbf{X}$ = vector of independent variables, and
$\mathbf{B}$ = vector of current estimates of the regression parameters.

This method is referred to by some authors as the two-step full-transform, and it appears to be as efficient as the maximum likelihood method (Ref 37). Furthermore, it is the least demanding in terms of computer time. It was, thus, tentatively applied to one case; since it gave excellent results, it was chosen for data analysis in studies 1 and 2. Direct application of a model with auto-regressive errors, however, has one important drawback that renders its results almost useless for calibrating a predictive model. The estimates of the error term are part of the auto-regressive model, i.e., the predicted values are calculated as a function of the residuals of the previous estimates. This is not a problem for studies intended to investigate only the behavior of certain data. However, such a model cannot be used to predict values of the dependent variable, because no history of residuals is available to compute the auto-regressive part of the model. Once more this reflects the basic problem of estimating auto-correlated data, already stated in the first part of this chapter: a good temperature estimate at instant t requires good temperature estimates at previous instants. The strategy chosen to get around this problem and arrive at a usable practical model starts with the basic assumption that the pavement temperature at instant t=0 can be explained by a linear combination of the portable slab temperature at the same instant and at instants t-1, t-2, etc., and of the effect of some non-auto-regressive regression covariable. The model is written

$$Tpvt_t = a + \sum_{1=0}^{p} b_i Tps_{t-i} + cD + v_t \qquad (4.13)$$

where

$Tpvt_t$ = pavement temperature at instant t,
a, b, and c = regression coefficients,
Tps_{t-i} = portable slab temperature at instant t-i,
D = depth within pavement,
n_t = error term, possibly auto-regressive of degree n, and
p = number of lags.

The regression coefficients of the lags of the dependent variable are assumed to be a polynomial of the form

$$b_i = \sum_{k=0}^{d} a_k i^k \qquad (4.14)$$

where

b_i = as in Eq 4.13,
a_k = coefficient of the polynomial, and
i = 0, 1, 2, ..., p.

The reasons underlying the choice of this model can be better understood by inspecting the plots of raw data, shown in appendix A and sampled in Figures 4.2, 4.3, 4.4, and 4.5. These plots indicate that there is a better agreement between temperatures in the heating-up phase of the cycle than in the cooling-down phase. This means that coefficients of the explicative variables are not constant but vary with the phase of the cycle. The simplest way to express this fact is by fitting a model in which the coefficients of the lagged independent variable are a linear function of the number of lags, as depicted in Eq 4.14.

PRESENTATION OF RESULTS AND CONCLUSIONS

STUDY 1. INVESTIGATION OF THE INFLUENCE OF AGGREGATE TYPE ON PAVEMENT TEMPERATURE ESTIMATES

As stated previously, the objective of study 1 was to verify whether or not the aggregate type has a significant influence on pavement temperature estimates. This study was the first to be performed, so data set number 1 was used. Inspection of the raw data already suggests that there is some difference between temperatures for different aggregate types and that it tends to manifest itself more intensely in the heating-up phase than in the cooling-down one. However, achieving more consistent conclusions requires statistical analysis of the data.

Analysis of variance (ANOVA) is the statistical method most widely used for answering questions such as the one being investigated in this study. However, temperature data do not meet the ANOVA underlying assumptions. F-values would be biased and the significant test would be meaningless. Therefore, auto-regressive models of the second order, to predict the temperatures in the river gravel portable slabs as a function of those in the limestone slabs, were calibrated with the two-step full-transform method for each thermocouple location in each pair of slabs. Nine models were thus obtained. The influence of the aggregate types on the pavement temperatures was considered non-significant if the fitted models had zero intercept, 45° slope, and negligible auto-regressive coefficients. Table 4.3 summarizes the results of the nine models. Figures 4.11 to 4.19 show the plots of the raw data for each thermocouple location in each pair of slabs. Figures 4.20 to 4.28 depict outputs of the auto-regressive models. In these figures, part a shows the plots of predicted versus observed values, part b, the residuals from the structural part, and part c, the total residuals. In order to emphasize the auto-correlation features of the data, both types of residuals were plotted against time.

The results show that the fits are extremely good for the auto-regressive model. The lack-of-fit of the structural part of the model, which is fitted by the least-squares method (Ref 37), can be seen in the cyclical residual plots depicted in part b of Figures 4.20 to 4.28. In all cases, the slopes remained within a narrow interval around one: the smallest slope is 0.87, whereas the largest is 1.04. This means that the rate of temperature change in both types of slabs is not very different. The intercepts were non-significant in three cases and, in cases where they were significant, the largest value was 9.21, whereas the smallest was 3.60. In all cases, the R^2 value was greater than 99 percent. These results indicate that the effect of aggregate type on temperature cannot be considered negligible. In addition, it seems that the river gravel slab tends to respond more intensely than the limestone to temperature changes. It is concluded that, ideally, the aggregate types of the portable slab and the pavement should match; however, since the difference is primarily due to some additive constant, calibration of separate models for the two aggregate types should yield satisfactory results.

STUDY 2. EFFECT OF BURYING THE SLABS ON PAVEMENT TEMPERATURES – RESULTS AND CONCLUSIONS

As stated previously, the objective of this study was to determine whether or not the reliability of the temperature estimates decreases when the sides of the portable slab are left in contact with air. Evidently, a relatively small slab simply resting on the ground cannot represent a pavement as well as another that has been buried and is subject to approximately the same heat dissipation conditions as the pavement. Consequently, the practice of banking earth around the slab seems advisable for better temperature estimates. However, a realistic look at the field work conditions, especially in a network level survey, reveals the practical difficulties associated with this practice. Digging on the side of the road requires special equipment whose presence can be more disruptive to traffic than the survey itself; digging is necessary to bank earth around the slab as well as to bury it. The time required to do and then undo this is very likely to be equal to or greater than that required to survey the test section. A pilot study to compare both situations is thus very useful, because if the study shows that temperature estimates with data taken at a portable slab simply sitting on the ground are unreliable, it can be concluded that this method of estimating pavement temperature is unfeasible for a network level survey.

Study 1 indicated that coarse aggregate type influences the pavement temperature. In addition, it is evident

TABLE 4.3. SUMMARY OF RESULTS FROM STUDY 1

TC Position	Thickness (in.)	Intercept Value	Intercept Standard Error	Intercept Probability of Par = 0	Slope Value	Slope Standard Error	Slope Probability of Par = 0	R^2	Autoregression Coefficient Lag 1	Autoregression Coefficient Lag 2
Top	6	8.76	1.302	0.0001	0.873	0.0168	0.0001	99.87	-1.26	0.36
Top	10	-3.92	1.419	0.0063	1.04	0.019	0.0001	99.77	-1.16	0.34
Top	14	7.90	0.838	0.0001	0.88	0.011	0.0001	99.97	-1.39	0.46
Middle	6	8.23	0.88	0.0001	0.88	0.0113	0.0001	99.98	-1.41	0.45
Middle	10	1.51	0.88	**0.0891**	0.96	0.012	0.0001	99.97	-1.29	0.33
Middle	14	5.31	0.559	0.0001	0.92	0.007	0.0001	99.88	-1.08	0.10
Bottom	6	9.21	0.712	0.0001	0.87	0.009	0.0001	99.98	-1.28	0.30
Bottom	10	3.60	0.903	0.0001	0.93	0.012	0.0001	99.96	-1.28	0.30
Bottom	14	-0.271	0.634	**0.6691**	0.994	0.009	0.0001	99.96	-0.66	-0.32

Bold numbers indicate non-significance.

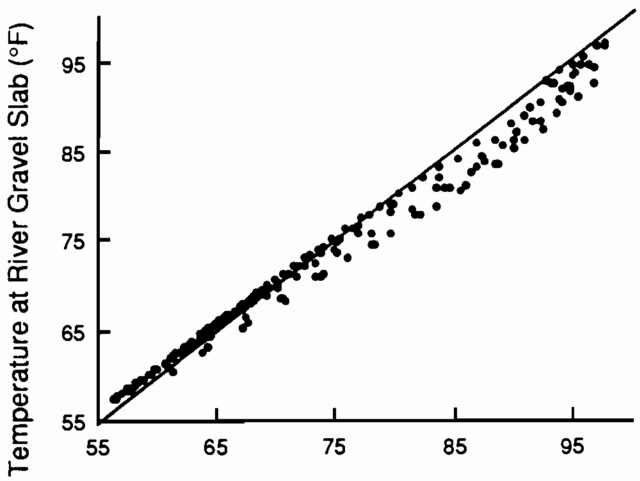

Fig 4.11. Temperatures at top thermocouples for 6-inch portable slabs.

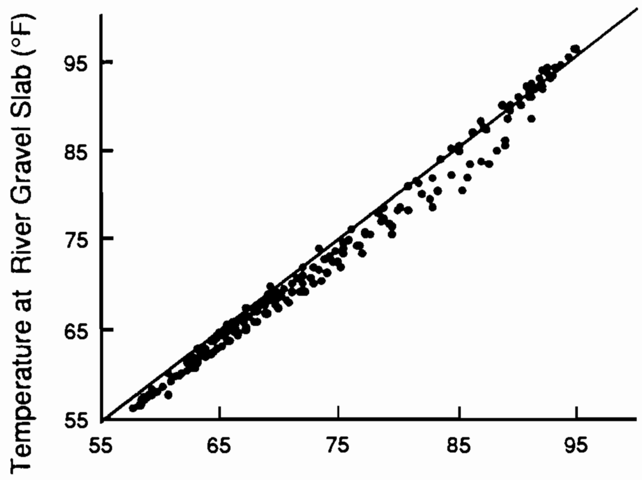

Fig 4.14. Temperatures at top thermocouples, 10-inch portable slabs.

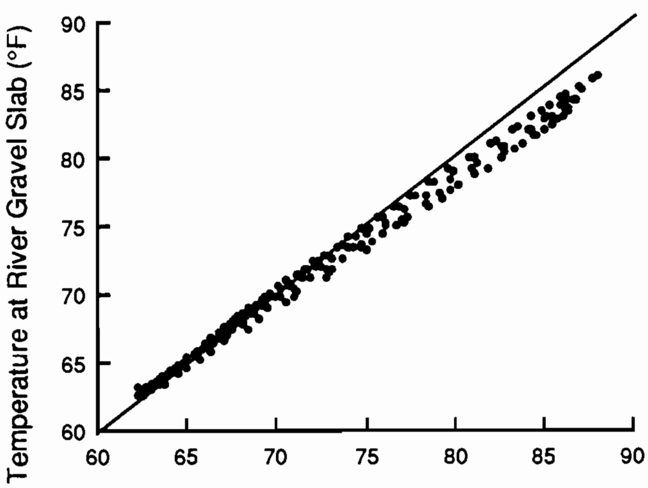

Fig 4.12. Temperatures at mid-depth thermocouples for 6-inch portable slabs.

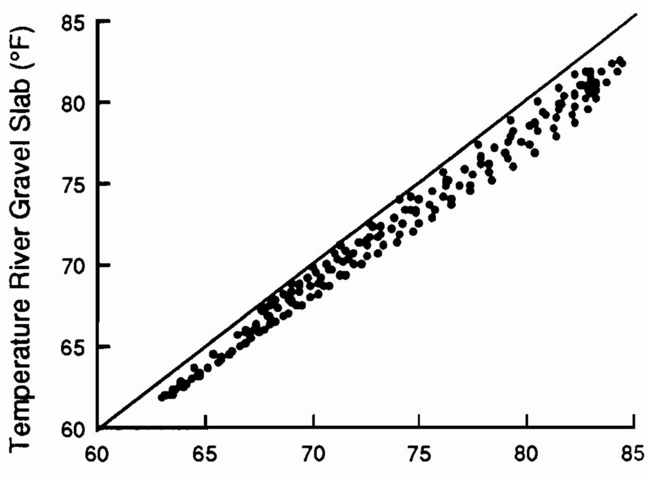

Fig 4.15. Temperatures at mid-depth thermocouples, 10-inch portable slabs.

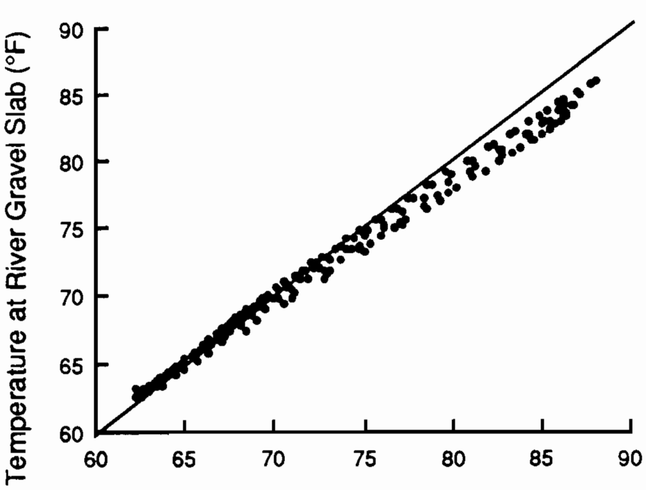

Fig 4.13. Temperatures at bottom thermocouples for 6-inch portable slabs.

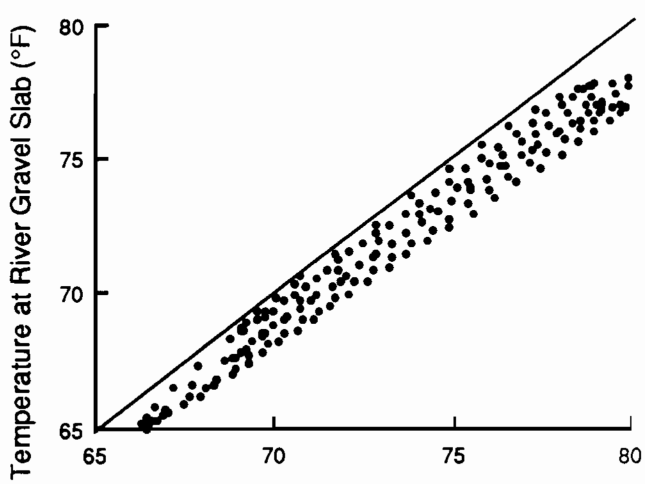

Fig 4.16. Temperatures at bottom thermocouples, 10-inch portable slabs.

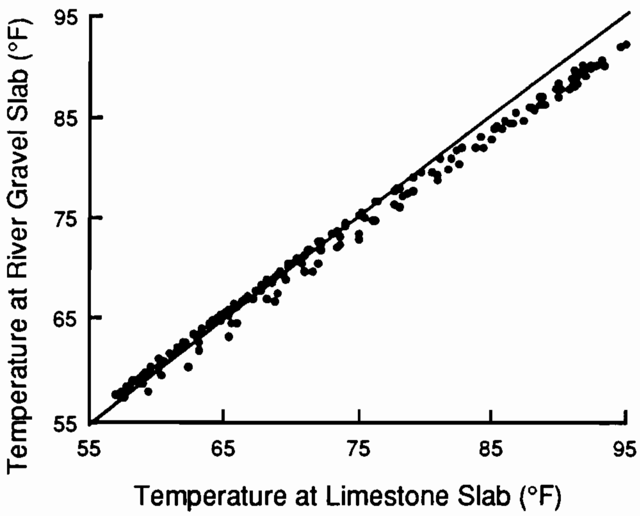

Fig 4.17. Temperatures at top thermocouples, 14-inch portable slabs.

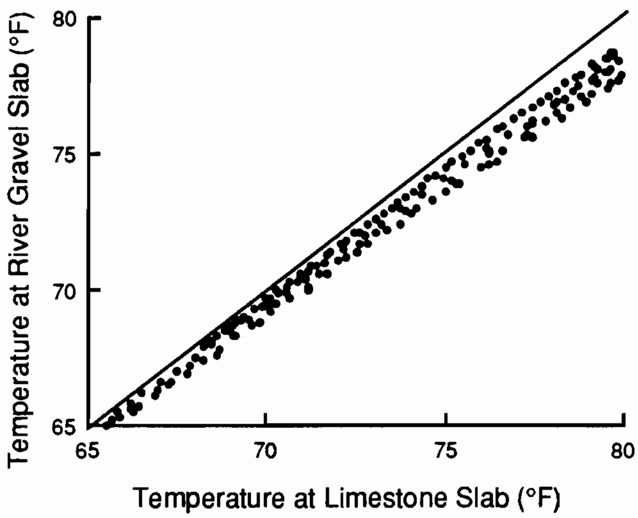

Fig 4.18. Temperatures at mid-depth thermocouples, 14-inch portable slabs.

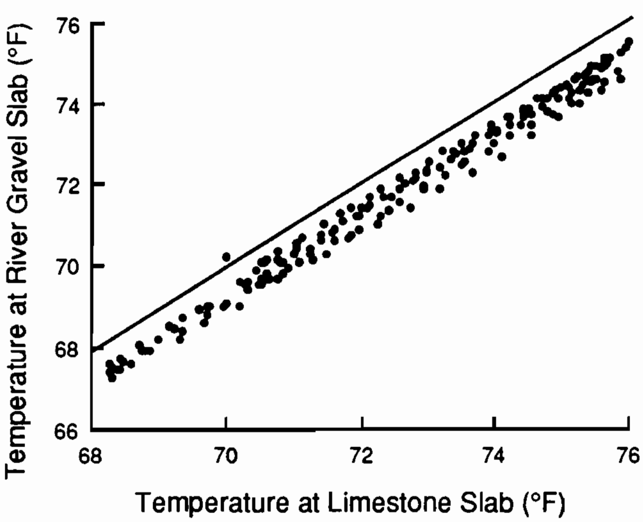

Fig 4.19. Temperatures at bottom thermocouples, 14-inch portable slabs.

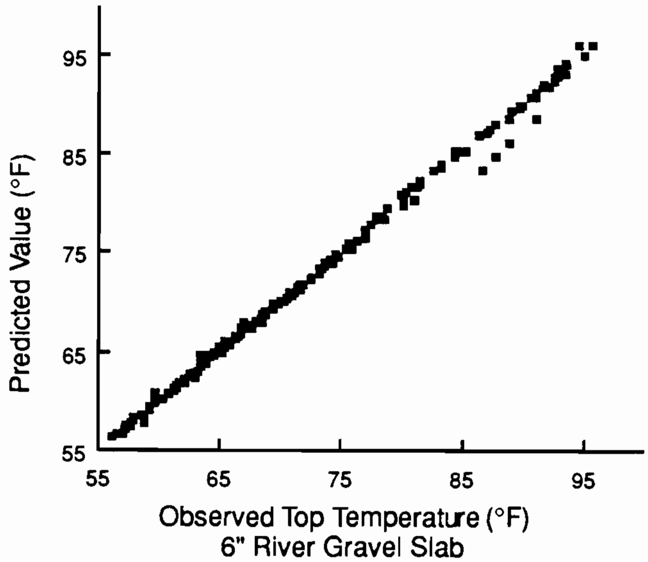

(a) Predicted versus observed values.

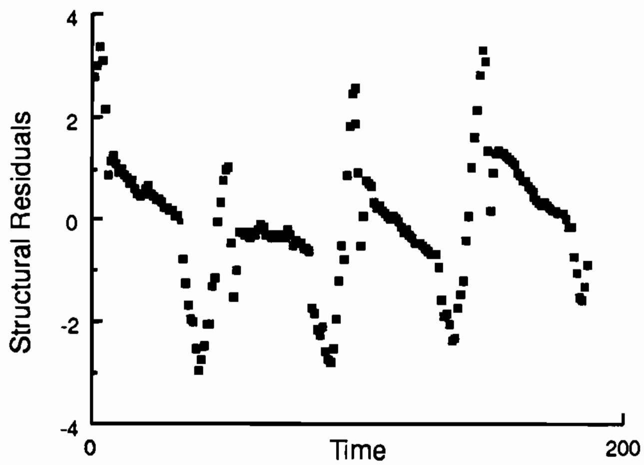

(b) Structural residuals versus time.

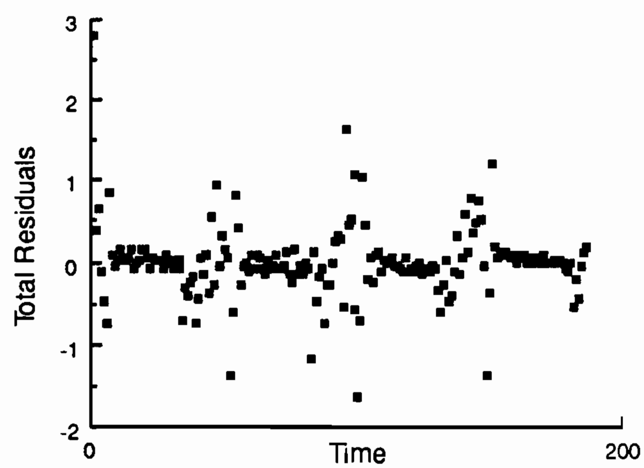

(c) Total residuals versus time.

Fig 4.20. Results of model for top temperatures, 6-inch-thick portable slabs.

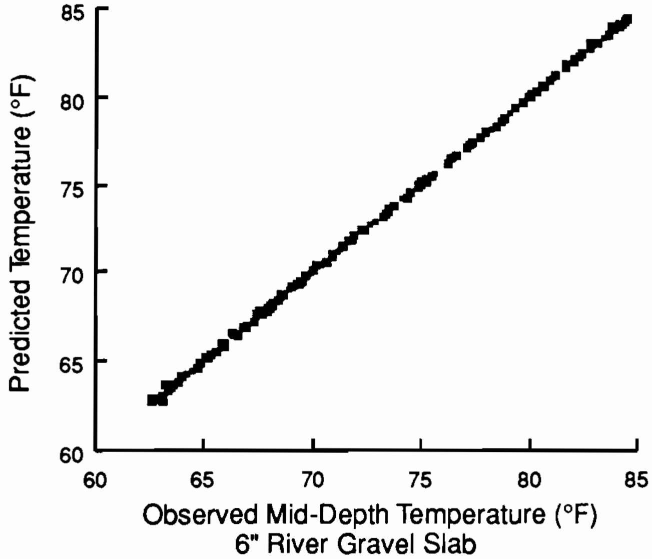

(a) Predicted versus observed values.

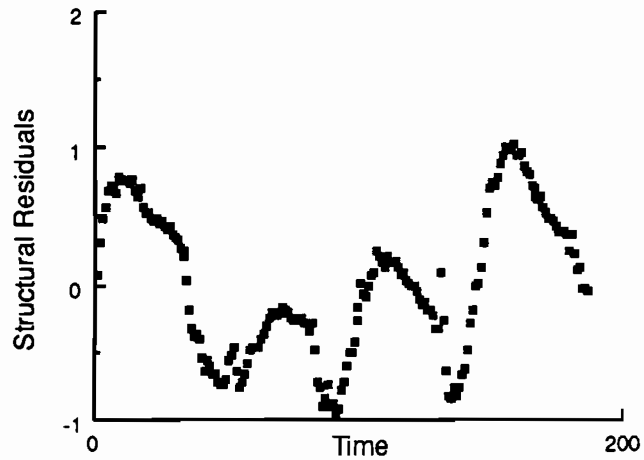

(b) Structural residuals versus time.

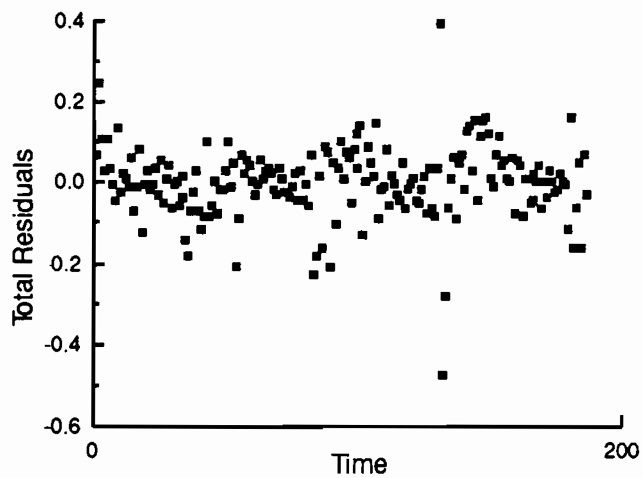

(c) Total residuals versus time.

Fig 4.21. Results of model for mid-depth temperatures, 6-inch-thick portable slabs.

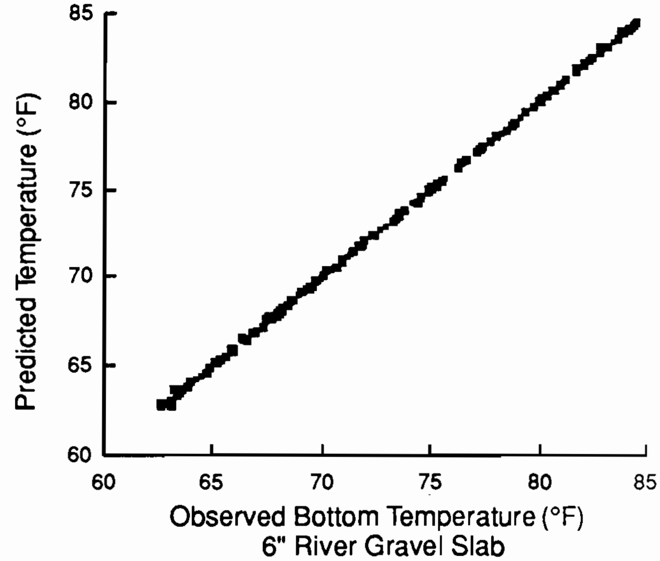

(a) Predicted versus observed values.

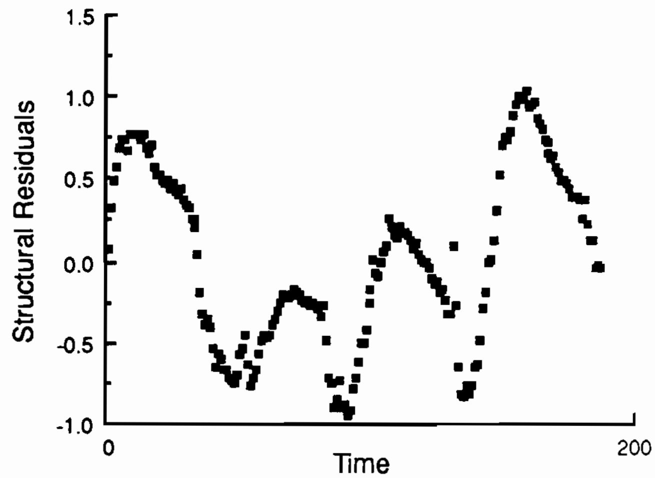

(b) Structural residuals versus time.

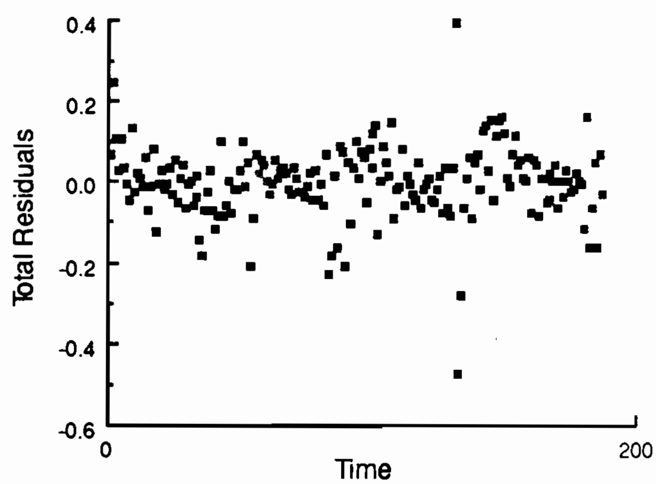

(c) Total residuals versus time.

Fig 4.22. Results of model for bottom temperatures, 6-inch-thick portable slabs.

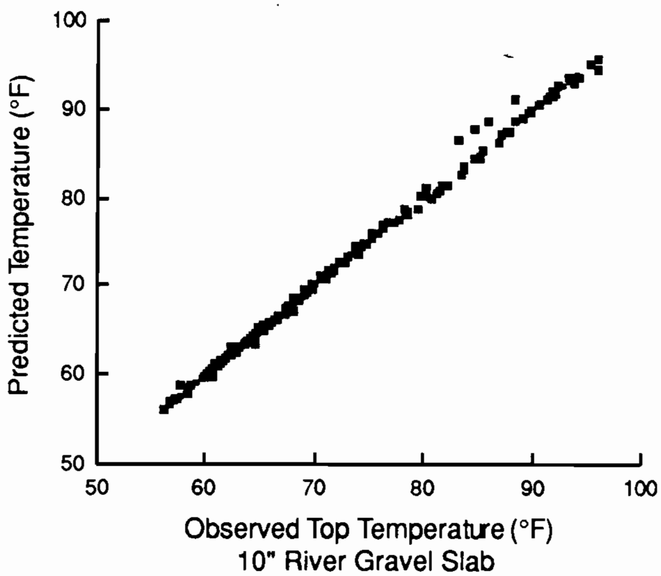

(a) Predicted versus observed values.

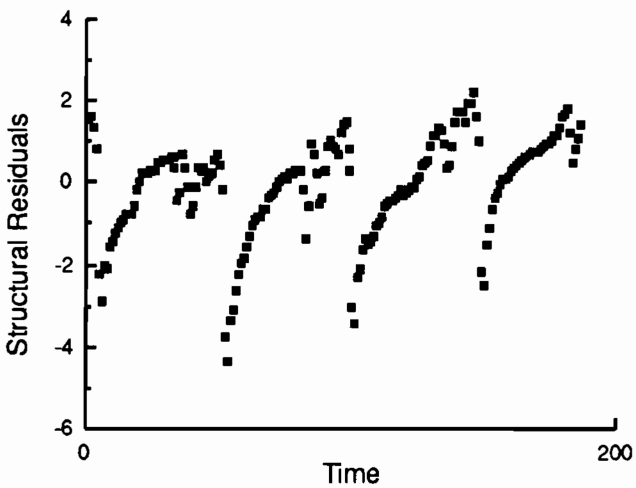

(b) Structural residuals versus time.

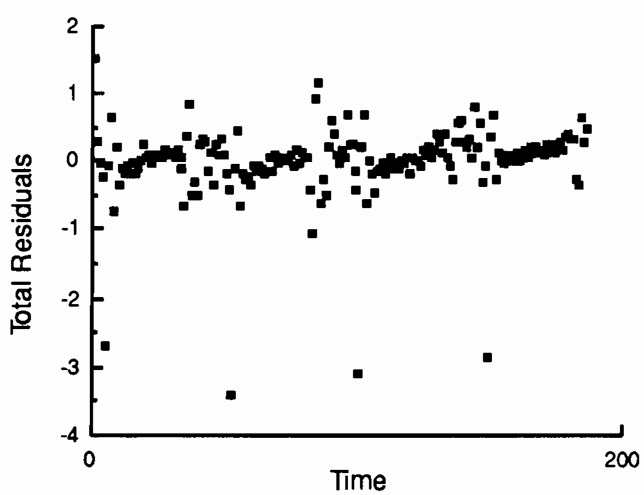

(c) Total residuals versus time.

Fig 4.23. Results of model for top temperatures, 10-inch-thick portable slabs.

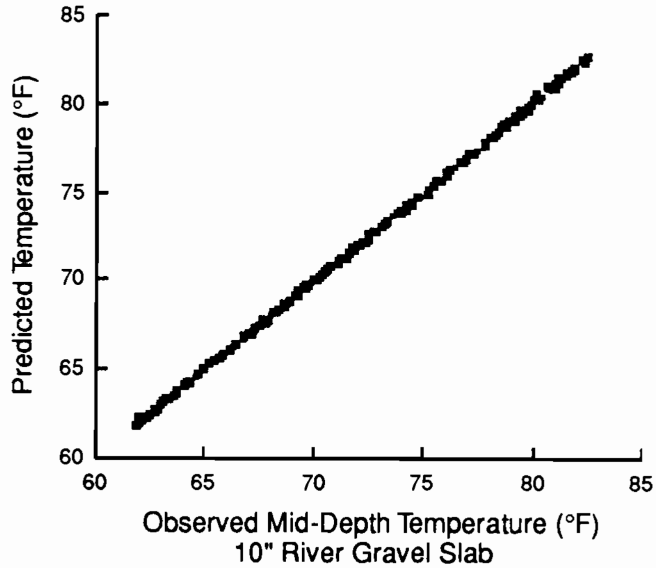

(a) Predicted versus observed values.

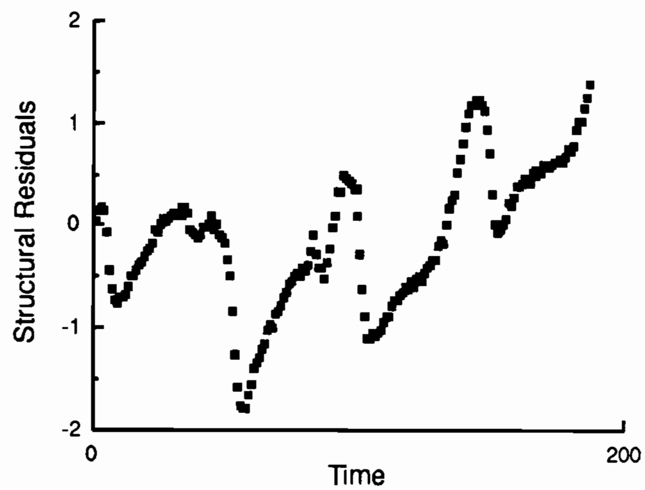

(b) Structural residuals versus time.

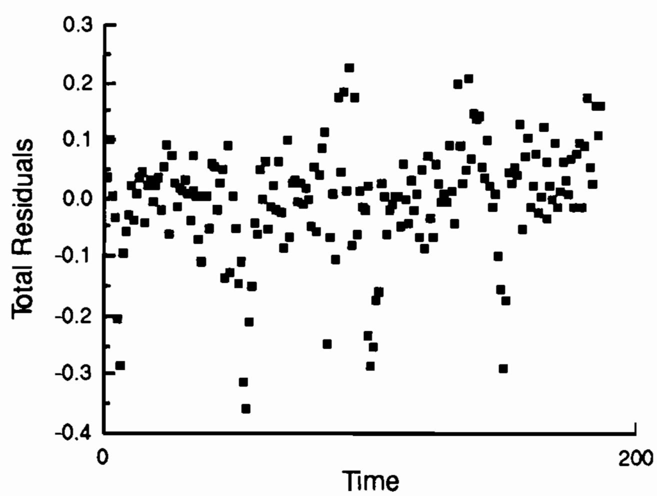

(c) Total residuals versus time.

Fig 4.24. Results of model for mid-depth temperatures, 10-inch-thick portable slabs.

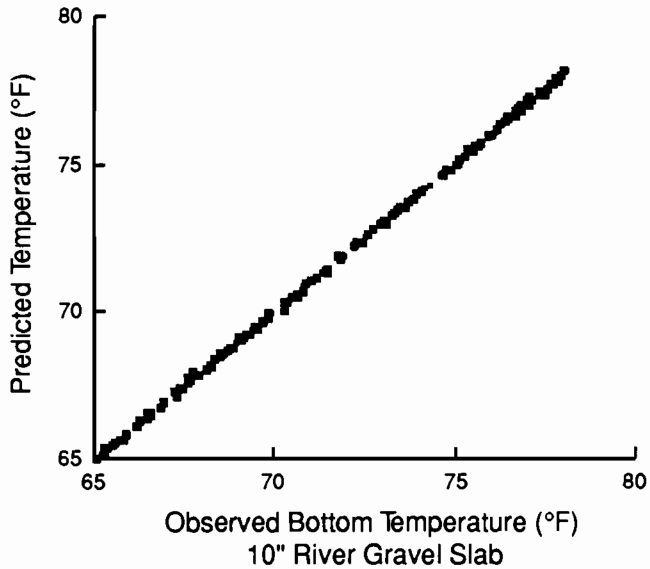

(a) Predicted versus observed values.

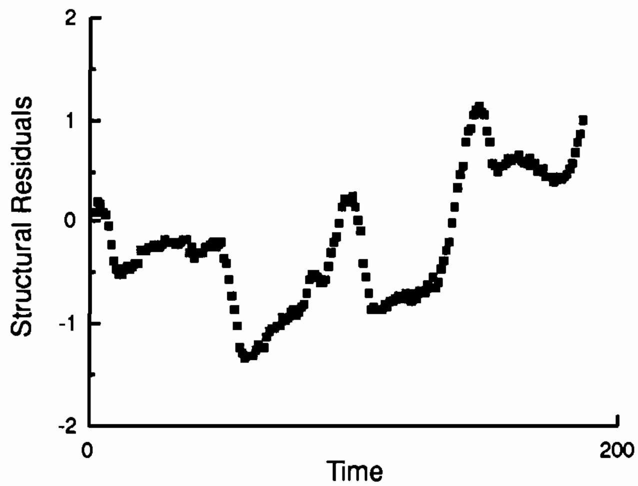

(b) Structural residuals versus time.

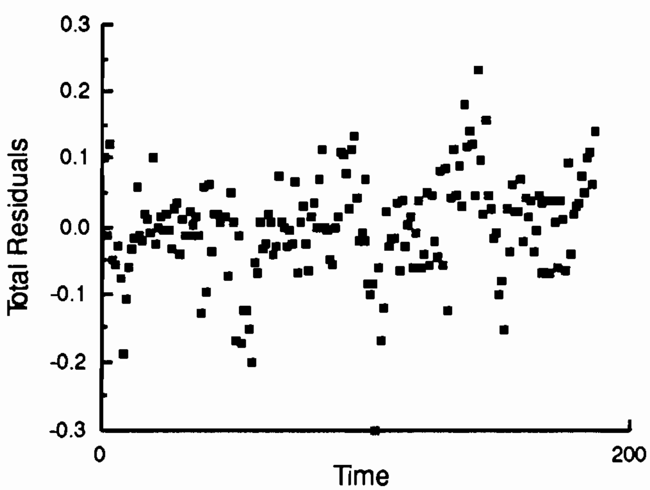

(c) Total residuals versus time.

Fig 4.25. Results of model for bottom temperatures, 10-inch-thick portable slabs.

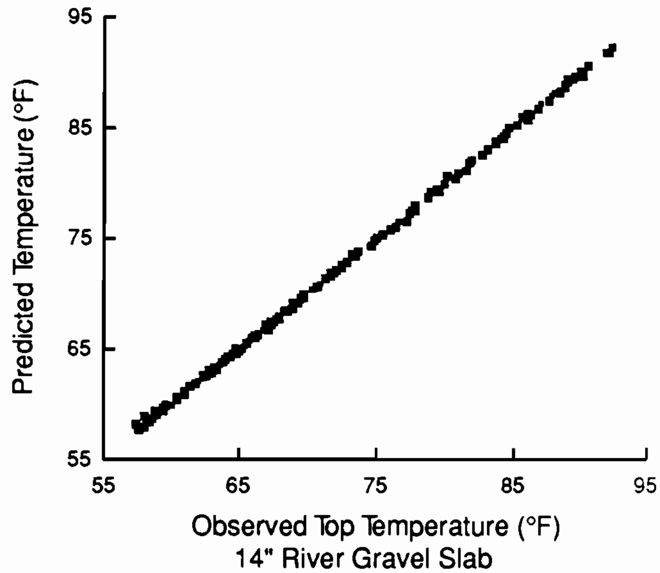

(a) Predicted versus observed values.

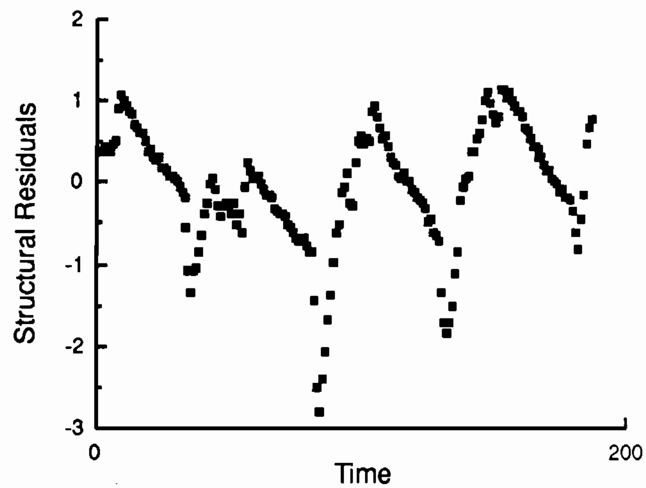

(b) Structural residuals versus time.

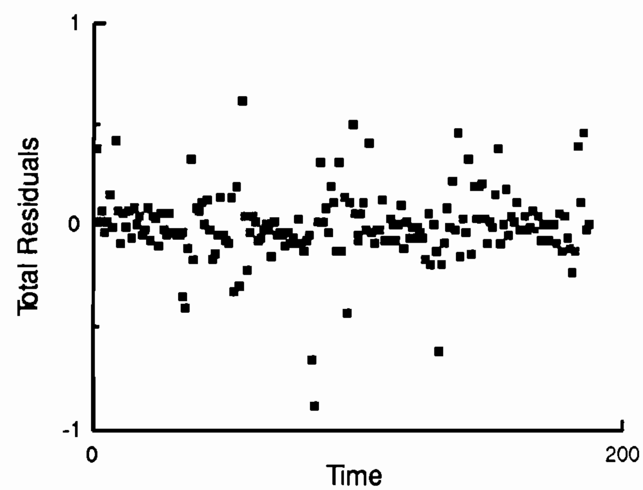

(c) Total residuals versus time.

Fig 4.26. Results of model for top temperatures, 14-inch-thick portable slabs.

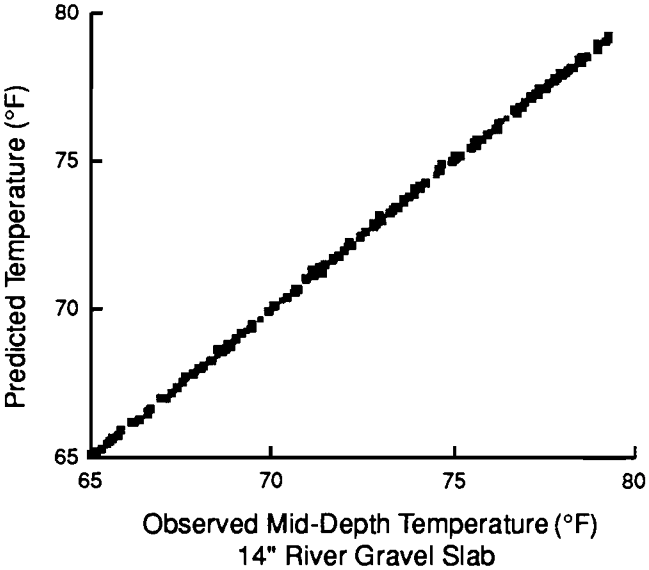

(a) Predicted versus observed values.

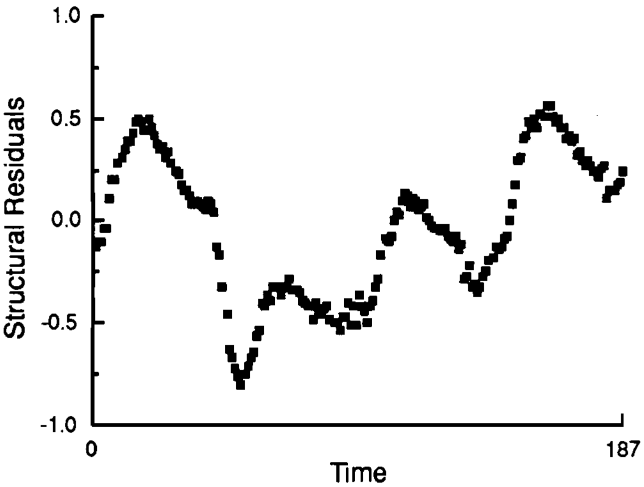

(b) Structural residuals versus time.

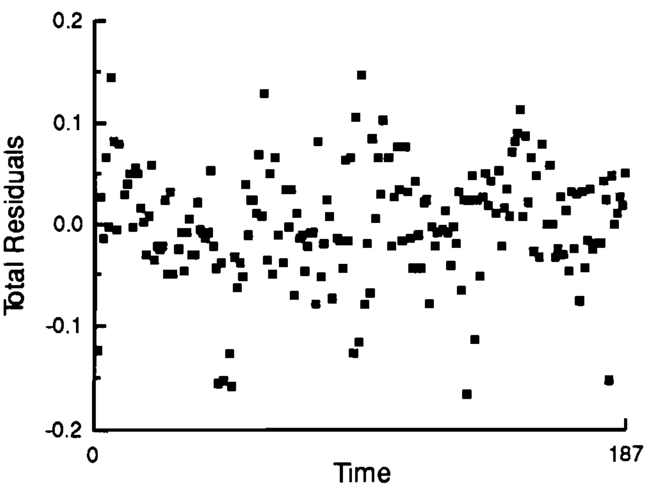

(c) Total residuals versus time.

Fig 4.27. Results of model for mid-depth temperatures, 14-inch-thick portable slabs.

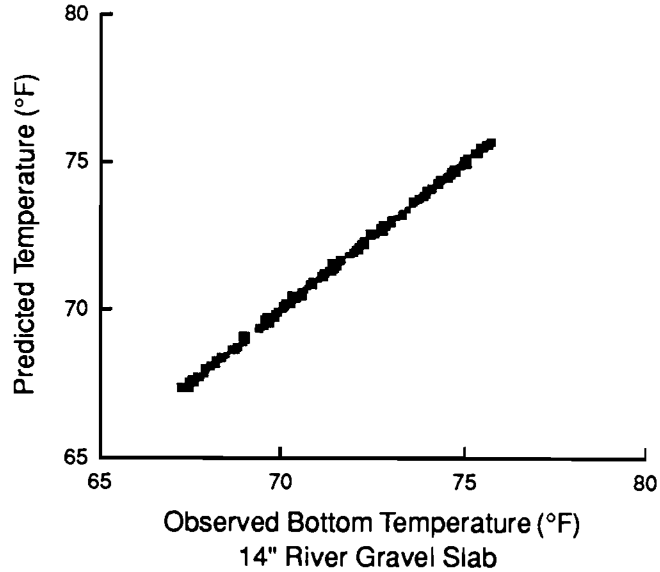

(a) Predicted versus observed values.

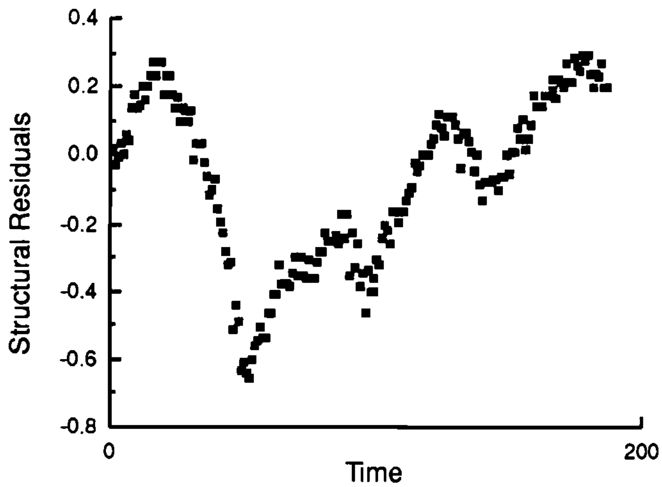

(b) Structural residuals versus time.

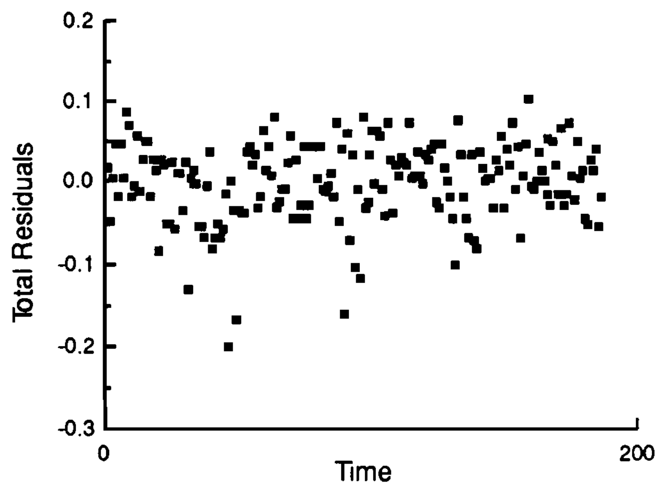

(c) Total residuals versus time.

Fig 4.28. Results of model for bottom temperatures, 14-inch-thick portable slabs.

that slab thickness will have some influence on the temperatures as well. In order to isolate the objective of this study, only the data taken from the 10-inch-thick limestone slab were used. If the pavement temperature data were not auto-regressive, a factorial experiment that would allow simultaneous investigation of the influences of all the interest factors and their interactions could have been designed. However, as discussed before, significance levels of the ANOVA would be biased and yield misleading conclusions. Therefore, the two-step full-transform method was applied in this study. The approach here was the same as that used in study 1: compare the results of auto-regressive models calibrated using both conditions—unburied and buried. These conditions are represented by data sets 1 and 2, respectively. Three models were calibrated for each data set to predict pavement temperatures as a function of those in the 10-inch limestone slab, for the top, mid-depth, and bottom thermocouple positions. Table 4.4 and Figures 4.29 to 4.34 depict the results of these models. In these figures, part a shows the raw data, part b, the plots of predicted versus observed values, and part c, the residuals versus time.

The results indicate that the corresponding models for the two data sets are different but equally reliable. The models calibrated using data set 1 (unburied slabs) presented higher values for slopes and smaller values for intercepts. Since both data sets 1 and 2 were taken on fairly hot days, those results are actually showing that unburied slabs, albeit insulated, are more susceptible than buried ones to temperature changes. The data calibrated for buried slabs has smaller intercepts, and none of the slopes is very different from one. In addition, the auto-regressive coefficients are fairly small. As already expected, these results indicate better agreement of pavement temperatures to those in the buried slabs than with those in the unburied ones. The quality of fit of models for data sets 1 and 2, however, is not very different. All R^2 are greater than 99 percent, and neither the residual plots nor the predicted versus observed plots present significant improvement when changing from models calibrated with data set 1 to those with data set 2. The conclusion is that, although the ideal situation would be to bury the slabs at the test site, the infeasibility of this service does not have a significant effect on the reliability of the models. It is thus concluded that the portable slabs can be used in the network-level diagnostic survey.

STUDY 3. CALIBRATION AND TESTING OF MODELS TO ESTIMATE PAVEMENT TEMPERATURES AT A GIVEN DEPTH

In this study, models to estimate pavement temperature at a desired depth were fit to the available data and then tested using the other data sets. The description of this study is divided into two parts:

Part 1 – Calibration of the models

Part 2 – Testing of the models obtained in Part 1

As discussed before, because the temperature data are auto-regressive, the ordinary least-squares technique may give biased results for the fitted models. Consequently, the auto-regressive least-squares method with lagged temperatures as explicative variables was used in order to account for the fact that pavement temperature in a given instant can be better explained by portable slab temperature history than by only its temperature at the same instant. The general format of the models was depicted in Eqs 4.13 and 4.14. As explained in the item pertaining to the data acquisition system, the temperatures were recorded every half-hour. This fact limited the number of lags in the model to three, because it would be unrealistic to expect field temperature measurements to require more than two hours per test section. The model is thus

$$Tpvt_t = a + \sum_{i=0}^{3} b_i \, Tps_{t-i} + cD + v_i \qquad (4.15)$$

where all parameters are as in Eq 4.13, and a second-degree polynomial was fit to the coefficients b_i (Eq 4.14).

Limestone is the coarse aggregate type for 50 percent of the CRCP test sections of the subject project. Therefore, a model to estimate temperatures in a limestone pavement from those in a limestone block can be used in 50 percent of the cases. As for the remaining

TABLE 4.4. SUMMARY OF RESULTS FROM STUDY 2

TC Position	Data Set	Intercept Value	Intercept Standard Error	Intercept Probability of Par = 0	Slope Value	Slope Standard Error	Slope Probability of Par = 0	R^2	Autoregression Coefficient Lag 1	Autoregression Coefficient Lag 2
Top	1	17.64	1.54	0.0001	0.78	0.02	0.0001	99.8	-1.21	0.29
Top	2	5.85	1.41	0.0001	0.95	0.02	0.0001	99.7	-0.82	-0.10
Middle	1	21.24	1.02	0.0001	0.73	0.01	0.0001	99.9	-1.40	0.44
Middle	2	12.06	1.02	0.0001	0.86	0.02	0.0001	99.9	-1.44	0.47
Bottom	1	16.24	1.14	0.0001	0.81	0.02	0.0001	99.9	-1.26	0.03
Bottom	2	10.92	1.71	0.0001	0.88	0.03	0.0001	99.9	-1.22	0.25

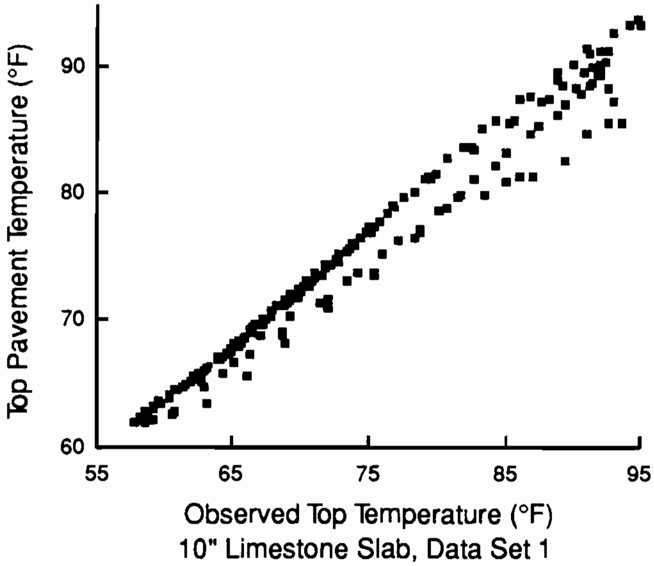

(a) **Pavement versus portable slab temperatures.**

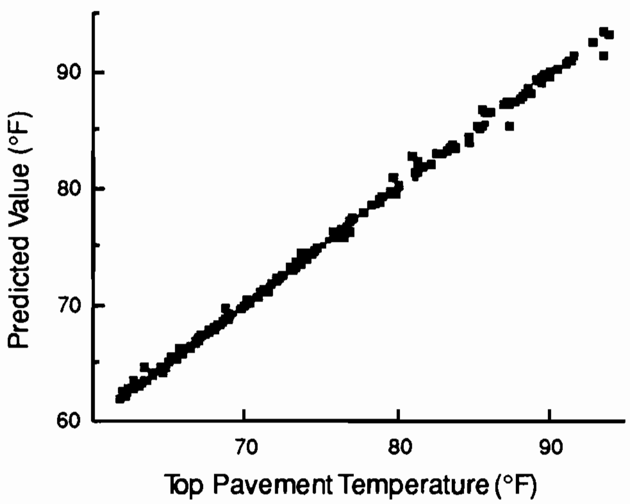

(b) **Predicted versus observed values.**

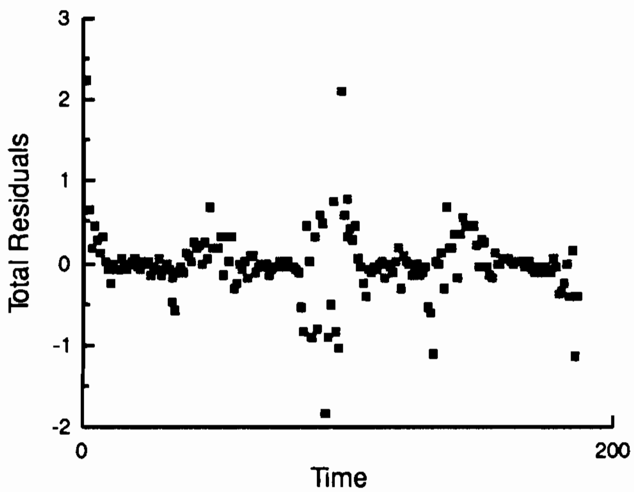

(c) **Residuals versus time.**

Fig 4.29. Results of auto-regressive model for top temperatures, data set 1.

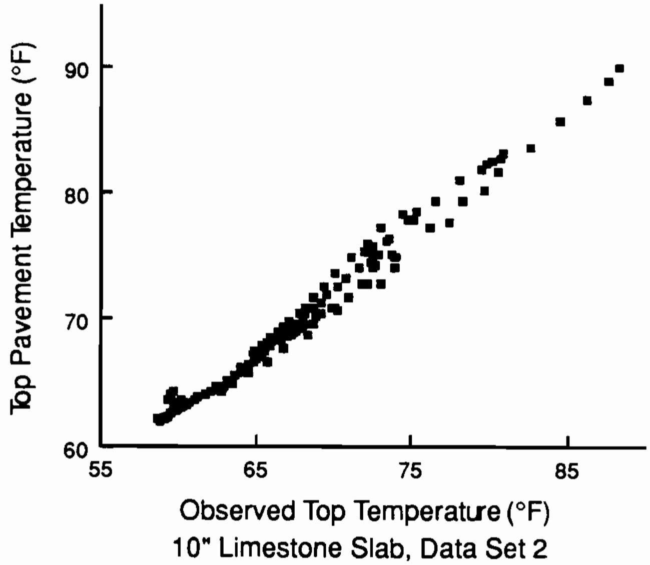

(a) **Pavement versus portable slab temperatures.**

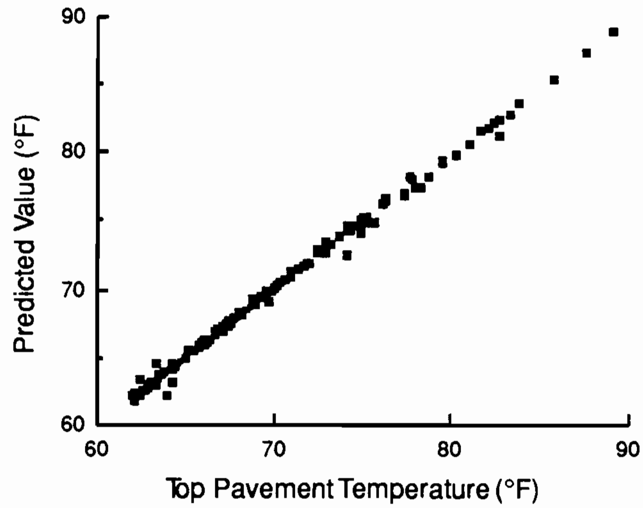

(b) **Predicted versus observed values.**

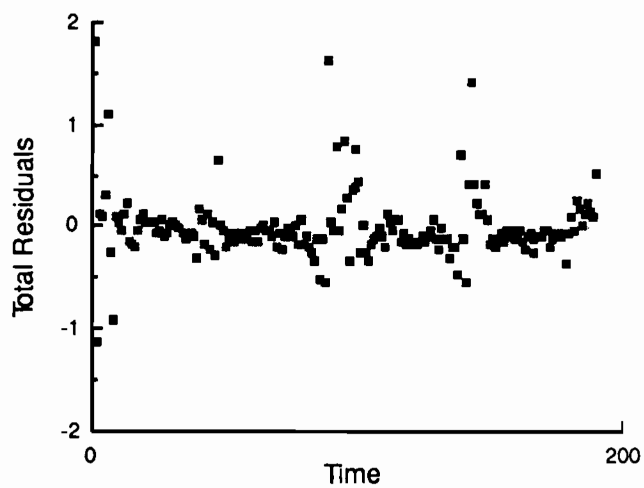

(c) **Residuals versus time.**

Fig 4.30. Results of auto-regressive model for top temperatures, data set 2.

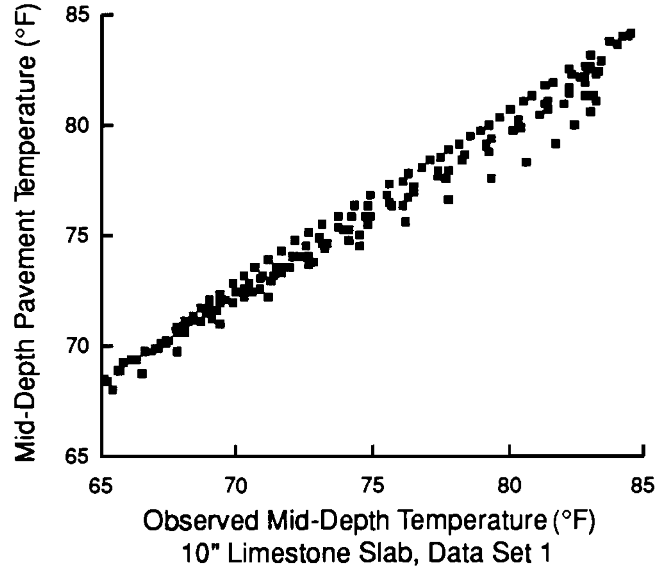

(a) Pavement versus portable slab temperatures.

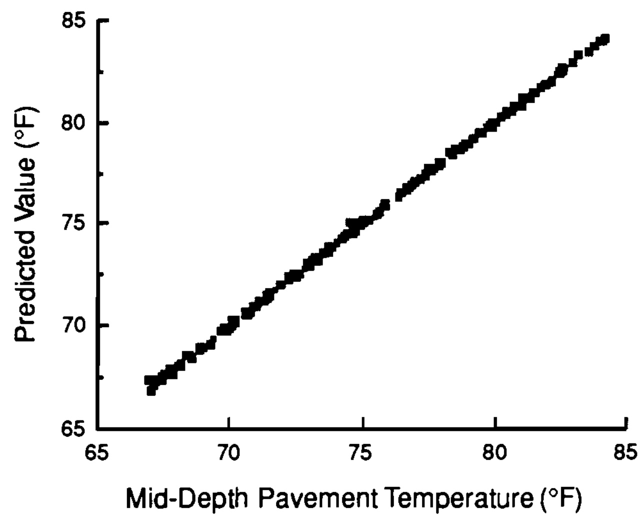

(b) Predicted versus observed values.

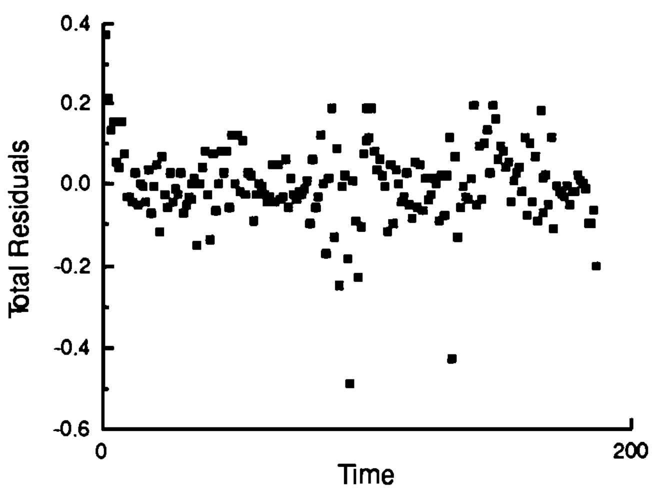

(c) Residuals versus time.

Fig 4.31. Results of auto-regressive model for mid-depth temperatures, data set 1.

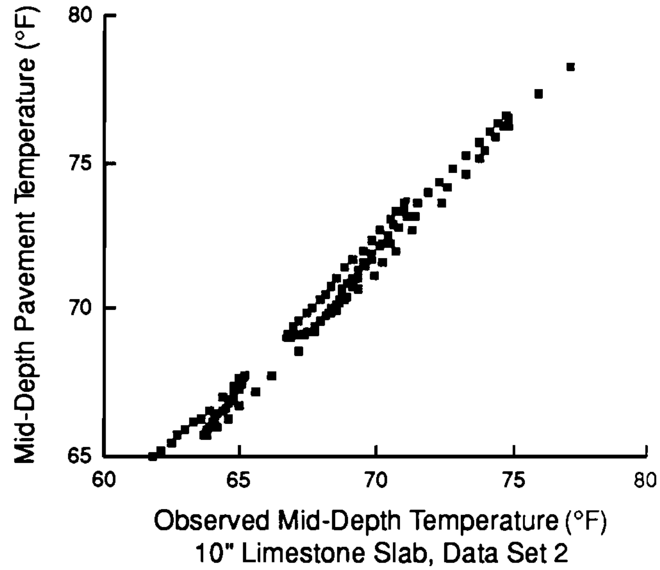

(a) Pavement versus portable slab temperatures.

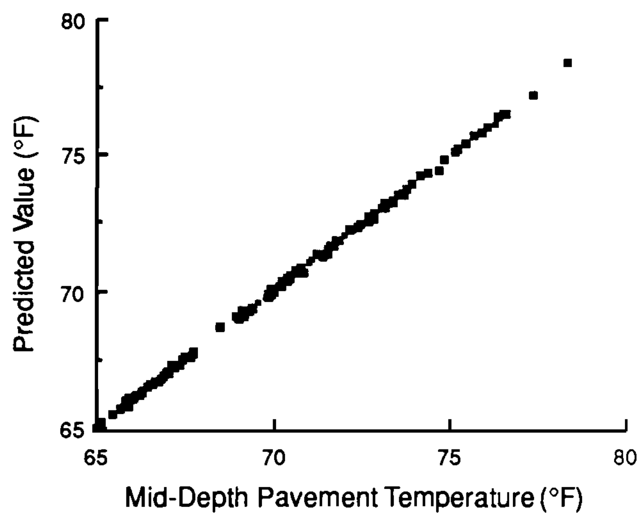

(b) Predicted versus observed values.

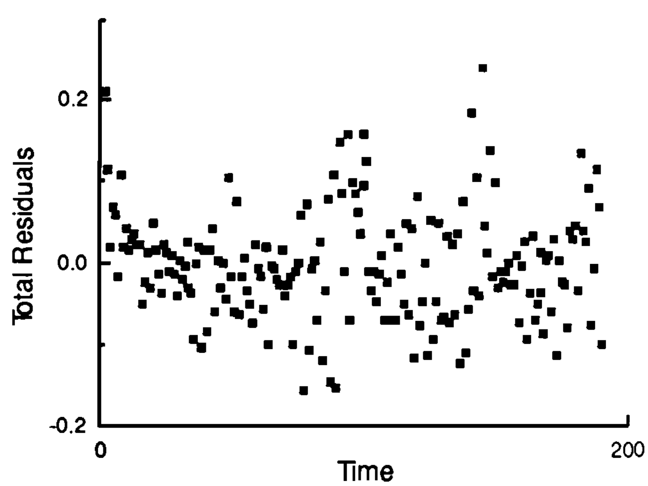

(c) Residuals versus time.

Fig 4.32. Results of auto-regressive model for mid-depth temperatures, data set 2.

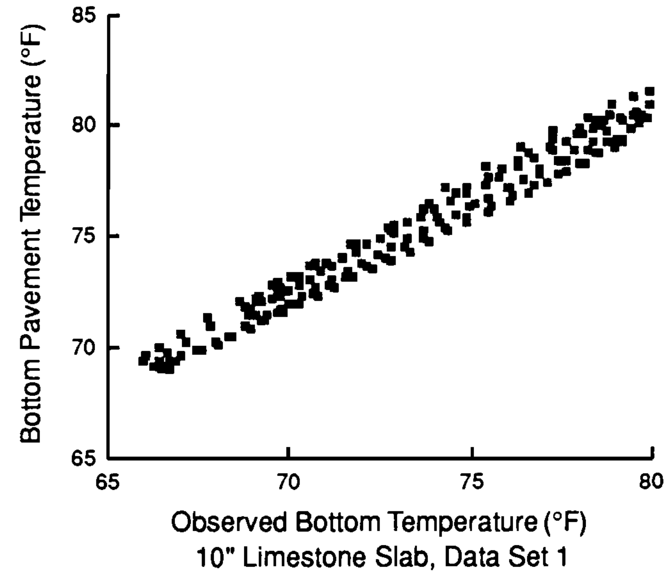

(a) Pavement versus portable slab temperatures.

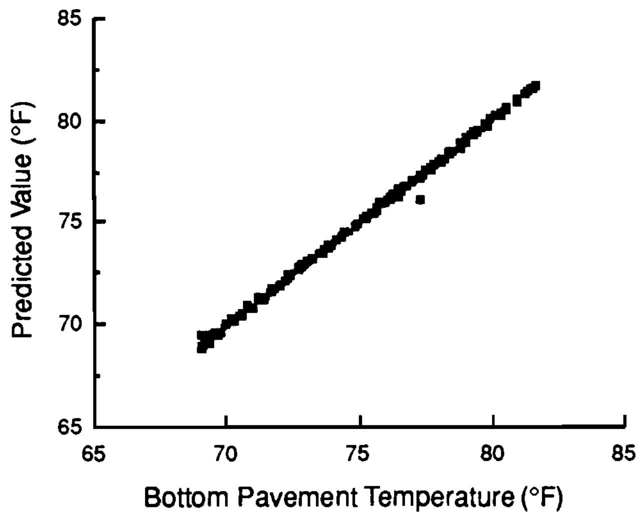

(b) Predicted versus observed values.

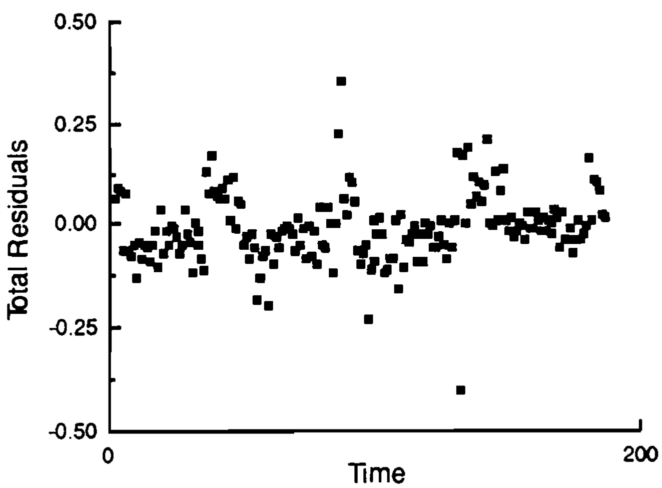

(c) Residuals versus time.

Fig 4.33. Results of auto-regressive model for bottom temperatures, data set 1.

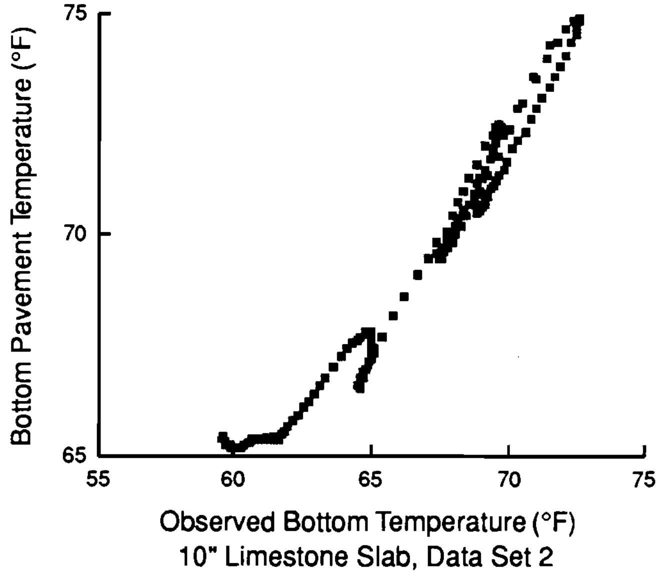

(a) Pavement versus portable slab temperatures.

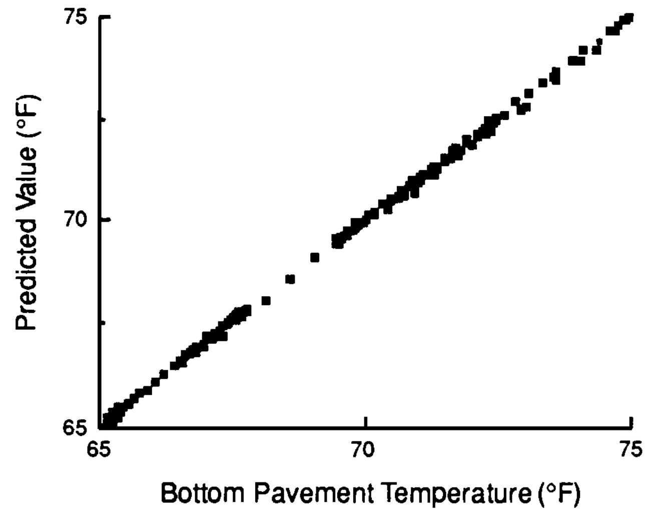

(b) Predicted versus observed values.

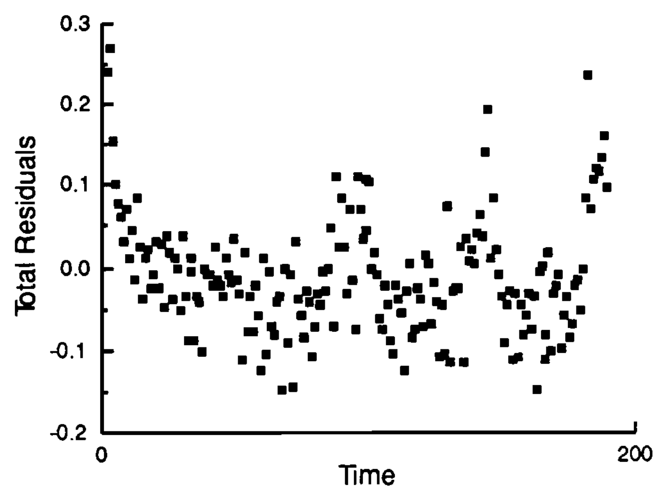

(c) Residuals versus time.

Fig 4.34. Results of auto-regressive model for bottom temperatures, data set 2.

test sections, 60 percent of them have silicious river gravel as aggregate type. Assuming that the field crews take only one block to the field, the following types of temperature models are needed for 80 percent of the test sections:

Situation 1 – A model to estimate limestone pavement temperatures as a function of depth and limestone block temperatures.

Situation 2 – A model to estimate river gravel pavement temperatures as a function of depth and limestone block temperatures.

The first model can be obtained directly from the available data, since the pavement of the test site is made of limestone. As for the second model, it will have to be assumed equivalent to some other model that can be calibrated with the available data. One possibility is to assume that a model that predicts temperatures in the river gravel block as a function of those in the limestone pavement can be used to predict temperatures of a river gravel pavement as a function of those in a limestone block. This assumption implies that aggregate type is the prevalent factor influencing the temperatures. However, inspection of raw data figures in Appendix A shows that, for all data sets, the slab size seems to have more effect on the temperature than does the aggregate type. Those figures indicate that temperatures of the two types of blocks are always much more similar to each other than to those in the pavement. Consequently, another possibility is to calibrate a model that predicts pavement temperatures as a function of those in the river gravel portable slabs, and to assume that it can equally well predict temperatures in a river gravel pavement from those of a limestone slab. Although the latter suggestion seems more reasonable, both models were calibrated and examined.

The three models examined in this study are:

Model 1 – Pavement temperatures as a function of limestone block temperatures.

Model 2 – Pavement temperatures as a function of river gravel block temperatures.

Model 3 – River gravel block temperatures as a function of pavement temperatures.

Data set 4, the largest continuous data set available, was used for the calibration. Table 4.5 summarizes the results for the three models. Figure 4.35 shows the results for model 1, Fig 4.36 for model 2, and Fig 4.37 for model 3. In these figures, part a shows the raw data, part b, the predicted versus observed values, and part c, the residuals versus time.

TABLE 4.5. SUMMARY OF RESULTS FROM STUDY 3 – MODELS TO ESTIMATE PAVEMENT TEMPERATURES AT A GIVEN DEPTH

Model 1:

$$Tpvt_t = A + B_0 * TLS_{t-0} + B_1 * TLS_{t-1} + B_2 * TLS_{t-2} + B_3 * TLS_{t-3} + C * D$$

$R^2 = 99.6\%$

$F_{4.1394} = 92052$

Coefficient	Estimate	Standard Error	Problem (Coef = 0)
A	3.205	0.647	0.0001
C	0.020	0.002	0.0001
B_0	0.390	0.004	0.0001
B_1	0.022	0.004	0.0001
B_2	0.062	0.004	0.0001
B_3	0.512	0.004	0.0001

Model 2:

$$Tpvt_t = A + B_0 * TLS_{t-0} + B_1 * TLS_{t-1} + B_2 * TLS_{t-2} + B_3 * TLS_{t-3} + C * D$$

$R^2 = 99.6\%$

$F_{4.1394} = 99763$

Coefficient	Estimate	Standard Error	Problem (Coef = 0)
A	1.257	0.474	0.0081
C	0.038	0.002	0.0001
B_0	0.415	0.004	0.0001
B_1	0.054	0.003	0.0001
B_2	0.073	0.003	0.0001
B_3	0.471	0.004	0.0001

Model 3:

$$Tpvt_t = A + B_0 * TLS_{t-0} + B_1 * TLS_{t-1} + B_2 * TLS_{t-2} + B_3 * TLS_{t-3} + C * D$$

$R^2 = 99.0\%$

$F_{4.1394} = 34091$

Coefficient	Estimate	Standard Error	Problem (Coef = 0)
A*	– 0.814	0.552	**0.1405**
C	– 0.041	0.004	0.0001
B_0	0.771	0.008	0.0001
B_1*	– 0.002	0.004	**0.5636**
B_2	– 0.142	0.004	0.0001
B_3	0.353	0.008	0.0001

* Non-significant

Model 1 presents a very high R^2, and all regression coefficients are highly significant. The values of the coefficients for the temperature lags, as well as their high significance, imply that the chosen format of the model was adequate. In terms of statistical results, models 2 and 3 are as good as model 1; however, the values of the coefficients of model 3 indicate that it may not be suitable for estimating temperatures in a pavement from those in the portable slab. The intercept is non-

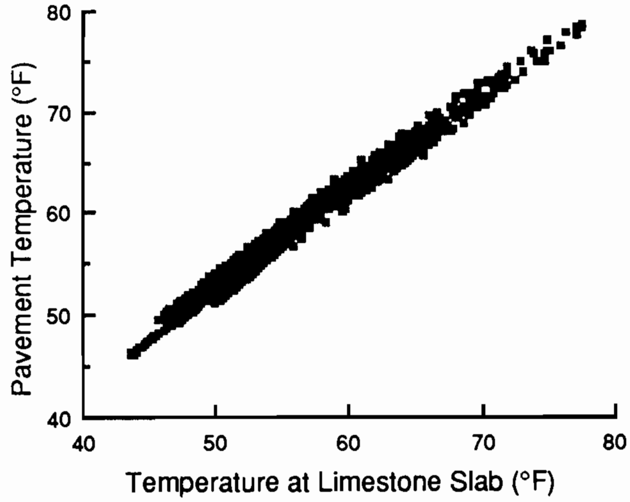

(a) Pavement versus limestone slab temperatures.

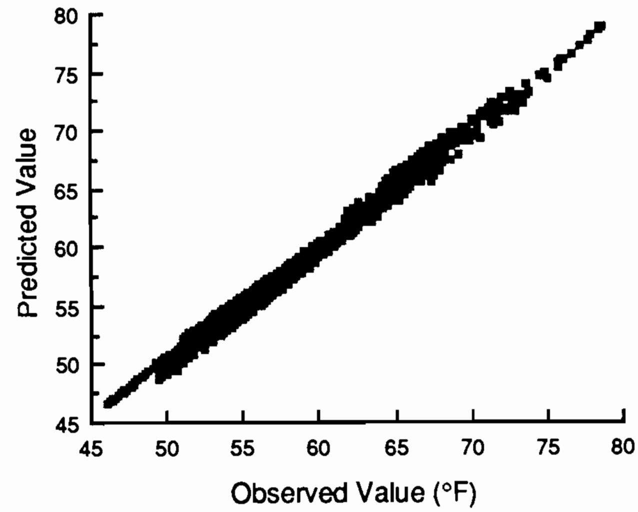

(b) Predicted versus observed values.

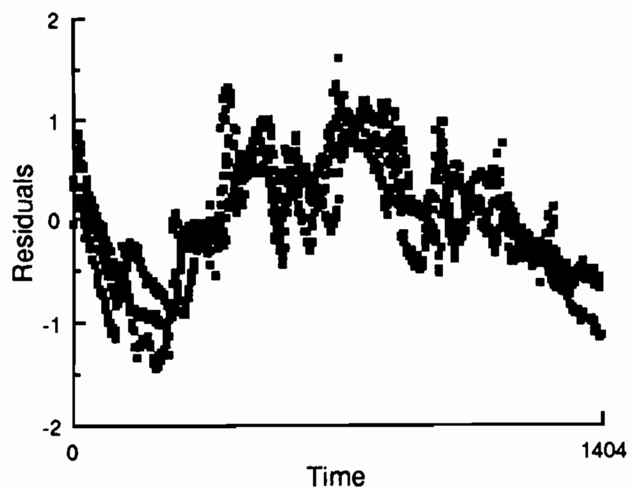

(c) Residuals versus time.

Fig 4.35. Results of auto-regressive model for temperatures, model 1.

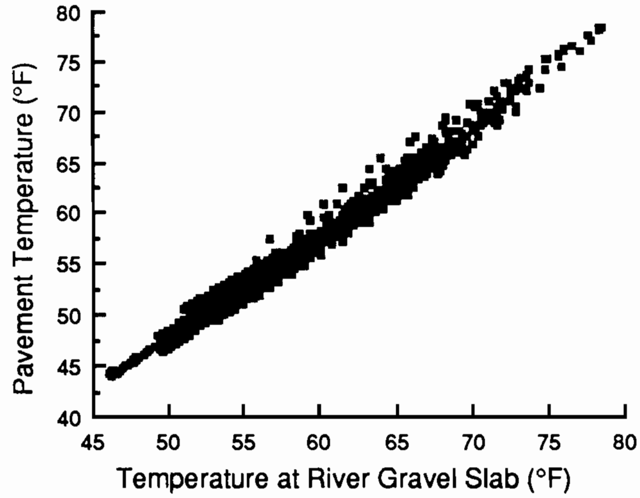

(a) Pavement versus river gravel slab temperatures.

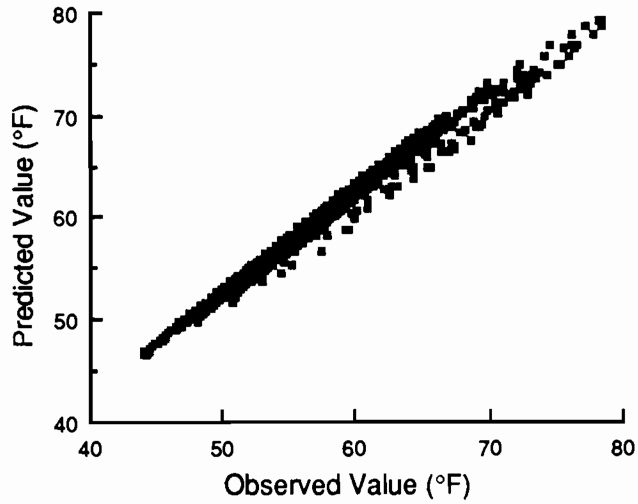

(b) Predicted versus observed values.

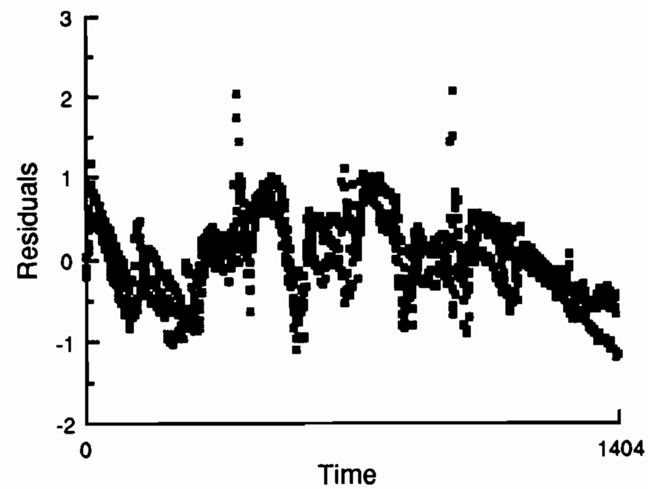

(c) Residuals versus time.

Fig 4.36. Results of auto-regressive model for temperatures, model 2.

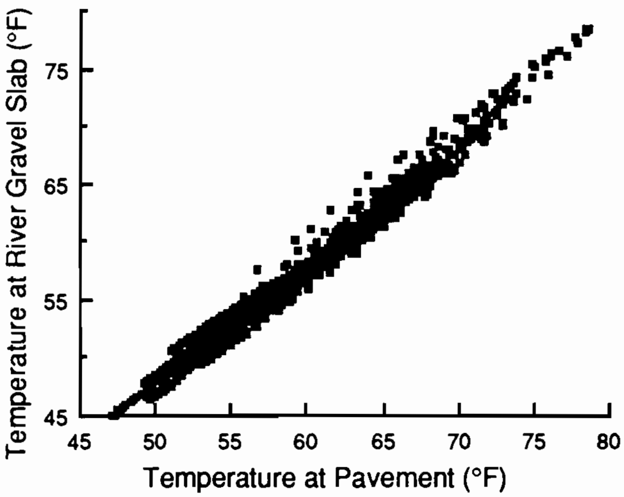

(a) River gravel slab versus pavement temperatures.

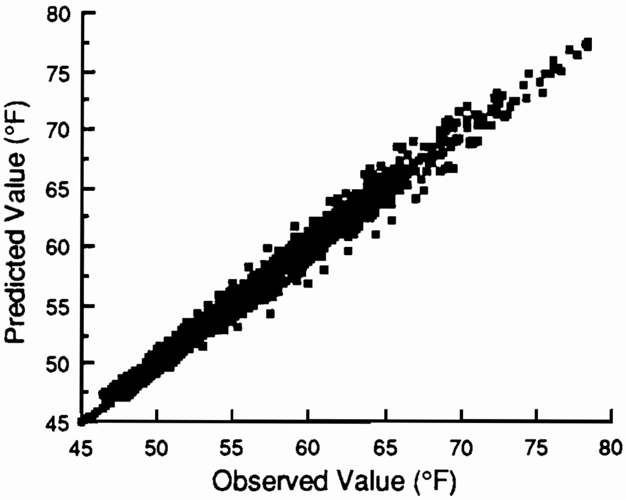

(b) Predicted versus observed values.

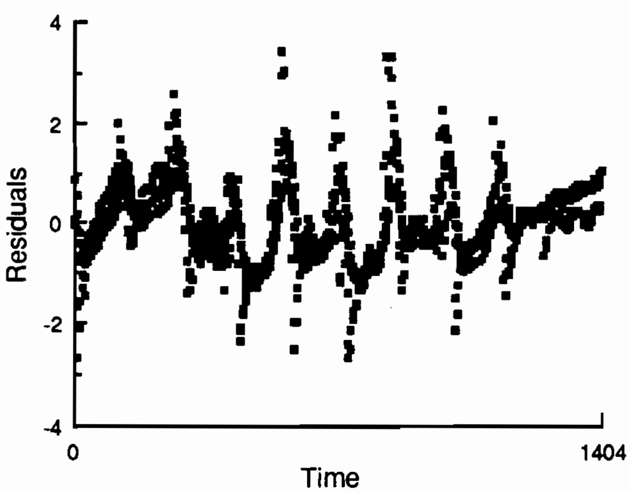

(c) Residuals versus time.

Fig 4.37. Results of auto-regressive model for temperatures, model 3.

significant, and some slopes are negative, while models 1 and 2 have significant intercepts and positive slopes. Models 1 and 2, despite the difference in aggregate types, have similar trends, while model 3 has a different trend, which is evidently due to the fact that it predicts block temperatures as a function of pavement temperatures instead of the opposite. Model 2 is thus recommended in lieu of model 3 for predicting pavement temperatures when block and pavement aggregate types do not match.

All residual plots are somewhat cyclical, showing that, despite the measures taken to deal with the auto-regressive data, some lack-of-fit still exists due to the autocorrelation. This suggests the necessity of testing the models with data taken under other conditions. Data set 4, taken during cold days, was used for calibration, because it is the biggest continuous set of data available. Therefore, data sets 1 and 2, taken during warm fall days, were used to test the models. In addition, the models were also tested with data set 3, which comprises only cloudy days. The testing consisted of comparing observed temperatures to those estimated with the models. The results of testing the models with data set 1 are depicted in Figs 4.38 (model 1) and 4.39 (model 2). The results of testing the models with data set 2 are depicted in Figs 4.40 (model 1) and 4.41 (model 2). The results of testing the models with data set 3 are depicted in Figs 4.42 (model 1) and 4.43 (model 2). Model 3 was not tested, due to the considerations discussed above.

Figures 4.38 to 4.43 indicate that, for all cases, temperatures at the top thermocouples are more accurately predicted than those at deeper thermocouples. The scatter is larger for model 2 (different aggregate types) than it is for model 1 (matching aggregate types). Some tendency to overestimate the lower temperatures can be observed for some of the deeper thermocouples in data sets 1 and 2. This tendency is more accentuated for data set 2 than it is for data set 1. For data set 3, however, this tendency is reversed, i.e., the bottom thermocouples temperatures are underestimated. This is probably a consequence of the observed lack-of-fit depicted in the cyclical residual plots: the model loses some of its accuracy when used for temperature ranges different from those in the calibration process. A summary of the models obtained through this study can be found later in this chapter.

STUDY 4. CALIBRATION AND TESTING OF MODELS TO ESTIMATE PAVEMENT TEMPERATURE GRADIENTS

As explained earlier in this chapter, estimates of temperature gradients are also needed when analyzing pavement data. Therefore, this study consisted of calibrating models for direct temperature gradient estimates. The underlying methods and reasoning are perfectly analogous to those used in study 4. The only difference is that, in lieu of temperatures, explicative and

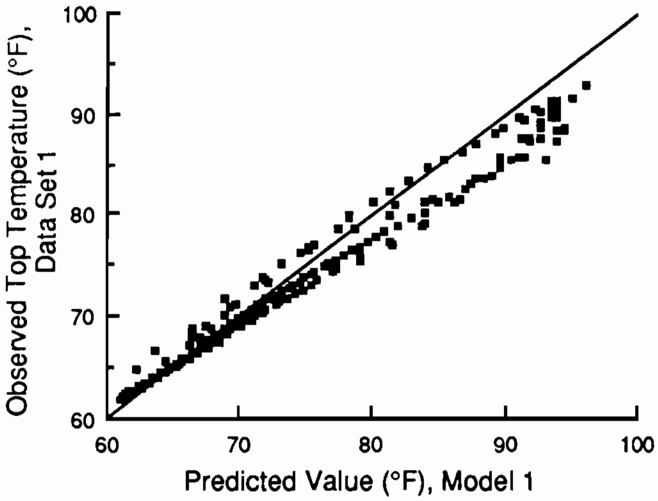

(a) Top temperatures.

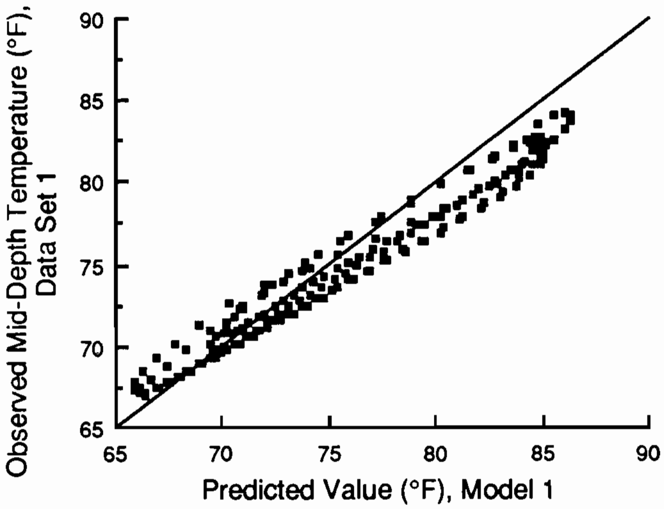

(b) Mid-depth temperatures.

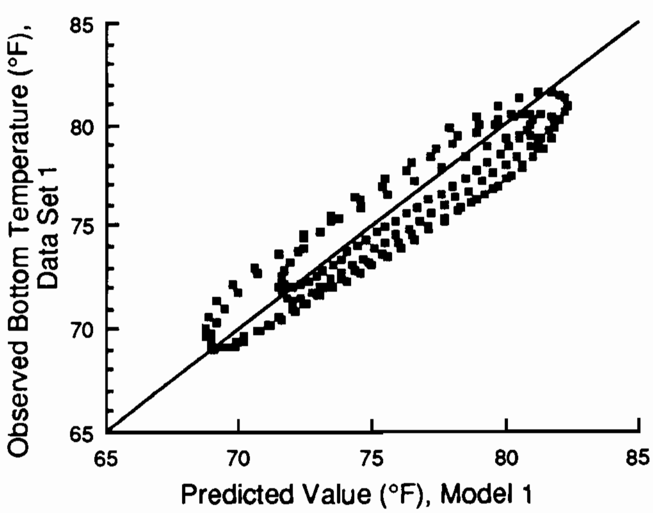

(c) Bottom temperatures.

Fig 4.38. Results of testing temperature model 1 with data set 1.

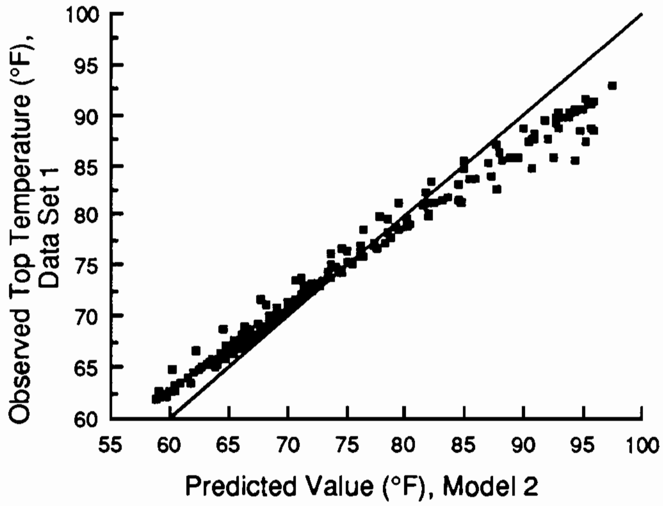

(a) Top temperatures.

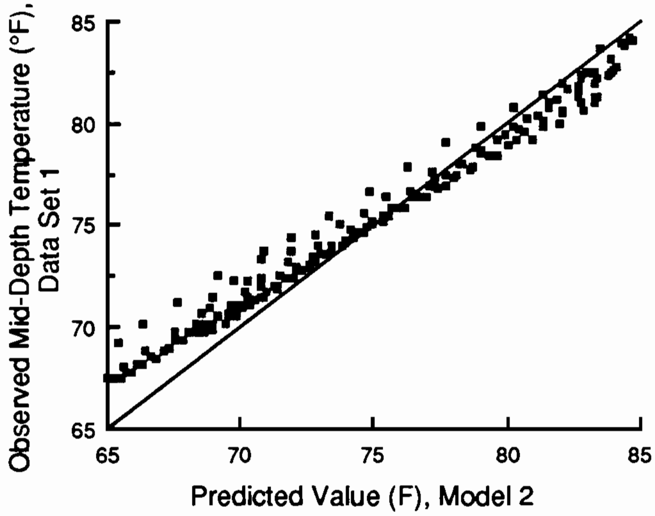

(b) Mid-depth temperatures.

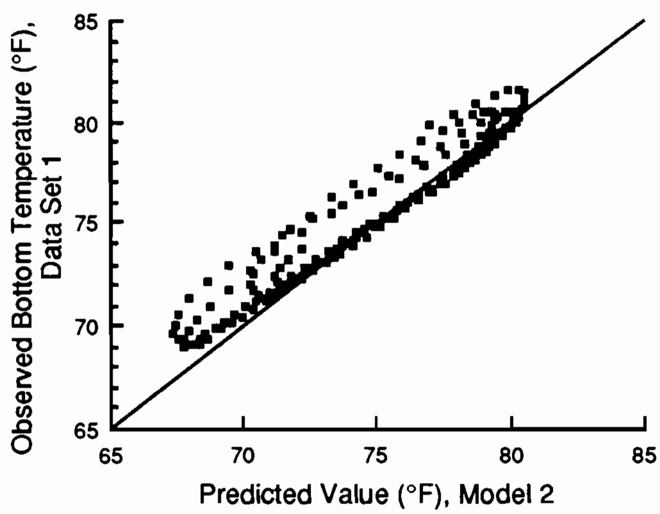

(c) Bottom temperatures.

Fig 4.39. Results of testing temperature model 2 with data set 1.

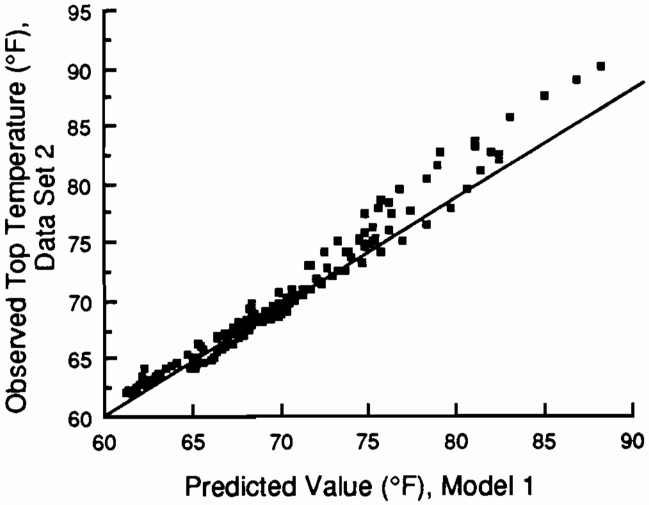

(a) Top temperatures.

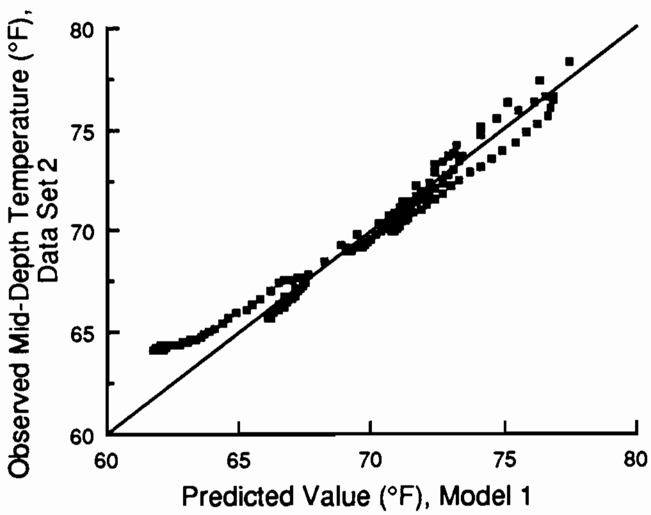

(b) Mid-depth temperatures.

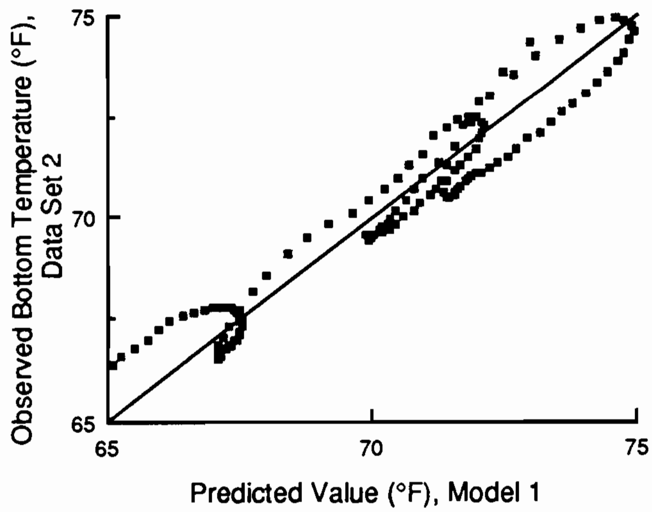

(c) Bottom temperatures.

Fig 4.40. Results of testing temperature model 1 with data set 2.

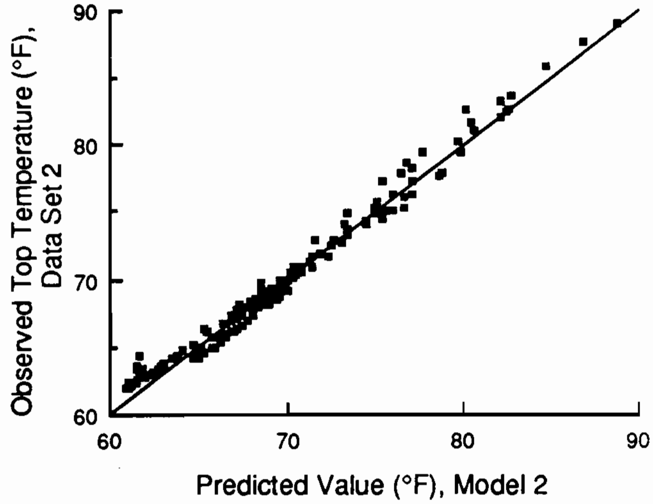

(a) Top temperatures.

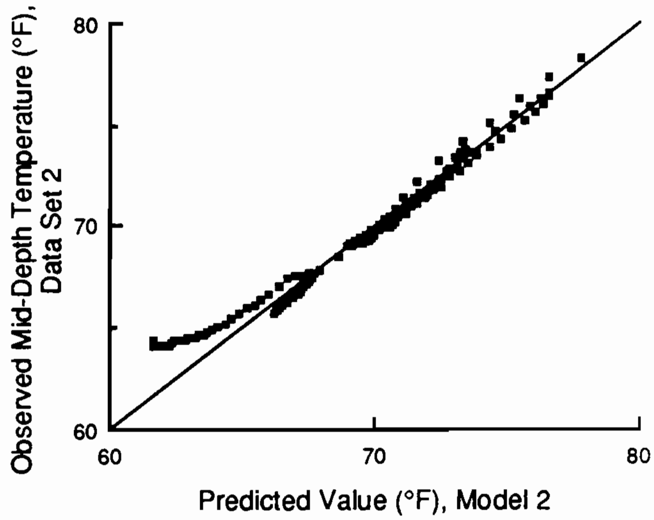

(b) Mid-depth temperatures.

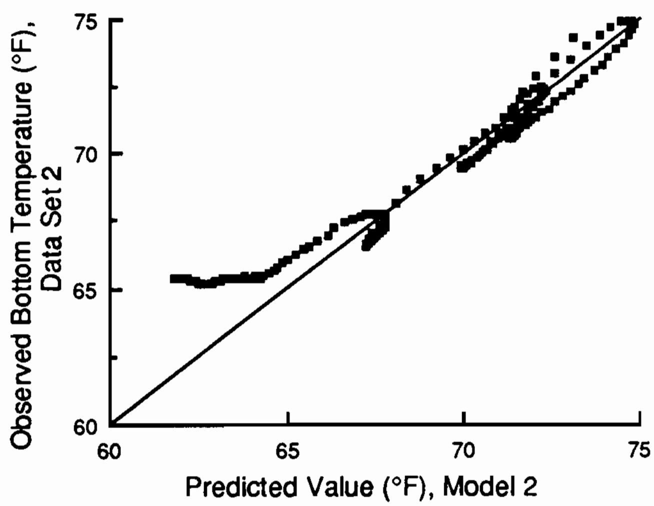

(c) Bottom temperatures.

Fig 4.41. Results of testing temperature model 2 with data set 2.

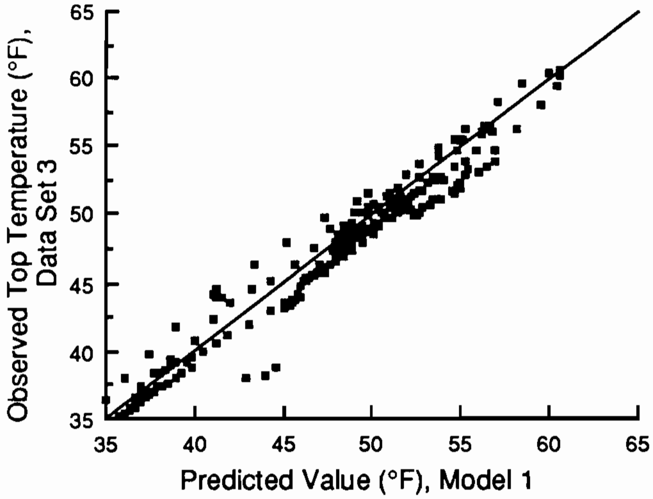

(a) Top temperatures.

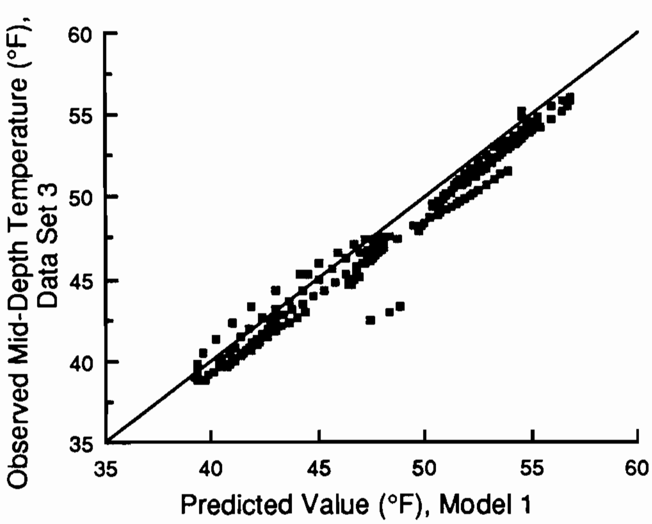

(b) Mid-depth temperatures.

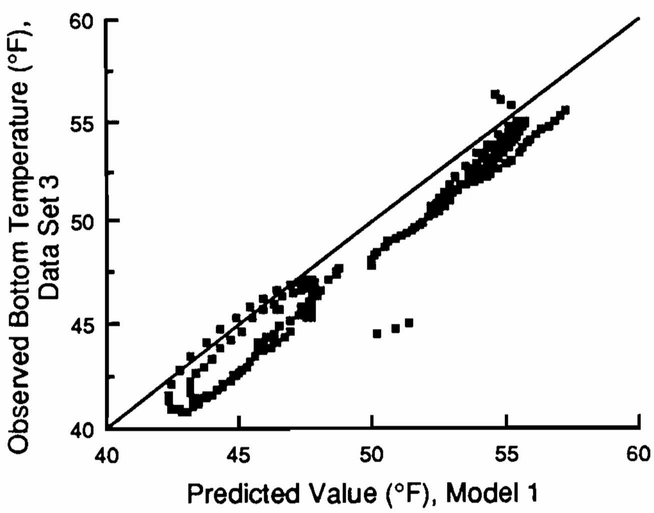

(c) Bottom temperatures.

Fig 4.42. Results of testing temperature model 1 with data set 3.

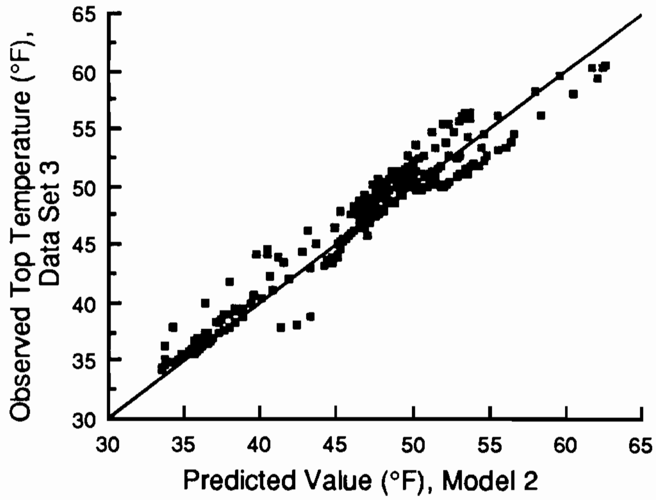

(a) Top temperatures.

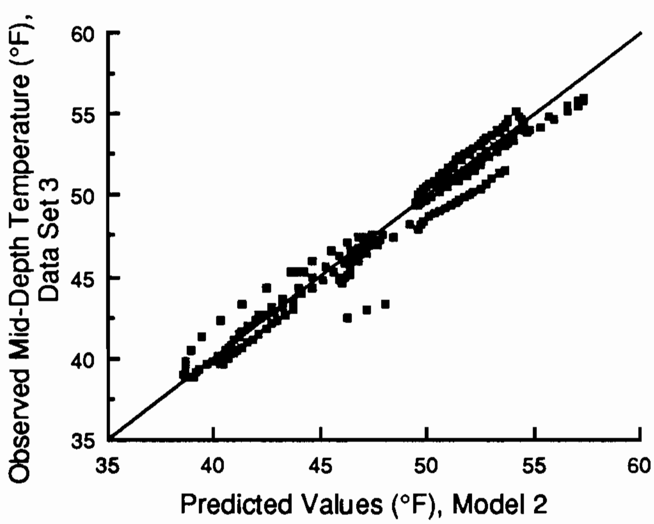

(b) Mid-depth temperatures.

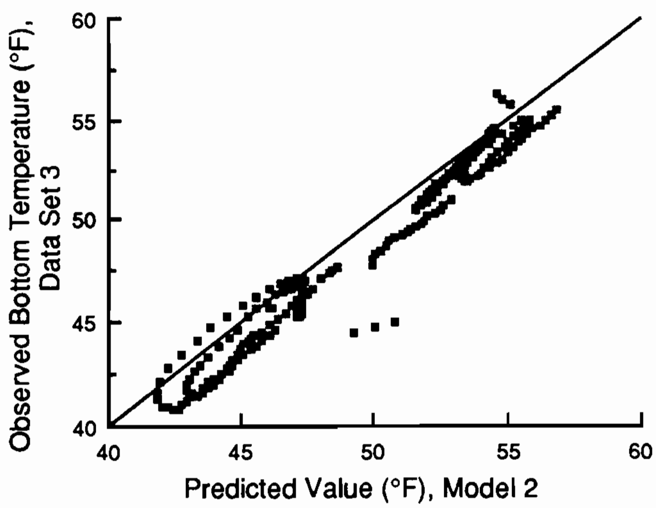

(c) Bottom temperatures.

Fig 4.43. Results of testing temperature model 2 with data set 3.

dependent variables are temperature gradients. Moreover, since study 3 revealed that model 3 is not adequate for predicting pavement temperatures, only models originally calibrated with pavement temperatures as the independent variable were used.

Table 4.6 depicts the summary of the results for models 1 (limestone/limestone) and 2 (limestone/river gravel). Figure 4.41 shows the results for model 1, and Fig 4.42, the results for model 2.

Models 1 and 2 are highly significant, with both R^2 around 99 percent. Both intercepts are non-significant, thus indicating that zero gradients in the portable slab correspond to zero gradients in the pavement. The high significance of the coefficients for the lags of the variable indicate that the auto-correlation is important. However, cyclical residual plots can still be seen despite the measures to deal with the auto-regressive data. It is thus advisable to test the models for other conditions. Results of testing the models with data set 1 are depicted in Fig 4.46 for model 1 and 4.47 for model 2. Results of testing the models with data set 2 are depicted in Fig 4.48 for model 1 and 4.49 for model 2. Tests with data set 3 are shown in Fig 4.50 for model 1 and 4.51 for model 2.

The lack-of-fit depicted in the cyclical residual plots manifested itself in the somewhat cyclical scatters depicted in Figs 4.46 to 4.51. The cyclical pattern is more defined in tests with data set 1. This is probably due to the fact that data set 1 was taken with the slabs sitting on the ground, rather than buried. For all data sets, the predictions of the upper gradients (top minus mid-depth) were more accurate than those of the lower (mid-depth minus bottom) and total (top minus bottom) gradients. Both models showed some tendency to overestimate the higher gradients of data set 1; for data set 2, this trend was reversed. As for data set 3, both models tended to underestimate gradients, especially the lower and total ones. Scatters for all data sets remained in a range of approximately ±4° F, which means that the models cannot be expected to predict small temperature gradients reliably.

TABLE 4.6. SUMMARY OF RESULTS OF STUDY – MODELS FOR ESTIMATING PAVEMENT TEMPERATURE GRADIENTS

Model 1:

$$\Delta Tpvt_t = A + B_0 * \Delta TRS_{t-0} + B_1 * \Delta TRS_{t-1} + B_2 * \Delta TRS_{t-2} + B_3 * \Delta TRS_{t-3} + C * \Delta D$$

$R^2 = 99.0\%$

$F_{4.1394} = 33421$

Coefficient	Estimate	Standard Error	Problem (Coef = 0)
A*	− 0.017	0.031	0.5765
C	− 0.018	0.005	0.0002
B_0	0.315	0.007	0.0001
B_1	− 0.051	0.003	0.0001
B_2	0.029	0.003	0.0001
B_3	0.557	0.007	0.0001

Model 2:

$$\Delta Tpvt_t = A + B_0 * \Delta TRG_{t-0} + B_1 * \Delta TRG_{t-1} + B_2 * \Delta TRG_{t-2} + B_3 * \Delta TRG_{t-3} + C * \Delta D$$

$R^2 = 99.2\%$

$F_{4.1394} = 40989$

Coefficient	Estimate	Standard Error	Problem (Coef = 0)
A*	− 0.009	0.028	0.7492
C	0.037	0.004	0.0001
B_0	0.350	0.005	0.0001
B_1	− 0.026	0.003	0.0001
B_2	0.015	0.003	0.0001
B_3	0.473	0.005	0.0001

* Non-significant parameters

SUMMARY OF FINDINGS

The findings of the four studies described above can be summarized a follows:

(1) Differences in temperatures due to aggregate type were primarily due to an additive constant, while the rates of change in temperature in both aggregate types are roughly the same. For data set 1, the temperatures of the river gravel slabs were 2° F to 4° F smaller than those of the limestone slabs in almost all cases.

(2) Differences in temperatures due to aggregate type can be accounted for by means of the appropriate models.

(3) Models calibrated with data taken with buried slabs did not show any significant improvement as compared to those obtained with unburied slabs. Therefore, it is possible to obtain accurate predictions with the slabs sitting on the ground.

(4) The following model can be used to predict pavement temperatures from those at the portable slab when the aggregate types in the slab and the pavement are the same:

$$Tpvt_t = 3.205 + 0.390 * TLS_{t-0} + 0.022 * TLS_{t-1} + 0.062 * TLS_{t-2} + 0.512 * TLS_{t-3} + 0.020 * D$$

(5) The following model can be used to predict pavement temperatures from those at the portable slab when the aggregate types in the slab and in the pavement are not the same:

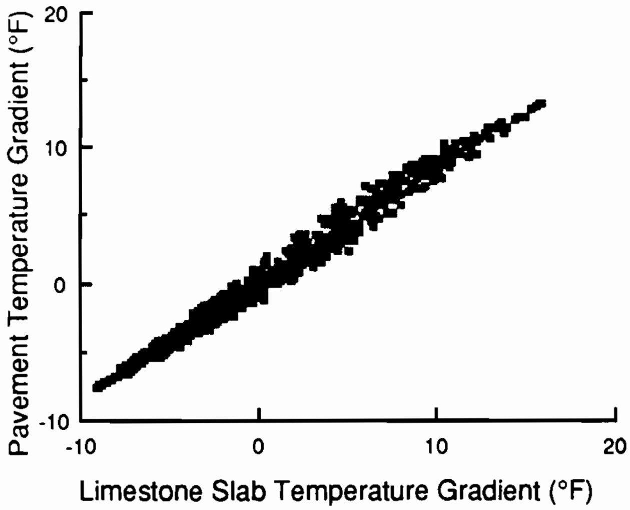

(a) Pavement versus limestone slab gradients.

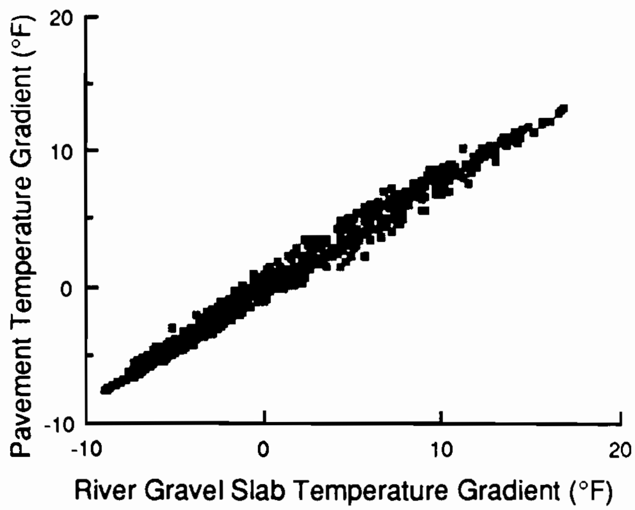

(a) Pavement versus river gravel slab gradients.

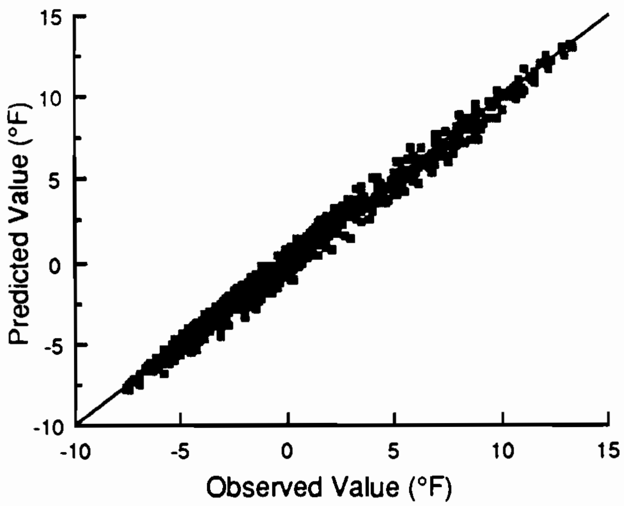

(b) Predicted versus observed gradients.

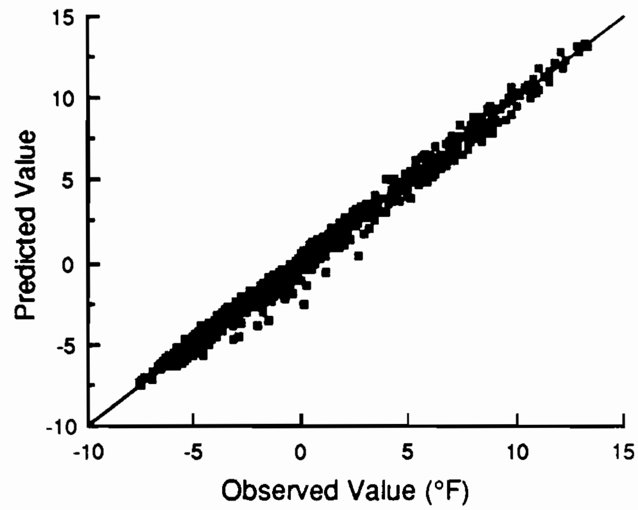

(b) Predicted versus observed gradients.

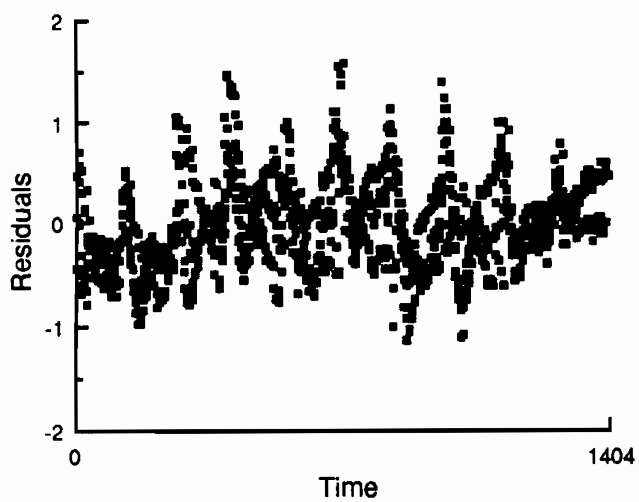

(c) Residuals versus time.

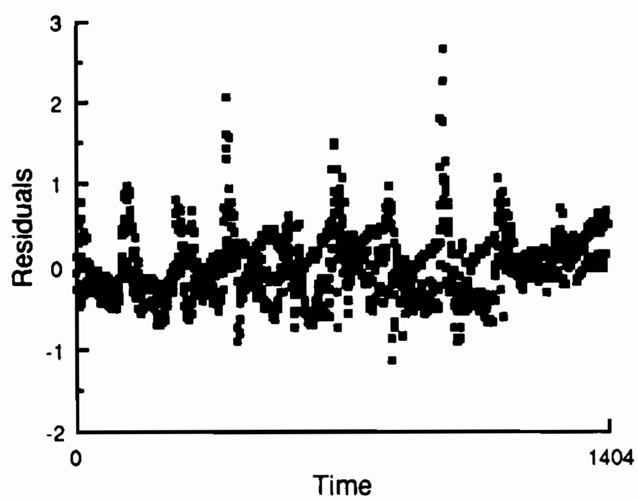

(c) Residuals versus time.

Fig 4.44. Results of auto-regressive model for temperature gradients, model 1.

Fig 4.45. Results of auto-regressive model for temperature gradients, model 2.

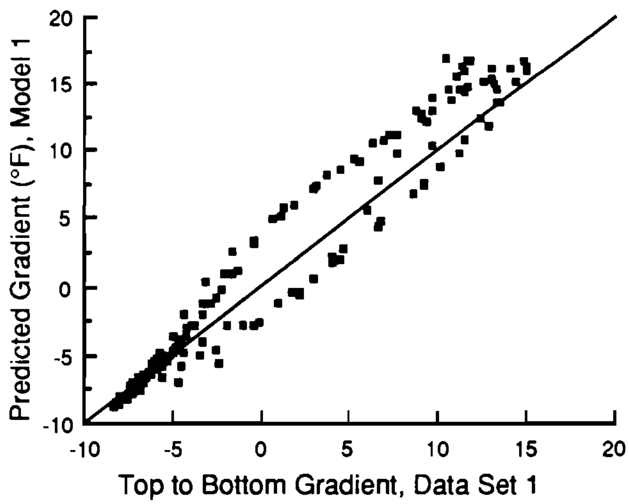

(a) Top - bottom gradients.

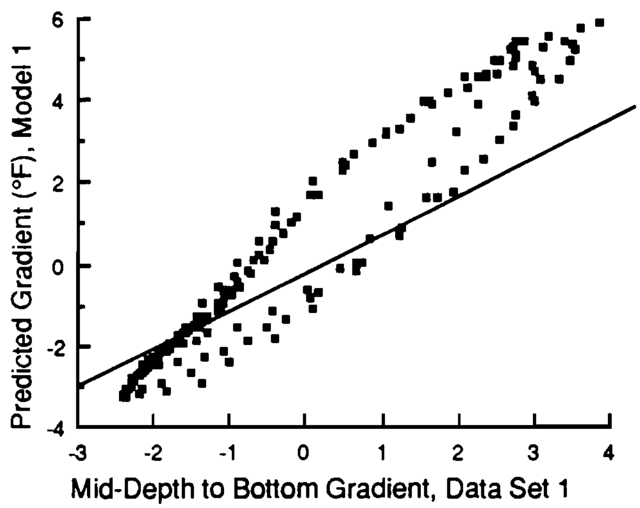

(b) Mid-depth - bottom gradients.

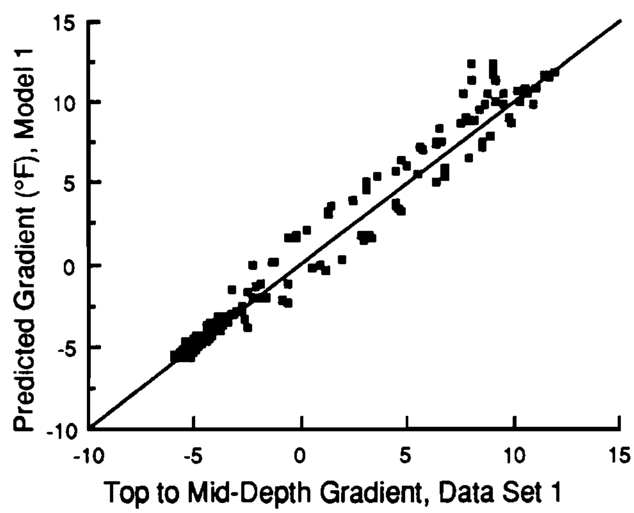

(c) Top - mid-depth gradients.

Fig 4.46. Results of testing temperature gradients model 1 with data set 1.

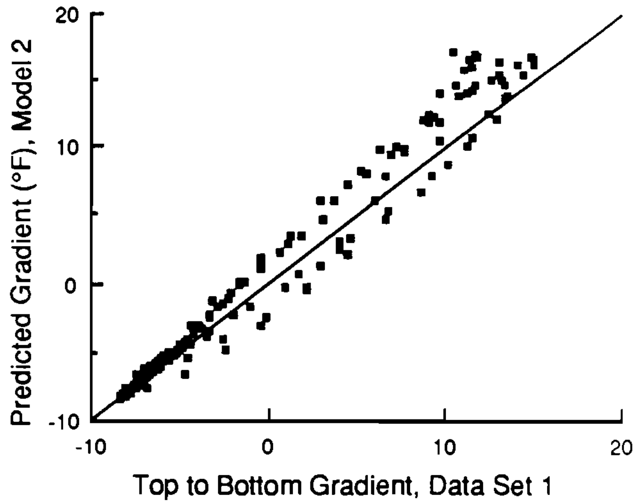

(a) Top - bottom gradients.

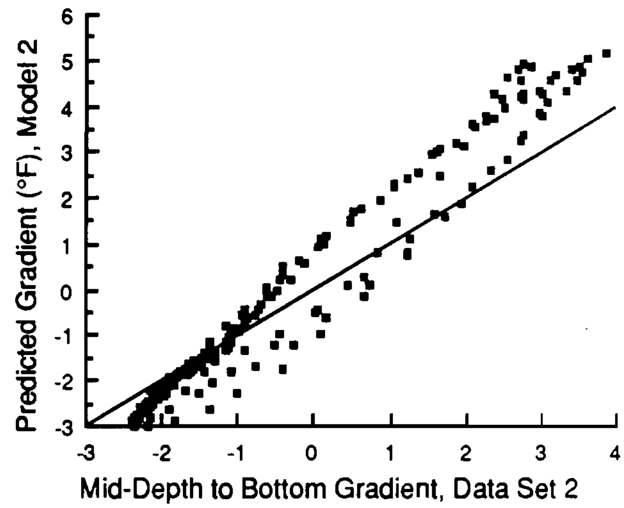

(b) Mid-depth - bottom gradients.

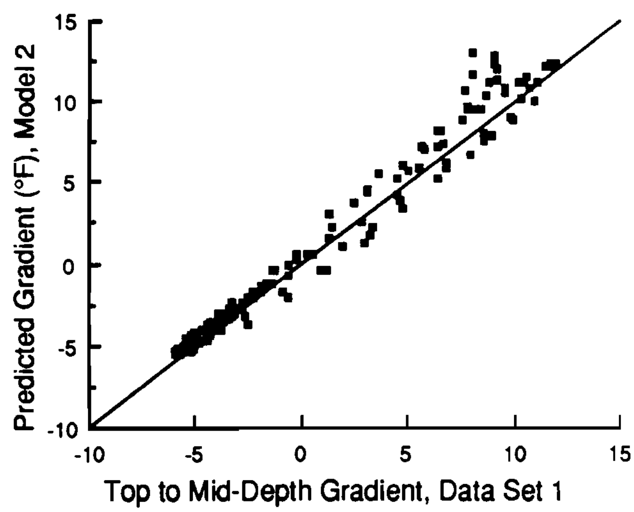

(c) Top - mid-depth gradients.

Fig 4.47. Results of testing temperature gradients model 2 with data set 1.

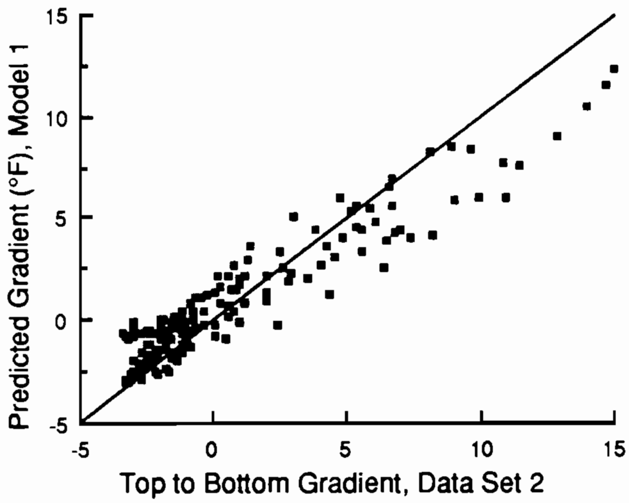

(a) Top - bottom gradients.

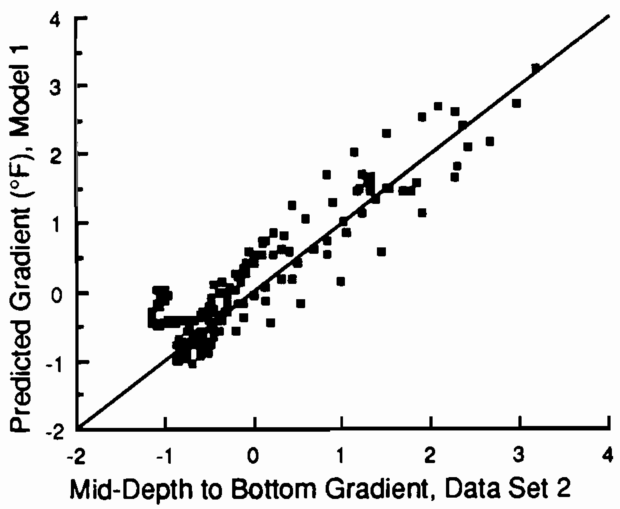

(b) Mid-depth - bottom gradients.

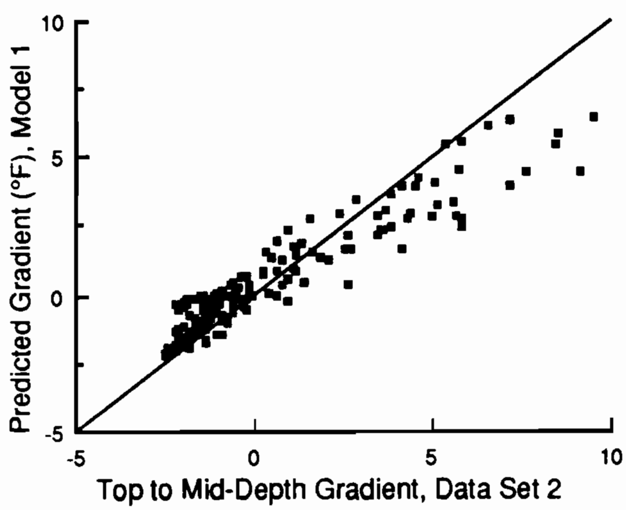

(c) Top - mid-depth gradients.

Fig 4.48. Results of testing temperature gradients model 1 with data set 2.

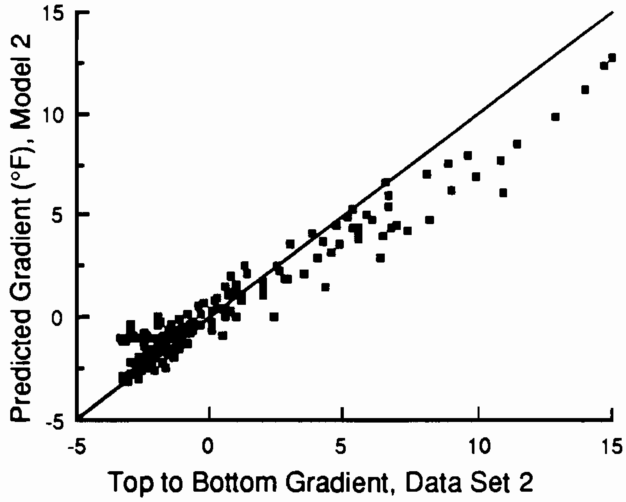

(a) Top - bottom gradients.

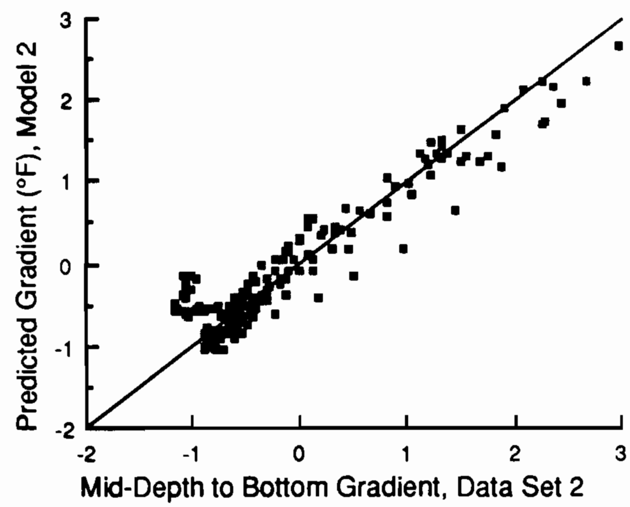

(b) Mid-depth - bottom gradients.

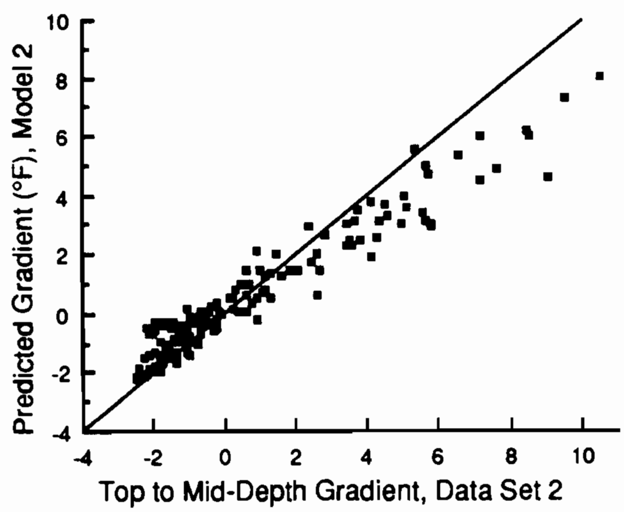

(c) Top - mid-depth gradients.

Fig 4.49. Results of testing temperature gradients model 2 with data set 2.

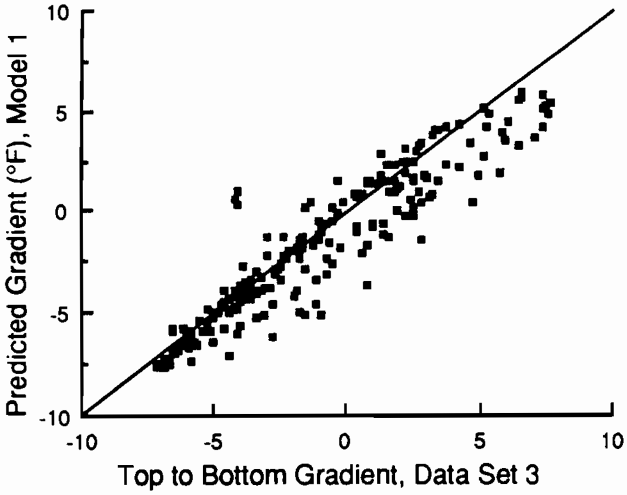

(a) **Top - bottom gradients.**

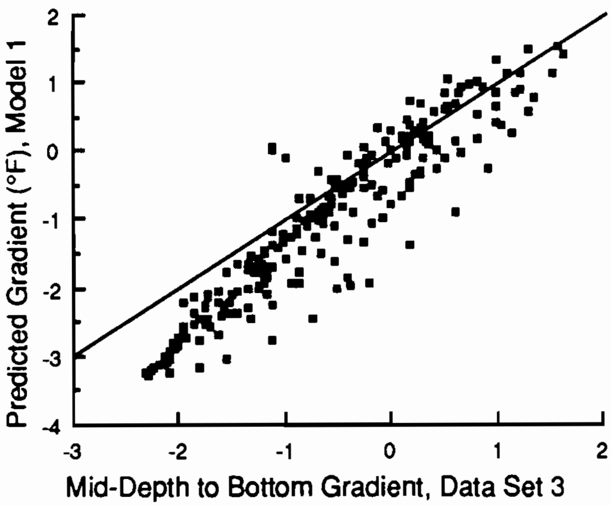

(b) **Mid-depth - bottom gradients.**

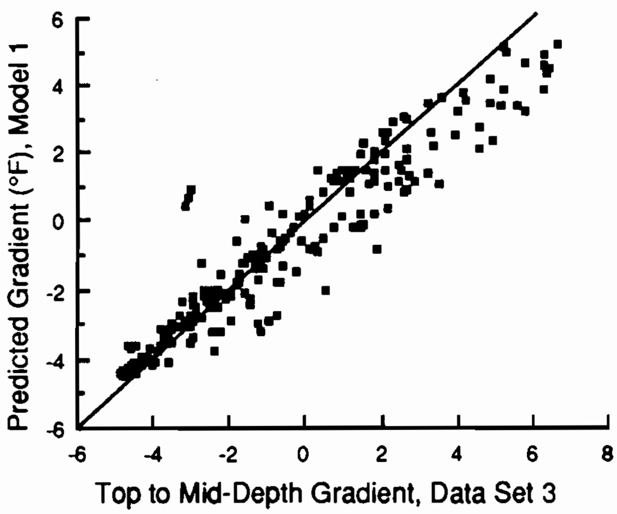

(c) **Top - mid-depth gradients.**

Fig 4.50. Results of testing temperature gradients model 1 with data set 3.

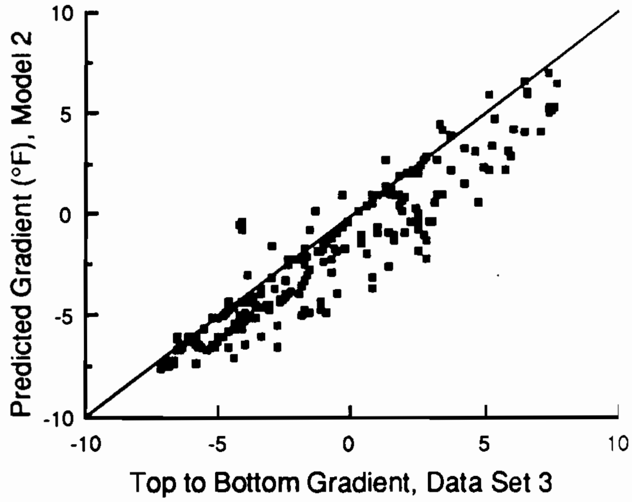

(a) **Top - bottom gradients.**

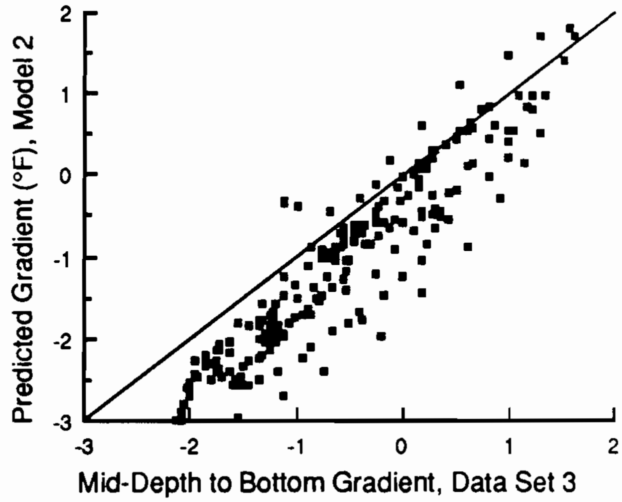

(b) **Mid-depth - bottom gradients.**

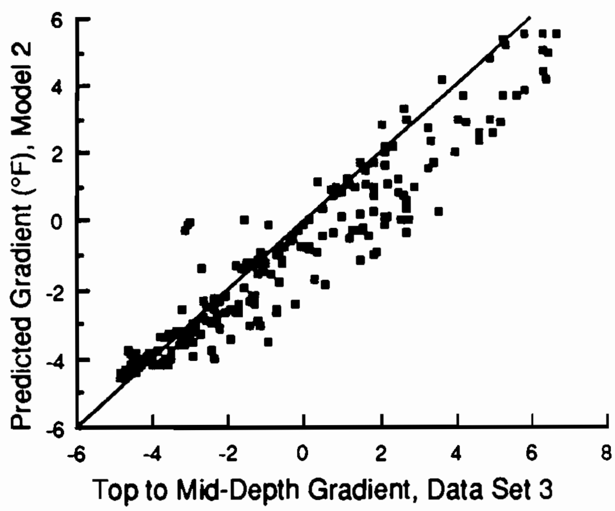

(c) **Top - mid-depth gradients.**

Fig 4.51. Results of testing temperature gradients model 2 with data set 1.

$$Tpvt_t = 1.257 + 0.415 * TLS_{t-0} + 0.054 * TLS_{t-1} + 0.073 * TLS_{t-2} + 0.471 * TLS_{t-3} + 0.038 * D$$

(6) The following model can be used to predict temperature gradients in the pavement from those at the portable slab when the aggregate types in the slab and in the pavement are the same:

$$\Delta Tpvt_t = 0.315 * \Delta TLS_{t-0} - 0.051 * \Delta TLS_{t-1} + 0.029_2 * \Delta TLS_{t-2} + 0.557 * \Delta TLS_{t-3} - 0.018 * \Delta D$$

(7) The following model can be used to predict temperature gradients in the pavement from those at the portable slab when the aggregate types in the slab and in the pavement are not the same:

$$\Delta Tpvt_t = 0.35 * \Delta TLS_{t-0} - 0.026 * \Delta TLS_{t-1} + 0.015 * \Delta TLS_{t-2} + 0.473 * \Delta TLS_{t-3} + 0.037 * \Delta D$$

(8) The models for estimating temperature gradients are not suitable for accurately predicting low temperature gradients, because a scatter of approximately ±4° F was observed in the plots of predicted versus observed gradients.

(9) Some lack-of-fit due to the auto-regressive characteristics of the data is present in all models, but fairly accurate predictions were obtained when the models were tested with the available data.

CONCLUSIONS AND RECOMMENDATIONS

The experiment described in this chapter was undertaken with data on a single pavement at a single site. Therefore, use of these models to predict pavement temperatures at test sections throughout the state requires assuming that the conditions at the test site will hold approximately for all other pavements state-wide. Due to the impossibility of conducting a larger experiment under the subject project, awareness of this limitation is very important for interpretation of field data.

The pavement at the test facility consists of reinforced concrete with a steel mesh somewhat coarser than is usually found in actual pavements. Since the thermal properties of the concrete and the steel are different, it seems reasonable to expect pavements with other—or even no—reinforcement to present different temperatures.

The time-series techniques previously described were used to fit the models, after the realization that the problem consisted of auto-correlated data, for which procedures such as least-squares and ANOVA are inadequate. The good results obtained with this technique demonstrate that it is appropriate to analyze temperature data. However, to be efficiently applied, these mathematical methods demand continuity of the samples. In practice, continuous data are very difficult to obtain, especially in the case of the test site used in this experiment, due to the practical constraints imposed on the data acquisition system.

Two types of models were fit to the data in an attempt to represent the following situations:

(a) pavement and portable slab have the same coarse aggregate type;

(b) pavement and portable slab have different aggregate types.

Since the pavement at the test site is made of limestone, situation a is actually represented by a model for limestone pavement/limestone block aggregate types, whereas situation b is represented by a model obtained from limestone pavement/river gravel block data. It is thus very important to emphasize that use of these models for other combinations of aggregate types implies the assumption that the influence of other aggregate types can be accurately represented by the available models. It is recommended that some data for other aggregate types be taken in order to verify this assumption.

The inaccuracies found in the experiment described herewith are not easy to solve using measurements of thermal properties of the pavement in conjunction with theoretical solutions of the heat transfer equation. According to Ref 61, heat transfer experiments are difficult and uncertain. Thermophysical properties of the materials are not well known. For example, thermal conductivity of metals with very low amounts of impurities cannot be measured with less than ±20 percent uncertainty (Ref 61). The uncertainty in these measurements increases drastically with heterogeneity; and portland cement concrete is considerably less homogeneous than a metal with few impurities. An accurate solution to the problem of obtaining pavement temperatures in the field seems to be beyond the current state-of-the-art in heat transfer studies, especially for the case of network-level surveys, which require expeditious and cheap procedures to be feasible.

The portable slab procedure for estimating pavement temperatures meets the requirements of quickness and cheapness demanded by a network-level diagnostic survey. As for the accuracy, it is concluded that, although improvements would be desirable, the current state-of-the-art in heat transfer studies does not permit us to expect more sophisticated procedures to yield improved results.

The procedure for measuring pavement temperature in the diagnostic survey, based on the findings described in this chapter, is presented in Chapter 6.

CHAPTER 5. DEVELOPMENT OF PROCEDURE FOR COLLECTING DEFLECTIONS

INTRODUCTION

The deflection data were collected in the diagnostic survey in order to fulfill two immediate research purposes:

(1) estimating stiffness of pavement layers and
(2) estimating load transfer coefficients.

In addition, since the study of edge loading conditions and the benefits of tied shoulders requires deflection data at the edge and interior of the pavement to be available, this type of data was collected as well. The available equipment for this task was the falling weight deflectometer (FWD).

EQUIPMENT FOR DATA COLLECTION

FUNDAMENTALS

The FWD applies to the pavement an impulse load by dropping a known mass from a pre-determined height, as illustrated in Fig 5.1. The mass falls on a foot plate connected to a rigid base plate by rubber buffers that act as springs. The peak force acting on the surface where the mass falls, which is measured by a load cell, can theoretically be calculated using the following relationship:

$$P = \sqrt{2\,m\,g\,h\,k} \tag{5.1}$$

where

P = peak force,
g = acceleration due to gravity,
h = height of drop of the mass,
m = mass of the FWD, and
k = spring constant.

The peak deflections are calculated by integrating the impact velocity, which is proportional to the output voltage in the velocity transducers, also termed geophones. In other words, the FWD is a tool capable of obtaining deflections through measurements of a surrogate variable, the velocity. Reference 47 discusses results of

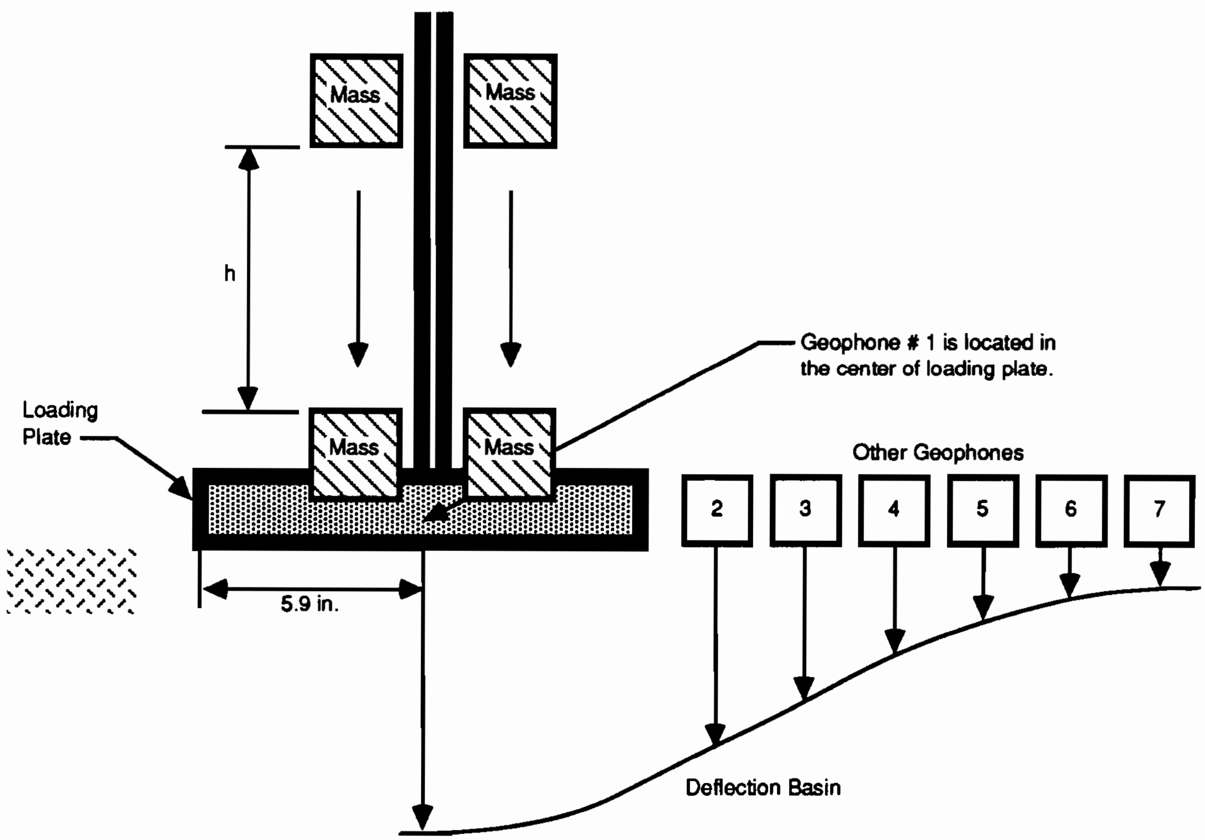

Fig 5.1. FWD loading plate and geophones.

studies comparing the FWD signals and those measured under a moving wheel load. In general, those studies found good agreement between those types of signals. However, the duration of the FWD deflection is around 0.025 second, somewhat smaller than the duration of the deflection signal under a moving wheel load (Ref 45).

DESCRIPTION OF THE EQUIPMENT AND OF THE OPERATING PROCEDURE

The FWD is a trailer-mounted device that can be towed by any standard car or van at normal highway speeds. The total weight of the pulse-generating device and the trailer does not exceed 2,000 pounds. The transient pulse-generating device is the trailer-mounted frame, which is capable of causing a given preset mass configuration to fall from four different preset heights in a movement perpendicular to the surface.

The assembly consists of the masses, the frame, loading plates, and a rubber buffer. The operation of lifting and dropping the mass on the loading plate is based on an electro-hydraulic system. Figure 5.2 depicts the FWD with one of the possible geophone configurations.

The falling weight/buffer assembly is furnished so that four different configurations of mass can be employed. All four mass configurations produce a transient reproducible load pulse of 0.025 to 0.030 second in duration. Each of these falling weight/buffer combinations is constructed so that weight from different heights can be released, such that different peak loads for the four specified masses can be obtained in the ranges depicted in Table 5.1 (Ref 45).

TABLE 5.1. MASSES AND CORRESPONDING RANGES OF PEAK LOAD

Falling Mass (lb)	Peak Loading Force (lbf)
110	1,500 - 4,000
220	3,000 - 8,000
440	5,500 - 16,000
660	8,000 - 24,000

A loading plate 11.8 inches in diameter is used. The mass guide shaft is perpendicular to the road surface in the measuring mode as well as the transport mode. The system includes a load cell capable of accurately measuring the force that is applied to the load plate.

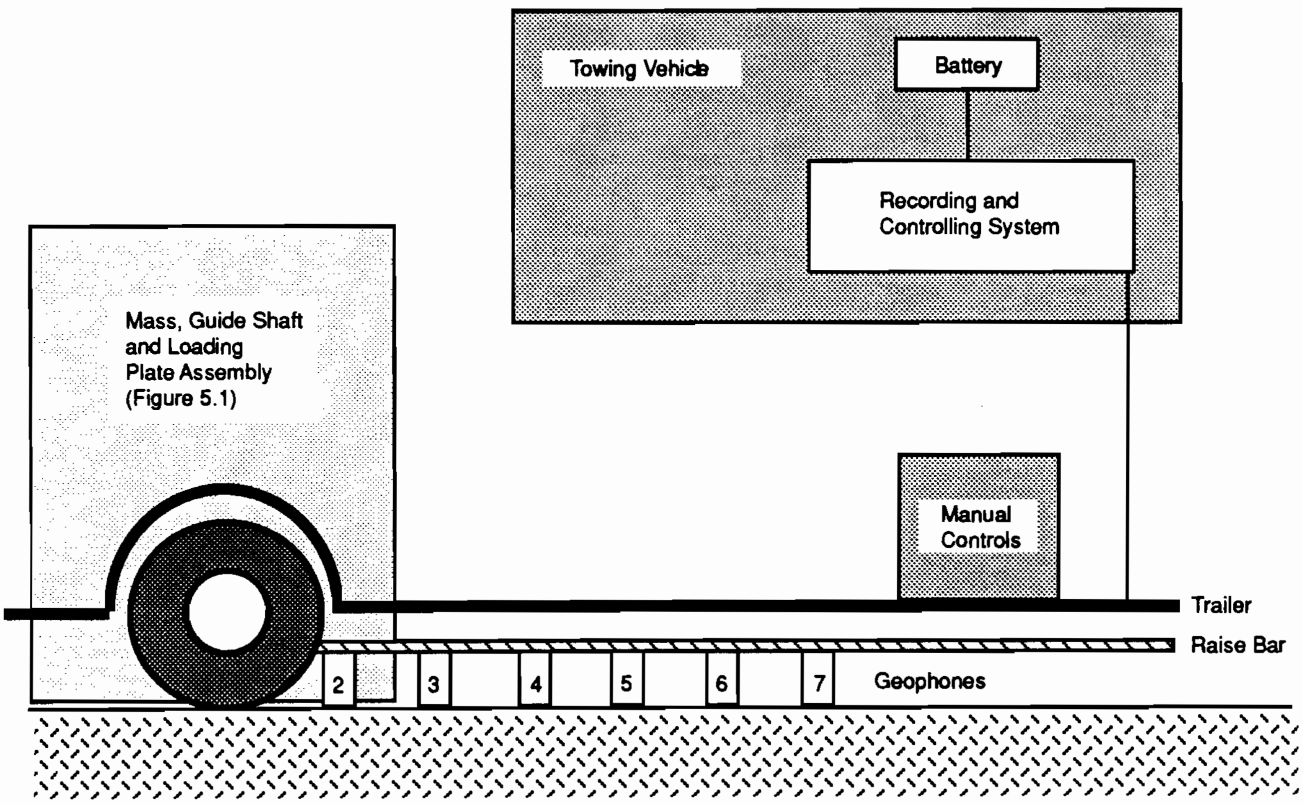

Fig 5.2. Scheme of the FWD and trailer (source: Ref 45).

The FWD can provide seven different deflection measurements per test. One of the velocity transducers (geophones) is located in the center of the loading plate, to the front and to the rear. All geophone holders ensure good contact between the transducers and the surface being tested. The electronic recording equipment is operated by a nominal 12-volt DC power and a printer, which automatically records data from field testing and also accepts keyed-in information.

The routine test procedure is:

(1) Select and secure the mass configuration in place; this is usually done before travelling to the test site.
(2) Position the trailer on the pavement so that the marked test location is directly below the center of the loading plate.
(3) Turn on the processing equipment and HP-85 computer, which are carried in the towing vehicle.
(4) Program a test sequence—drop height and number of drops per test point—from the HP-85 keyboard. When the operator enters the "RUN" command, the FWD loading assembly is lowered to the pavement surface. The mass is dropped the programmed number of times from the pre-programmed height, and the assembly is raised again. This step typically lasts no longer than two minutes.
(5) Inspect the data displayed on the HP-85 screen, and enter a "skip" command within a pre-programmed time if it is decided that the data should not be recorded; otherwise, the deflection data, the peak force magnitude, and site identification information are all stored on the HP-85 magnetic tape cassette. The data are also printed.

RECOMMENDED PROCEDURE FOR THE DIAGNOSTIC SURVEY

INTRODUCTION

As opposed to the case of crack width and pavement temperature, described in the previous chapters, the procedure to measure deflections at each test location does not need to be developed, because the equipment already has embedded in it what can be called "procedure for data collection". What is left to decide are where in the pavement to measure and how many times each test section should be replicated. Theoretically, the configurations of masses and of geophones could also be selected for the diagnostic survey; but it was decided to use whatever configurations were available at the particular FWD in each District, because the mass configuration is the same for all available FWD's in the SDHPT, and the default geophone configurations change very little. Thus, only the layout of the test locations and the number of replicates had to be decided upon. The former was decided based on what the data will be used for. Similarly to any other experiment, the number of replicates was decided based on a compromise between maximizing the number of replicates and minimizing the time spent in each test section.

LAYOUT OF DEFLECTION MEASUREMENTS ON A NON-OVERLAID TEST SECTION

As already explained in the introduction item, the deflection measurements should provide data to permit estimates of stiffness of pavement layers, and studies of load transfer and edge load conditions. The layout of the deflection measurements stations was planned based on these objectives.

The load transfer coefficient is a dimensionless number that attempts to capture the amount of load that can be transferred from one side of a pavement discontinuity to another. Evidently, 100 percent of load transfer would be the ideal situation, but joint efficiencies up to 50 percent have been reported (Ref 64). Efficiency of load transfer at CRCP cracks is more controversial (Ref 57). Reference 57 presents a comprehensive explanation of the concepts underlying the development of the load transfer coefficients recommended in the AASHTO Guide (Ref 1). This Guide always stresses the necessity for each agency to develop its own characteristic pavement design parameters that reflect local conditions. Therefore, a procedure for estimating load transfer coefficients for CRCP test sections is being developed under Project 1169 (Ref 51). This procedure was still unfinished at the time of this report; however, the basic idea underlying the estimate of load transfer by means of deflection data is that comparing the ratio of deflections measured on both sides of a discontinuity with the ratio of those taken in the interior of the slab can be a good indicator of load transfer. Figure 5.3 and Eq 5.2 clarify this concept. Theoretically, a deflection basin measured with the loading plate close to a discontinuity with 100 percent load transfer would present little difference from that measured with the loading plate at the interior of the slab, and coefficient LT in Eq 5.2 would be

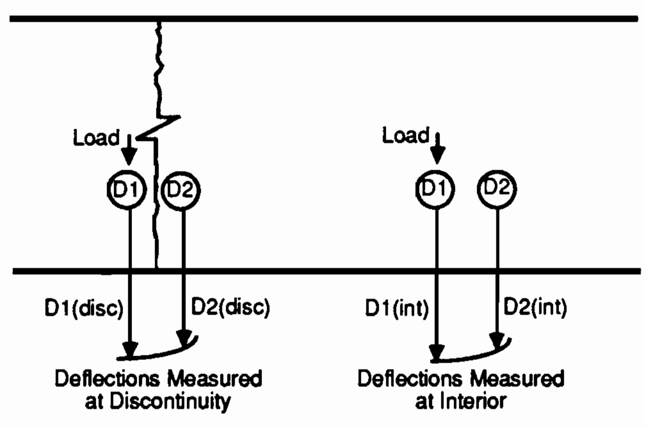

Fig 5.3. A concept of load transfer coefficient.

very close to one. Experimental evidence supporting these concepts has been reported (Ref 57).

$$\frac{\dfrac{D_2(disc)}{D_1(disc)}}{\dfrac{D_2(int)}{D_1(int)}} = LT \qquad (5.2)$$

where

LT = a possible indicator of load transfer, and

other parameters = those depicted in Fig 5.3.

The basic idea underlying the process of back-calculating stiffness of pavement layers is that, since elasticity moduli, load, geometric characteristics, and deflections are related, the former can be estimated from the rest. There are some programs that can take deflection basins, geometric characteristics, and loading as inputs and, using equations from layered theory, interactively select a combination of elasticity moduli that satisfies the specific combination of inputs (Refs 22, 27, and 47). Alternatively, the subgrade stiffness can be estimated from Westergaard equations (Ref 60) and the slab elasticity modulus from experimental data in other projects (Ref 16). Reference 57 presents a detailed comparative discussion about the adequacy of those methods. Whatever method is used, the pavement stiffness should ideally be back-calculated from the deflection basins measured at the interior of the slab, as far as possible from discontinuities. It has been suggested (Ref 33) that the interior slab measurement point be located in a spot within cracks at least eight feet from one another, in order to make sure that influences from discontinuities are not present in the deflection data taken at this spot. However, since inspection of crack spacing data taken in the 1987 condition survey indicates that not all test sections have maximum crack spacing greater than eight feet, it is recommended that the interior point be located between cracks spaced as closely as possible to the maximum spacing in the 1987 data.

Therefore, it is necessary to have the following deflection data in each test section:

(1) at the interior of the slab, to provide data for back-calculating pavement stiffness;

(2) at an edge, but far enough from a discontinuity to avoid its influence, to provide data for future studies of edge loading conditions; and

(3) at both sides and at a crack, to provide data for load transfer coefficients.

Figure 5.4 depicts a scheme for these five locations. Evidently, although the same type of data is

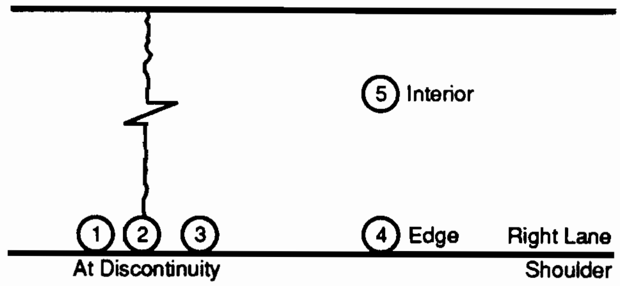

Fig 5.4. Scheme of the test locations in a non-overlaid section.

desired from the overlaid test sections, presence of the overlay does not permit the test points above to be located. An alternate procedure for the overlaid test sections is described in the next item. The number of replicates of the layout depicted in Fig 5.4 is discussed in the pertaining item.

LAYOUT OF DEFLECTION MEASUREMENTS ON AN OVERLAID TEST SECTION

Among the locations depicted in Fig 5.4, only the pavement edge can be identified with certainty in an overlaid test section. Evidently, locations arbitrarily selected in the interior of the pavement can be tested, but it is impossible to know for sure if there is some discontinuity, like a punchout, underneath it. No load transfer studies are possible, but back-calculation of layer moduli can still be done, and edge loading conditions can still be examined if enough replications are available for the edge and interior positions. The number of replications for both overlaid and non-overlaid cases are discussed below.

NUMBER OF REPLICATES

Once the trailer is positioned, the deflection measurement procedure itself is entirely automated and takes only about two minutes. Therefore, the governing factor in the time spent on each sub-section is the trailer alignment. Evidently, positioning the trailer in the interior of the slab does not take much time; however, accurate positioning of the loading plate at an edge or at a crack, takes more time. The amount of test sections to be surveyed, together with the fact that only the three summer months can be used for the diagnostic survey, recommends that a minimum amount of time be spent on each section, but not at the expense of accuracy.

Through conversations with experienced FWD operators it was found that the time needed to align the trailer in the more difficult positions might exceed five minutes. Since any plans to spend more than about an hour and a half per test section are not realistic in terms of the planned network-level survey, the maximum number of replicates per non-overlaid test section was limited to five. In the case of the overlaid sections, ten replicates were recommended, which were expected to take approximately the same time as the five replicates in the non-overlaid section, because the positioning of the trailer is easier. Moreover, the fact that the pavement has been overlaid means that discontinuities under the overlay are probably frequent, and a higher number of replicates is necessary to compensate for this.

SUMMARY

This chapter presented the development of the procedure for measuring deflections in the diagnostic survey, and a description of the equipment to use (the FWD). The procedure to apply at each point or station is given by the FWD manufacturer. This chapter discussed the objectives of the deflection measurements and the procedures to attain these, while observing the practical constraints imposed on the network-level survey.

CHAPTER 6. INSTRUCTIONS FOR THE DIAGNOSTIC SURVEY

BACKGROUND AND OBJECTIVE

The diagnostic survey undertaken in Project 472 involved the collection of three parameter types: crack width, deflections, and pavement temperature. While the previous chapters have described the development of procedures to obtain those data, this chapter summarizes those findings as instructions to the field crews, including field forms and other practical material. Most of the material presented in this chapter comes from Ref 55, a tech memo that serves as an instruction manual for field crews. The crews were also provided with maps and instructions on how to locate the test sections, and with additional data to help in deciding on the locations of the measurement stations. However, this material does not help in understanding the data collection procedure and it is therefore not included here.

One of the findings of Chapter 3 is that previous training is very important in achieving reliable and reproducible crack width measurements. Moreover, previous experience is required to operate the FWD. Thus, the instructions in this chapter are necessary but not sufficient for preparing a diagnostic survey. In Project 472, sessions were given in which questions were answered and specific training was provided; such an approach cannot be replaced by written instructions. Another report under this Project explains the preparations for the diagnostic survey, discusses the training lessons, and describes the field work needed to collect the data. It complements this report as guidance for future surveys.

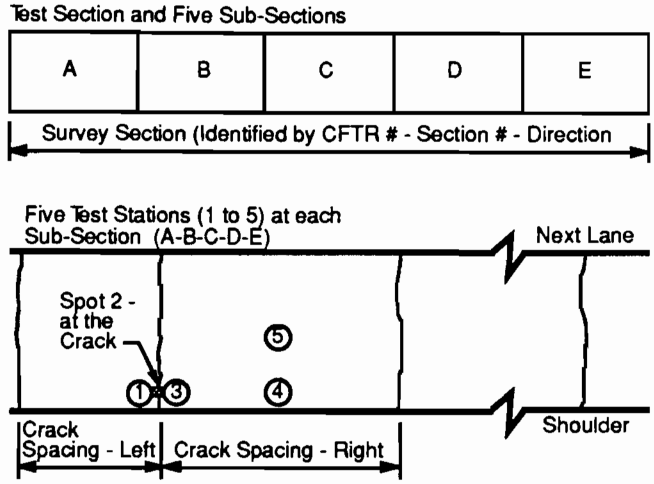

Fig 6.1. Non-overlaid test section: subsections and stations.

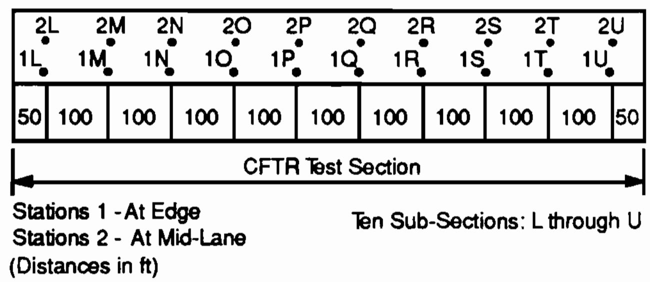

Fig 6.2. Overlaid test section subsections and stations.

PROCEDURES FOR MEASURING DEFLECTIONS

SUBSECTIONS FOR DEFLECTION MEASUREMENTS

Chapter 5 discusses the locations and the number of subsections in which deflections should be measured. This chapter concentrates on the procedure to apply at each subsection. Figure 6.1 shows a typical plan view of a non-overlaid test section divided into five subsections, each containing five stations at which to measure deflections. Figure 6.2 shows a plan view of the overlaid test section, with the ten subsections and the two stations at each subsection.

Although the identification of the stations can be assigned as the operator wishes, it is suggested that a unique identification be used throughout the survey. A possible identification system is suggested in Figs 6.1 and 6.2. Subsections are identified by letters A through E in the non-overlaid test sections, and L through U in the overlaid ones. Measurement stations are numbered 1 to 5 for the non-overlaid and 1 to 2 for the overlaid. This system ensures that subsections, i.e., the replicates the test section was divided into, are identified by letters, while stations within subsections are identified by numbers, for both overlaid and non-overlaid cases. In addition, the range of letters indicates whether or not the section is overlaid, thus eliminating the need for additional computer memory to store this information.

The temperature of the test slab should be recorded simultaneously with the deflection measurements in a coordinated procedure that is described below.

SELECTION OF THE TEST STATION LOCATION

Although theoretically the CRCP cracks are held together by the reinforcement (leading to no structural discontinuity), progressive damage may modify this condition. Thus, Chapter 5 suggests that station 5 (interior of the slab) should be located between two cracks as far apart as possible from one another, to ensure that the desired "interior load condition" is not more like "edge load condition." Crack spacing data were available from the previous condition survey, undertaken in 1987 (Ref 6). Thus, the field crews were provided with a printout of the minimum, average, and maximum crack spacings expected in each test section. They were instructed to make every effort to locate the measurement station between cracks spaced approximately as the maximum crack spacing; however, due to progressive cracking that may have occurred in the past year, it is possible that some sections have smaller crack spacings than the maximum values showed in the crack spacing data. For those cases, the crews were instructed to do their best to select stations located between cracks as far as possible from one another. Sometimes, it was known beforehand that a good "interior condition" could not be found, due to the small crack spacing observed in 1987. Because of those problems, the crack spacing at the deflection station was also recorded. The form used for this purpose is depicted in Fig 6.3. The same procedure should be applied in overlaid test sections if it is evident that the overlay presents reflective cracks that repeat the crack pattern of the pavement underneath. For overlays in good condition, the procedure for overlaid sections should be applied.

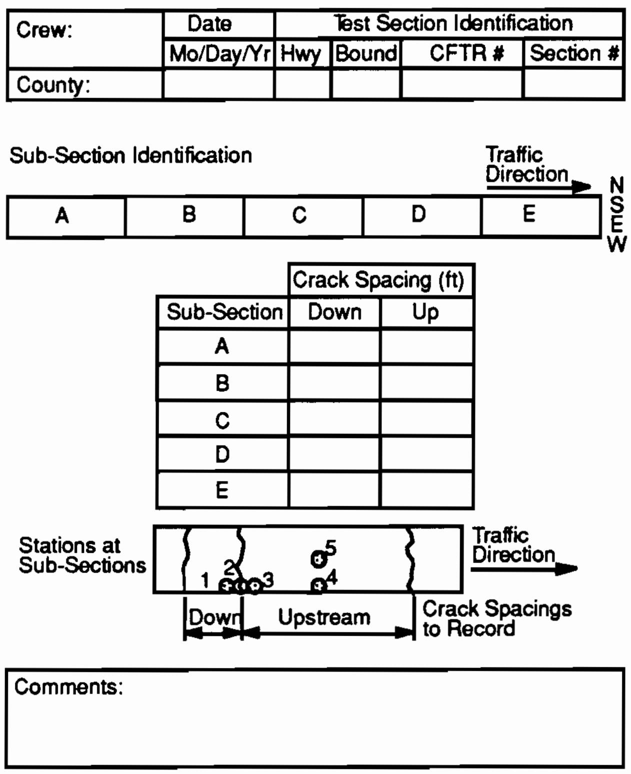

Fig 6.3. Station position form.

MASSES, HEIGHTS, AND GEOPHONE CONFIGURATION IN THE FWD

Due to practical difficulties in changing masses and configurations of the FWD, it is suggested that the standard mass of 200 kg (440 lb) be used throughout the experiment. All four drop heights should be used. The geophone configuration already set in each district can be used without change, as long as it is recorded clearly.

FIELD PROCEDURE

Once the trailer is correctly positioned at the station, one operator must stay in the van to monitor the FWD data acquisition system, while the other records pavement temperatures on the appropriate forms according to procedure described in the pertaining item. A third operator, a driver, is also necessary. Without this third person, the process will either slow down or require adjustments. Once all four drops are done, the trailer is moved to the next station and the procedure is repeated.

The stations in the interior of the slab need only to be visually positioned approximately halfway between the cracks. However, for measurements at the edge and at the cracks, the FWD must be positioned as close as possible to positions depicted at Fig 6.1, in order to obtain accurate data for edge load conditions. It is suggested that all edge stations be done first, for all subsections, as the trailer proceeds forward in the same line. Then, the trailer is moved back to the beginning of the test section, and the interior stations are surveyed. This method is better than proceeding forward in a zigzag, because of the practical difficulties in maneuvering and aligning the FWD trailer.

PROCEDURE FOR MEASURING CRACK WIDTH

SPECIFIC TRAINING

Chapter 3 results showed that it is extremely important that the operators receive a training lesson on how to measure crack width. Such a lesson was provided by CTR to the personnel sent out into the field to measure the crack widths. This lesson is documented in another report about the preparations for the survey and the field work.

SELECTION OF THE CRACKS

Three cracks should be selected out of every test section in order to represent cracks closely spaced, average spaced, and widely spaced. As mentioned above, the operators were provided with the figures of the minimum, maximum, and mean crack spacing for each particular section. Time and personnel availability restricted the number of cracks per test section to three, although more replicates would be desirable.

With the help of the rolotape and the data provided on minimum, maximum, and mean crack spacing, the operator looked for three cracks that had approximately these spacings from their neighboring cracks. In addition, all efforts should be made to find cracks that are approximately equally spaced from their neighbors; it is

Instructions for Filling the Crack Width Form	Date	Test Section Identification			
	Mo/Day/88	Hwy	CFTR Number	Test Section #	Bound

Crack	Closely Spaced	Medium Spaced	Widely Spaced
Crack Spacing	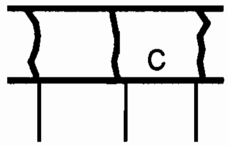	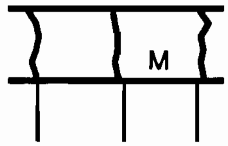	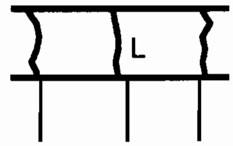
Microscope Readings			

Special Situations				
	Tick if Applicable	☐ Spacing Smaller than Expected	☐ Spacing Smaller than Expected	☐ Spacing Smaller than Expected
		☐ Spalled or Stepped Crack	☐ Spalled or Stepped Crack	☐ Spalled or Stepped Crack
		☐ Unable to Find Big Patch	☐ Unable to Find Big Patch	☐ Unable to Find Big Patch
		☐ Overlay / Seal Coat		☐ Sealed Cracks
		☐ Crack Spacing Approximately Constant		
		☐ Test Section Marks Were Not Visible		
	Other (Please Describe)			

Fig 6.4. Crack width form.

recognized, though, that this type of spacing cannot be found in every test section.

Chapter 3 explains the problems that can be found in reading crack width. In order to save time, it is advisable to take one or two tentative readings of each preliminary selected crack. If it seems that the crack is the kind of crack to be avoided, another selection should be made.

It is suggested that the selected cracks be marked so as to relate them with the crack spacing. For instance, they can be marked C (for close spacing), M (for mean spacing), and W (for wide spacing). The spacing between the selected crack and the two neighboring cracks should be measured with the rolotape and marked on the form in the appropriate box. Figure 6.4 depicts the form for recording the crack width readings and the spacings from the surveyed crack to its neighbors.

PROCEDURE TO TAKE THE READINGS

Once the cracks to be measured are selected, the operator should take six readings out of each in a time interval preferably no longer than two hours. The time constraint is important in order to make absolutely sure that crack opening and closing due to temperature differentials will not affect the results of the experiment to any extent, since it is arguable whether or not those thermal movements are detectable by the 0.001-inch microscope. Because crack width readings usually take no more than fifteen minutes per crack, the time constraint is not expected to be a problem. The readings should be recorded in the appropriate columns on the crack width form.

Each reading should be taken at a different location along the crack. At each location, the operator, using his or her best judgment, should attempt to put the microscope in what appears to be a non-spalled, non-faulted area. The operator should then focus the microscope, carefully sliding it back and forth until he/she is confident that what is being seen is actual width and not microscopic spalling or the distance between the crack wall and a piece of pulled-off aggregate: the former case gives falsely large widths, whereas the latter can yield falsely narrow readings. Figure 6.5 sketches those cases. In addition, faulted cracks are difficult to read because their edges are at two different levels, and, since the microscope can focus on only one level at a time, one side will always be fuzzy, thus increasing the possibilities for error in the readings. All those cases were discussed in Chapter 3 and were illustrated in the training lesson to the field crews.

Once the first reading is taken, the operator should write it down on the form and then repeat the procedure for another location randomly selected at the same crack. If the selected crack turns out to be spalled or faulted or both, it is recommended that another selection be made, if possible, to avoid bad results.

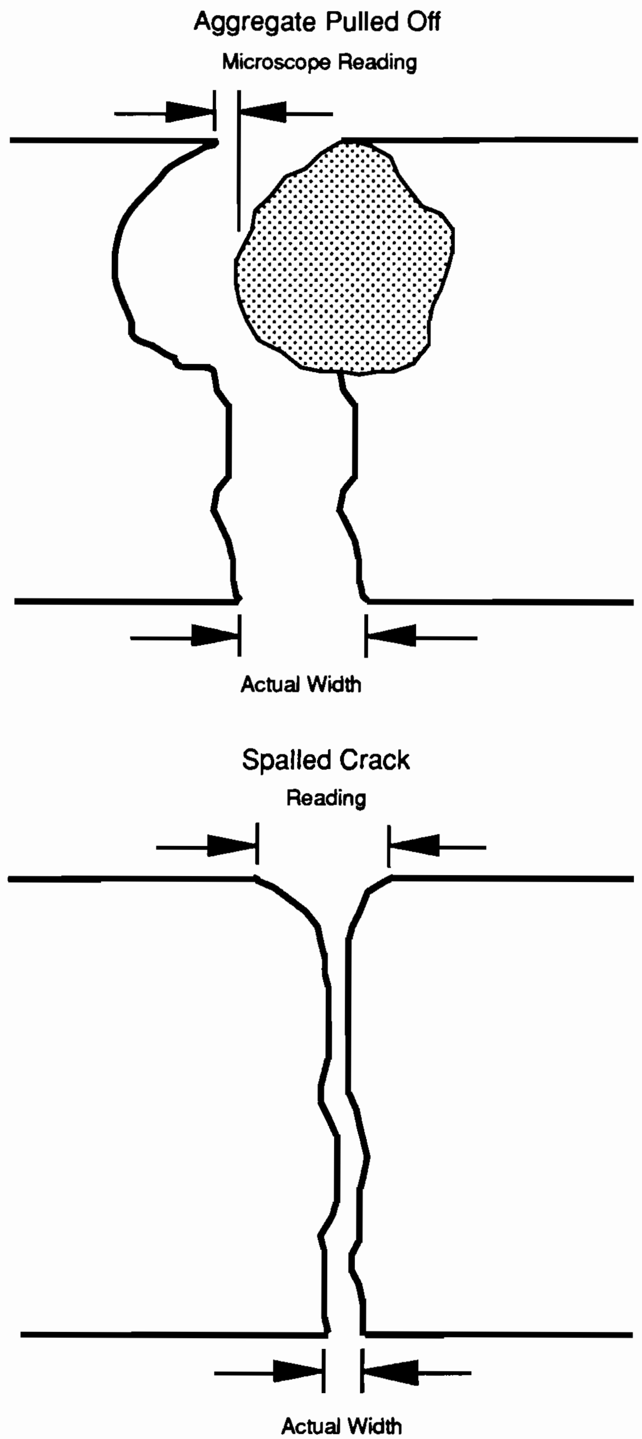

Fig 6.5. Situations to avoid in crack width readings.

In the experiment reported in Chapter 3, it was observed that the reading of crack widths requires the use of a pillow or small mat to provide a cushion against the rough (and, in the summer, hot) pavement.

PROBLEMS THAT CAN BE EXPECTED AT SOME TEST SECTIONS

(1) ***Changes in Crack Spacing.*** Data on crack spacing provided to the field crew were based on the statewide condition survey undertaken in 1987. Therefore, it is possible that by 1988 the crack spacing was smaller, due to progressive cracking of the test section. If this is the case, the operators should select three cracks to represent what they visually see as close, mean, and wide spacing, and then check, in the crack width form (Fig 6.4), the appropriate box stating that this problem has occurred.

(2) ***Crack Spalling.*** Results of the study undertaken on crack width have shown that readings in spalled or faulted cracks do not give reliable results. There may be cases in which the operator is not able to find representative cracks that will give reliable results because, for instance, all the cracks are spalled. In this case, the appropriate box must be checked on the form to indicate that the particular crack or cracks are subject to high error.

(3) ***Constant Crack Spacing.*** In some test sections the crack spacing is approximately constant, and available data on crack spacing can reveal this fact beforehand. In these cases, the operator just checks the appropriate box in the crack width form and selects the cracks only on the basis of reading ease.

(4) ***Other.*** Inspection of crack spacing data shows that it is difficult to find cracks approximately equally spaced for several test sections. Nothing can be done about this, but awareness of this fact is very important for further data analysis, especially if some unexpected behavior or trend must be explained.

PROCEDURE TO MEASURE PAVEMENT TEMPERATURE

TEMPERATURE READINGS

Chapter 4 describes the development of a procedure for estimating pavement temperatures from those in a portable slab (which should be put at the test site at least six hours before starting the deflection measurements). Those portable slabs have thermocouples embedded in them, and there are three pairs of wires emerging from the slabs, identified with tags stating top, mid-depth, and bottom. Chapter 4 describes the portable slabs and explains how the thermocouple works.

To take a reading, the operator simply puts the wires in the appropriate slots of the thermocouple reader and writes down the number in the appropriate box on the form depicted in Fig 6.6. One set of readings, spaced every half-hour, should be taken for each test section.

It is important that the test slab and the pavement be subject to the same environmental conditions. Otherwise, it is evident that the portable slab readings will not reflect the pavement temperature. Thus, the following procedure should be followed in moving the portable slab from one test section to another:

- place the portable slab near one test section the night before the measurements;
- finish the job at the section the next day;
- put the portable slab in the van and drive to the next section;
- if trip time does not exceed about one hour, begin work in the next section immediately;
- if the lunch break will occur between measurement of two test sections, put the portable slab at the next section *before* lunch. (In the summer, excessive heat inside a car parked in the sun may make the portable slab hotter than the pavement and the temperature readings will be wrong.)

In the majority of cases, the test sections will be very close to each other. Significant changes in the portable slab temperature equilibrium are not expected to occur in a short time frame due to the insulation around the portable slab. However, it is advisable to cover it with material with some thermal insulation capability during short trips between test sections.

In overlaid sections, the portable slab temperature does not reflect exactly the pavement temperature. An estimate of the overlay temperature is also necessary in this case. The following devices are available for estimating pavement surface temperature:

- pyronometer,
- surface thermometer (flat surface for contact), and
- digital thermometer (probe for contact).

The accuracy and repeatability of all those instruments was checked as a part of the routine preparations for the survey. In addition, a training lesson on these readings was provided to the new personnel. Those studies, and the training lesson, are described in the next report about the diagnostic survey.

OTHER POSSIBLE PROBLEMS

Other problems that may occur include

(1) an overlaid or sealed test section,
(2) sealed cracks,
(3) a partially patched test section, and
(4) a test section at which marks are no longer visible.

Occurrence of the first problem is automatically recorded by means of the procedure used for measuring the deflections.

Occurrence of the second prevents crack width readings, but the FWD testing should proceed normally. The appropriate box should be marked in the crack width form.

Crew:	Date	Test Section Identification			
	Mo/Day/Yr	Hwy	Bound	CFTR #	Section #
County:					

Thermocouple Location	Temperature	Time
Surface		
Mid-Depth		
Bottom		
Tick Unit	°C °F	

Comments:

Fig 6.6. Temperature form.

Occurrence of the third should be treated as occurrence 1 is treated, as far as deflections are concerned. If it also affects crack width, the appropriate box should be marked in the crack width form.

Occurrence of the fourth problem can be overcome by using the instructions on locating the specific section, which usually include the distance from the closest mile post to the starting point of the section. The ending point is usually 1000 feet away from the starting point. The actual section length, however, was also provided. The section characteristics (cut, fill, at grade, or transition) were provided to make it easier for the crews to find the test sections. These data should be used to relocate the section when the marks made in 1987 are not visible. The appropriate box in the crack width form should be checked.

LIST OF MATERIAL

The material for each crew includes:

(1) 1 microscope precise to 0.001 inch;
(2) 1 portable slab;
(3) 1 thermocouple reader;
(4) crack width forms;
(5) temperature forms;
(6) station position forms;
(7) 1 set of maps with the Project locations;
(8) the database with the test section numbers, specific location, and length;
(9) data on expected crack spacings for every test section;
(10) 10 Floppy disks for FWD data storage;
(11) 10 tags for identifying the floppy disks;
(13) 1 rolotape;
(14) 1 pad or mat for kneeling on; and
(15) 10 cans of paint for marking the cracks.

SUMMARY

At the end of work on a test section (and if no problems were discovered), the following data should have been collected:

- A complete set of deflection measurements (four drop heights) at all stations, of each of the subsections, i.e., 100 deflection measurements for the non-overlaid sections and 80 for the overlaid.
- Five station position forms (Fig 6.3), one for each subsection, filled-in with the crack spacings around the station, for each subsection in the non-overlaid sections.
- One set of temperatures of the portable slab, i.e., one filled-in temperature form for each test section. If the deflection measurements took more than half an hour, an additional temperature form should have been completed. In the case of the overlaid sections, surface temperature should have also been measured, for every subsection. The device used should also have been recorded. Alternatively, this temperature can be entered in the computer that records the FWD measurements.
- Six crack width readings in each of the three selected cracks, i.e., 18 crack width readings; this makes one crack width form (Fig 6.4) per non-overlaid test section.

Whenever any of the special situations previously discussed occurs, the appropriate box in the forms should be checked. If any unexpected situation does occur that prevents the procedures above from being fully executed, the situation should be briefly described in the space on the forms provided for comments. Any other significant or unusual occurrence should also be reported in the comments.

REFERENCES

1. American Association of State Highway Officials, "AASHTO Guide for Pavement Structures," Vol 1, 1986.
2. American Association of State Highway Officials, "AASHTO Guide for Pavement Structures," Vol 2, 1986.
3. Anderson, V. L., and R. A. McLean, *Design of Experiments – A Realistic Approach*, Marcel Dekker Inc., 1974.
4. Barber, E. S., "Calculation of Maximum Pavement Temperatures from Weather Reports," HRB Bulletin #168, Highway Research Board, Washington, D. C., 1957.
5. Brook, R. J., and G. C. Arnold, *Applied Regression Analysis and Experimental Design*, Marcel Dekker Inc., 1985.
6. Chou, Chia-Pei, "Development of a Long-Term Monitoring System for Texas CRC Pavement Network," Research Report 472-2, Center for Transportation Research, The University of Texas at Austin, 1988.
7. Cuthbert, D., and F. S. Wood, *Fitting Equations to Data*, John Wiley & Sons, 1971.
8. Dossey, T., "Condition Survey Data Base," Tech Memo 472-23, Center for Transportation Research, The University of Texas at Austin, April 1988.
9. Gebhart, B., *Heat Transfer*, McGraw Hill Co., 1961.
10. Glass, G. V., V. L. Wilson, and J. M. Gottmann, *Design and Analysis of Time Series Experiments*, Colorado Associated University Press, 1975.
11. Haas, R., and W. R. Hudson, *Pavement Management Systems*, Robert E. Krieger Publishing Co., Fl., 1978.
12. "Synthesis of Highway Practice, Continuously Reinforced Concrete Pavements," NCHRP 16, Highway Research Board, Washington, D. C., 1973.
13. Kendall, M., and A. Stuart, "The Advanced Theory of Statistics," Vol 3, Design and Analysis and Time Series, Charles Griffin & Co., London, 1968.
14. Kleinbaum, D. G., and L. L. Kupper, *Applied Regression Analysis and Other Multivariable Methods*, Duxbury Press, 1978.
15. Lindsay, J. D., "A Ten-Year Report on the Illinois Continuously Reinforced Concrete Pavements," HRB Bulletin #214, Highway Research Board, Washington, D. C., 1959.
16. Lu, Jian, "Test of Significance Impact of Aggregate Type on ft, fc, E, Z, and ac," Tech Memo 422-39, Center for Transportation Research, The University of Texas ar Austin, September 1988.
17. Lundy, J., "Background Documentation of IAC 1530," Tech Memo 1503-1, Center for Transportation Research, The University of Texas at Austin, April 1987.
18. Lundy, J., "Design of Project 1530 Test Sections," Tech Memo 1503-2, Center for Transportation Research, The University of Texas at Austin, May 1987.
19. Lundy, J., "Equivalencies of Trucks Used on the Attorney General's Test Sections," Tech Memo 1503-3, Center for Transportation Research, The University of Texas at Austin, October 1987.
20. Lybas, J. M., et al, *Evaluation of Concrete Test Pavement Using the FWD and WESLIQUID*, University of Florida, 1985.
21. Lytton, R. L., W. M. Moore, and J. P. Mahoney, "Pavement Evaluation: Phase 1, Pavement Evaluation Equipment," FHWA-RD-75-78, Final Report, 1975.
22. Majdazeh, K., "Pavement Condition Evaluation Using Dynamic Deflection Measurements," Research Report OHIO-DOT-13-77, FHWA, 1977.
23. McCullough, B. Frank, and P. J. Strauss, "A Performance Survey of Continuously Reinforced Concrete Pavements in Texas," Research Report 21-1F, Center for Highway Research, The University of Texas at Austin, 1974.
24. McCullough, B. Frank, "Development of Equipment and Techniques for a Statewide Rigid Pavement Deflection Study," Research Report 46-1, Center for Highway Research, The University of Texas at Austin, January 1965.
25. McCullough, B. Frank, and H. Treybig, " Determining the Relationship of Variables in Deflection of Continuously Reinforced Concrete Pavements," Technical Report 46-4, 1965.

26. McCullough, B. Frank, A. Abou-Ayyash, W. R. Hudson, and J. Randall, "Design of Continuously Reinforced Concrete Pavements for Highways," NCHRP Research Report 1-15, 1975.

27. Michalak, C. H., et al, "Determining Stiffness Coefficients and Elastic Moduli of Pavement Materials from Dynamic Deflections," Research Report 207-1, Texas A&M University, 1976.

28. Miner, R., "Temperature Differential Prediction Techniques," Research Status Report for Project 460, Center for Transportation Research, The University of Texas at Austin, January 1988.

29. Nelson, C. R., *Applied Time Series Analysis for Managerial Forecasting*, Holden Days Inc., 1973.

30. Omega Engineering Inc., *Complete Temperature Measurement Handbook and Encyclopedia*, Omega Engineering Inc., 1987.

31. Price, G. E., "Curling of Rigid Pavement Slabs Due to Temperature," Master's Thesis, The University of Texas at Austin, 1987.

32. Ryan, B., et al., *Minitab Handbook*, Second Edition, Duxbury Press, 1796.

33. Saraf, C., "Project 472 Condition Surveys Deflection Data," Tech Memo 472-22, Center for Transportation Research, The University of Texas at Austin, January 1988.

34. Saraf, C., B. Frank McCullough, and W. R. Hudson, "Condition Surveys and Pavement Evaluation of Existing and Overlaid Rigid Pavements," Research Report 388-5F, Center for Transportation Research, The University of Texas at Austin, 1985.

35. SAS Institute Inc., *SAS User's Guide: Basics*, Version 5, SAS Institute Inc., 1982

36. SAS Institute Inc., *SAS/User's Guide: Statistics*, SAS Institute Inc., 1984.

37. SAS Institute Inc., *SAS/ETS User's Guide*, SAS Institute Inc., 1984.

38. Shahin, M. Y., and B. Frank McCullough, "Prediction of Low Temperature and Thermal Fatigue Cracking in Flexible Pavements," Research Report 123-14, Center for Highway Research, The University of Texas at Austin, 1972.

39. Snedecor, G. W., and W. G. Cochran, *Statistical Methods*, The Iowa State University Press, 7th Edition, 1982.

40. Strauss, P. J., J. Long, and B. Frank McCullough, "Development of Photographic Techniques for Performing Condition Surveys," Research Report 177-10, Center for Highway Research, The University of Texas at Austin, 1977.

41. Taute, A., and B. Frank McCullough, "Manual for Condition Survey of Continuously Reinforced Concrete Pavements," Research Report 177-19, Center for Transportation Research, The University of Texas at Austin, 1981.

42. Taylor, I. J., and W. J. Eney, "First Year Performance Report on Continuously Reinforced Concrete Pavements in Pennsylvania," HRB Bulletin #214, Highway Resarch Board, Washington, D. C., 1959.

43. Torres-Verdin, V., and B. Frank McCullough, "Effect of Environmental Factors and Loading Position on Dynaflect Deflections in Rigid Pavements," Research Report 249-4, Center for Transportation Research, The University of Texas at Austin, February 1982.

44. Torres-Verdin, V., C. L. Saraf, and B. Frank McCullough, "Evaluation of the Effect of Survey Speed on Network-Level Collection of Rigid Pavement Distress Data," Research Report 388-2, Center for Transportation Research, The University of Texas at Austin, 1984.

45. Tremper, B., "Continuously Reinforced Concrete Pavements in California after Eight Years Service," HRB Bulletin #214, Highway Research Board, Washington, D. C., 1959.

46. Treybig, H., "Performance of Continuously Reinforced Concrete Pavement in Texas," Research Report 46-8, Texas Highway Department, 1968.

47. Uddin, W., et al., "A Structural Evaluation Methodology for Pavements Based on Dynamic Deflections," Research Report 387-1, Center for Transportation Research, The University of Texas at Austin, July 1985.

48. Van Breemen, W., "A Ten-Year Report on Experimental Continuously Reinforced Concrete Pavements in New Jersey," HRB Bulletin #214, Highway Research Board, Washington, D. C., 1959.

49. Vedros, P., and W. R. Barker, "Case Studies of Pavement Performance. Phase 1 – Kentucky," FHWA-RD-77-103, Final Report, 1977.

50. Velasco, M. G., and B. Frank McCullough, "Summary for 1978 CRCP Condition Survey in Texas," Research Report 177-20, Center for Transportation Research, The University of Texas at Austin, 1981.

51. Wei, Chao, "Summary of the Methods for Obtaining J-value," Tech Memo 1169-12, Center for Transportation Research, The University of Texas at Austin, February 1989.

52. Weissmann, A. J., " Storage System and Nature of 1988 Survey Data," Tech Memo 472-32, Center for Transportation Research, The University of Texas at Austin, November 1988.

53. Weissmann, A. J., "Crack Width Measurements on CRCP," Tech Memo 472-19, Center for Transportation Research, The University of Texas at Austin, 1987.

54. Weissmann, A. J., "Experimental Designs for Crack Width and Slab Temperature Analysis," Tech Memo 472/21, Center for Transportation Research, The University of Texas at Austin, 1987.

55. Weissmann, A. J., "Instructions and Procedures for Measuring: Crack Width, Pavement Temperature, and Pavement Deflections with the FWD," Tech Memo 472-24, Center for Transportation Research, The University of Texas at Austin, July 1988.

56. Weissmann, A. J., "Preliminary Analysis of Slab Temperature Data," Tech Memo 472-20, Center for Transportation Research, The University of Texas at Austin, 1987.

57. Weissmann, A. J., "Sources of Data for the Performance Prediction Model," Tech Memo 472-36, Center for Transportation Research, The University of Texas at Austin, 1989.

58. Weissmann, A. J., and T. Dossey, "Comprehensive, User-Directed Description of the Statewide CRCP Condition Survey Data Base," Tech Memo 472-30, Center for Transportation Research, The University of Texas at Austin, September 1988.

59. Weissmann, A. J., "Diagnostic Data – Definitive Address of the Data Sets," Tech Memo 472-34, Center for Transportation Research, The University of Texas at Austin, December 1988.

60. Westergaard, H. M., "New Formulas for Stresses in Concrete Pavements for Airfields," *Transactions*, ASCE, Vol 133, Paper #2340, 1948.

61. White, F. M., *Heat and Mass Transfer*, Reading, Mass., 1988.

62. White, R., W. R. Hudson, A. H. Meyer, and K.H. Stokoe, II, "Design and Construction of a Rigid Pavement Research Facility," Research Report 355-1, Center for Transportation research, The University of Texas at Austin, September 1984.

63. Witkosky, F. C., and R. K. Shaffer, "Continuously Reinforced Concrete Pavements in Pennsylvania," HRB Bulletin #214, Highway Research Board, Washington, D. C., 1959.

64. Yoder, E., and M. W. Witzac, *Principles of Pavement Design*, John Wiley & Sons, Inc., N.Y., 1975.

65. Yoder, E. J., and R. T. Milhous, "Comparison of Different Methods of Measuring Pavement Condition," NCHRP, Interim Report #7, 1964.

66. Zuk, W., "Analysis of Special Problems in Continuously Reinforced Concrete Pavements," HRB Bulletin #214, Highway Research Board, Washington, D. C., 1959.

APPENDIX. RAW TEMPERATURE DATA FOR CHAPTER 4

This appendix presents the raw data pertaining to Chapter 4, "Development of Procedure for Estimating Pavement Temperature." The data are presented graphically in the form of plots of temperature versus time. The four data sets used in the analysis are presented in numerical order. Each plot shows temperatures at a given thermocouple location for the two portable slabs of the same thickness and for the pavement.

Figures A.1 to A.9 refer to data set 1, Figs A.10 to A.18 to data set 2, Figs A.19 to A.27 to data set 3, and Figs A.28 to A.36 to data set 4.

The following abbreviations are used in these figures:

RG-6": temperatures at the 6-inch-thick river gravel portable slab;

RG-10": same, 10-inch-thick;

RG-14": same, 14-inch-thick;

LS-6": temperatures at the 6-inch-thick limestone portable slab;

LS-10": same, 10-inch-thick; and

LS-14": same, 14-inch-thick.

PAVEMENT: temperatures at thermocouples in BRC test slab for thermocouple location 3 in Fig 1.2, Chapter 1.

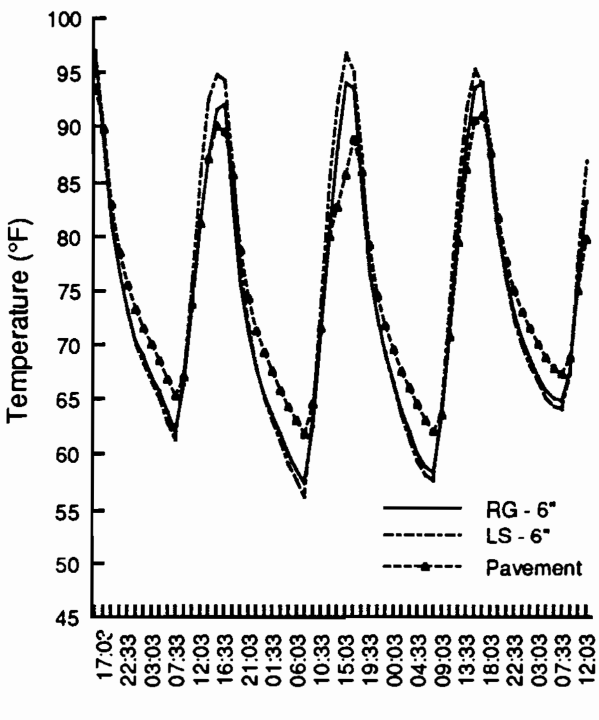

Fig A.1. Temperatures at top thermocouples, data set 1, 6-inch-thick portable slabs.

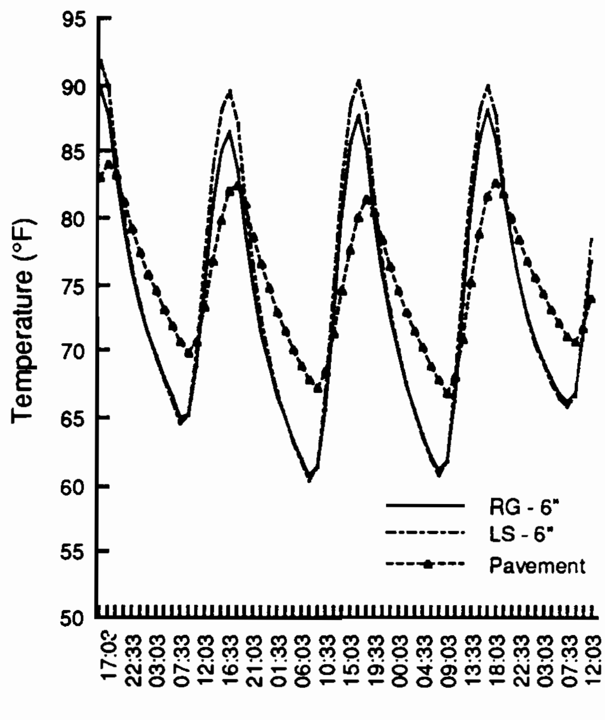

Fig A.2. Temperatures at mid-depth thermocouples, data set 1, 6-inch-thick portable slabs.

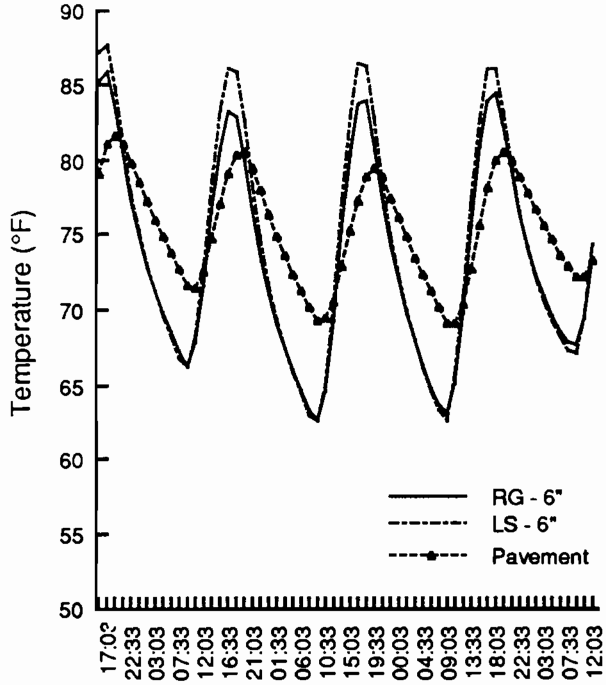

Fig A.3. Temperatures at bottom thermocouples, data set 1, 6-inch-thick portable slabs.

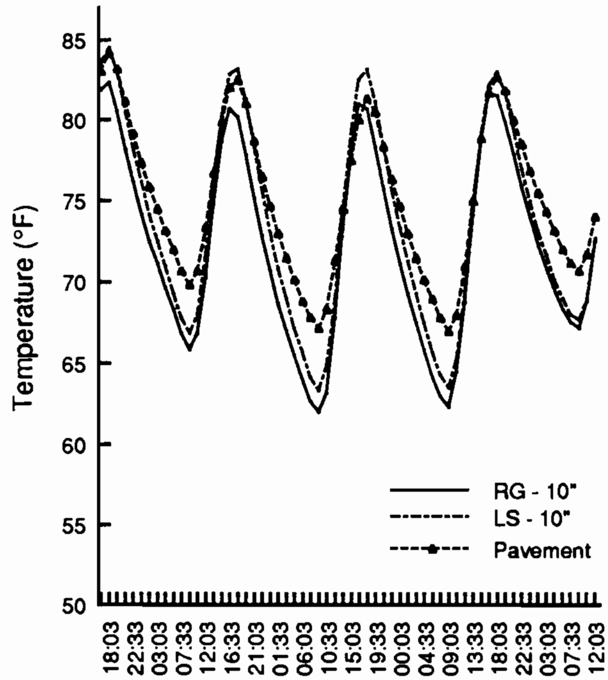

Fig A.5. Temperatures at mid-depth thermocouples, data set 1, 10-inch-thick portable slabs.

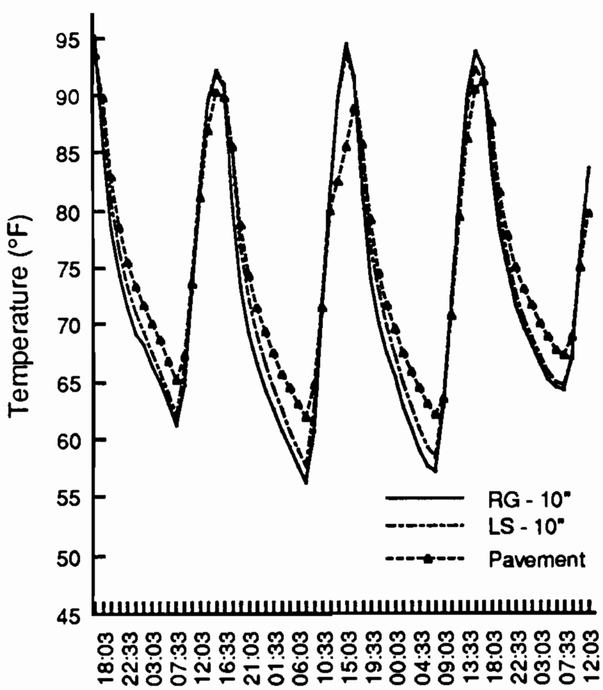

Fig A.4. Temperatures at top thermocouples, data set 1, 10-inch-thick portable slabs.

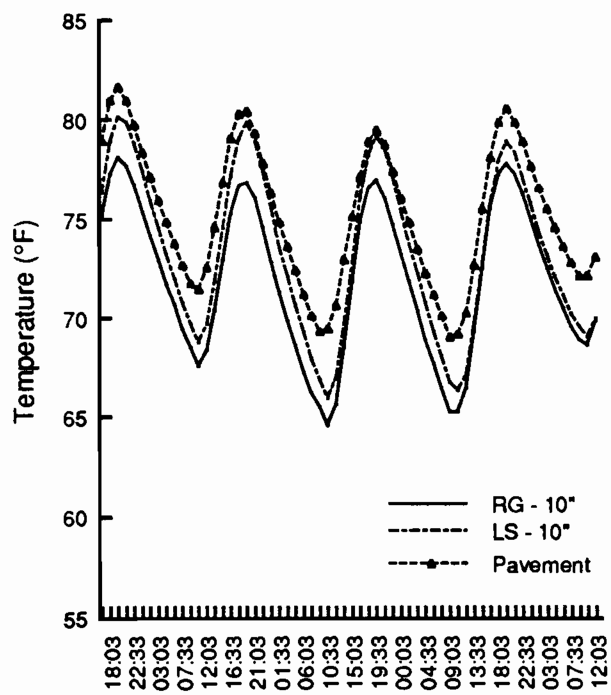

Fig A.6. Temperatures at bottom thermocouples, data set 1, 10-inch-thick portable slabs.

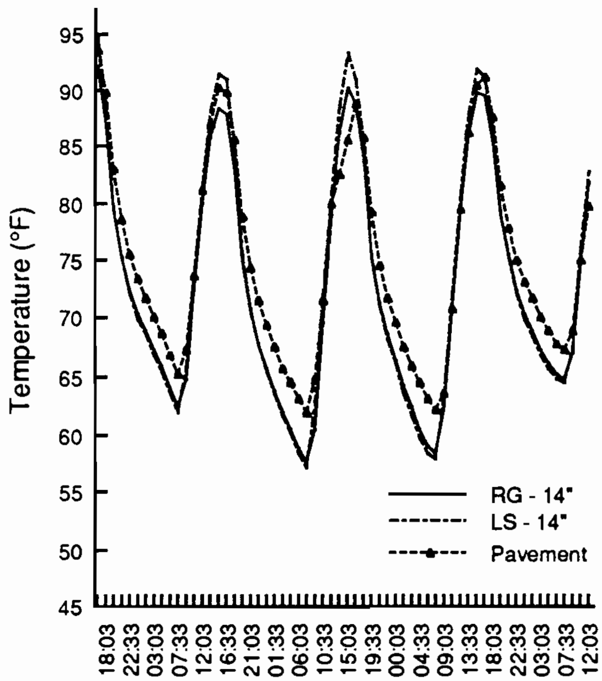

Fig A.7. Temperatures at top thermocouples, data set 1, 14-inch-thick portable slabs.

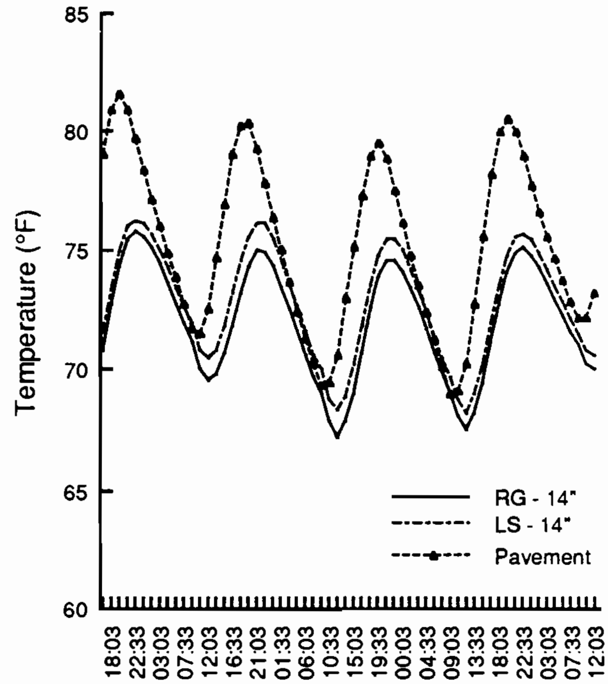

Fig A.9. Temperatures at bottom thermocouples, data set 1, 14-inch-thick portable slabs.

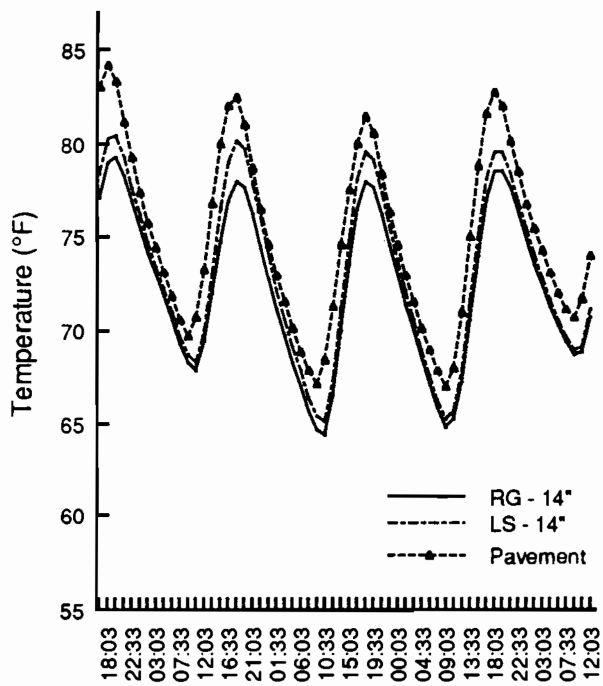

Fig A.8. Temperatures at mid-depth thermocouples, data set 1, 14-inch-thick portable slabs.

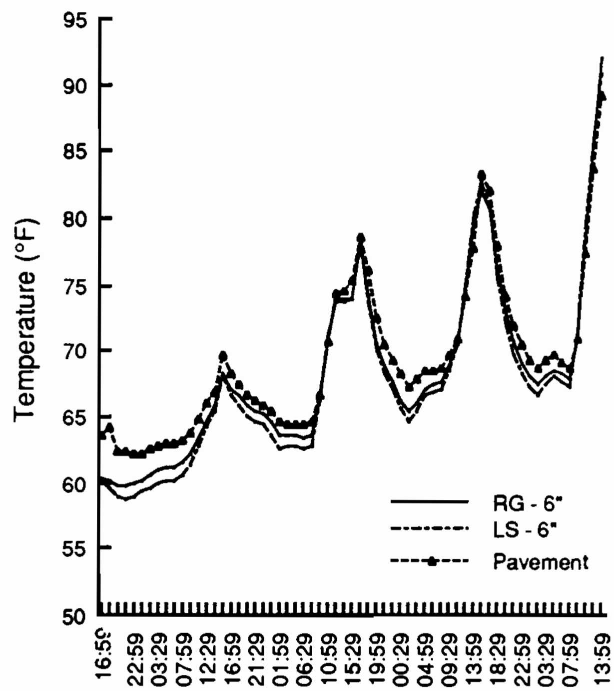

Fig A.10. Temperatures at top thermocouples, data set 2, 6-inch-thick portable slabs.

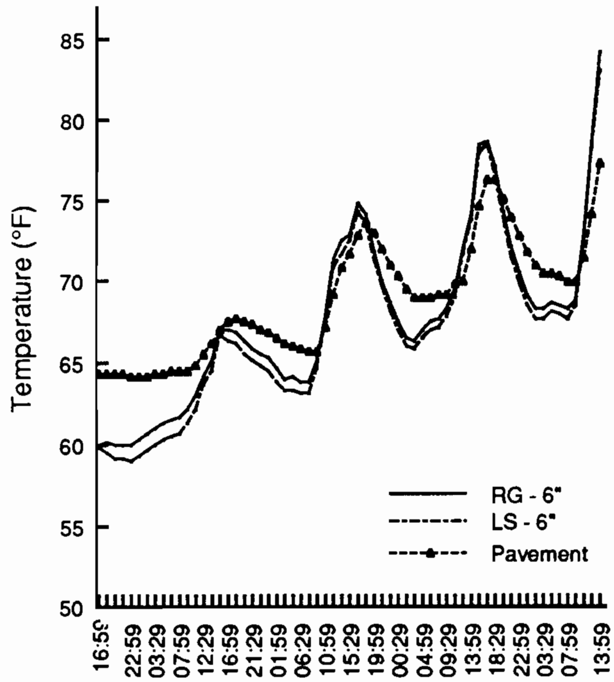

Fig A.11. Temperatures at mid-depth thermocouples, data set 2, 6-inch-thick portable slabs.

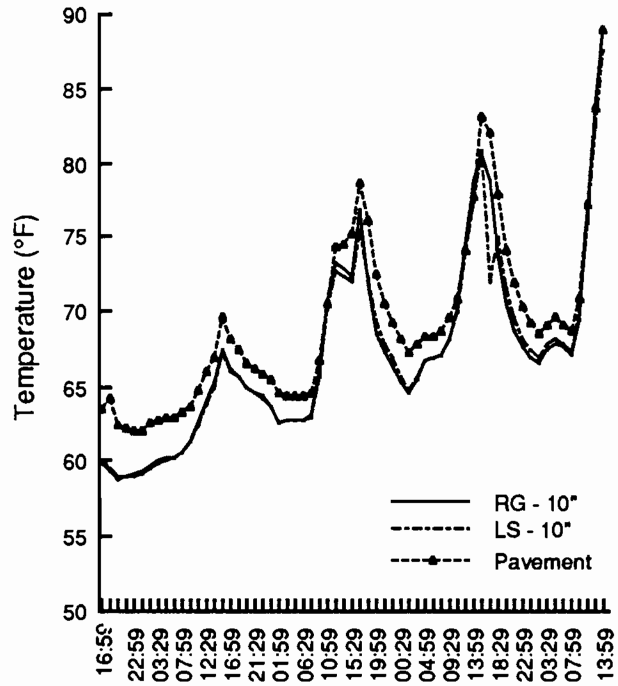

Fig A.13. Temperatures at top thermocouples, data set 2, 10-inch-thick portable slabs.

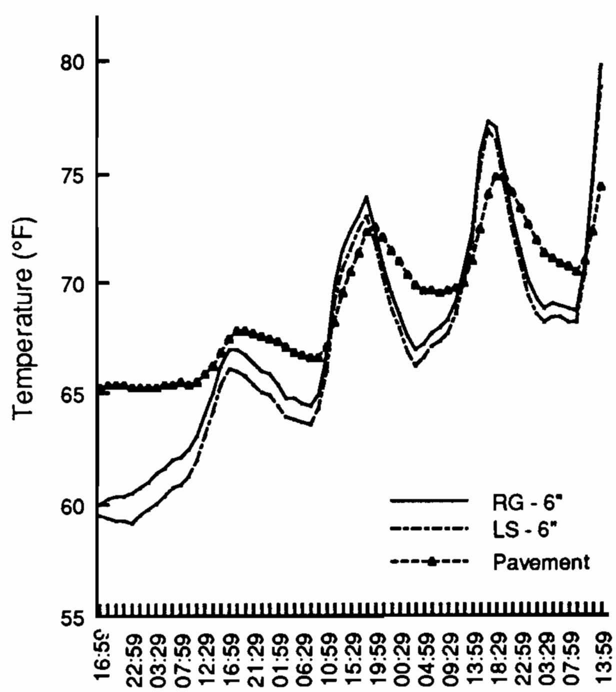

Fig A.12. Temperatures at bottom thermocouples, data set 2, 6-inch-thick portable slabs.

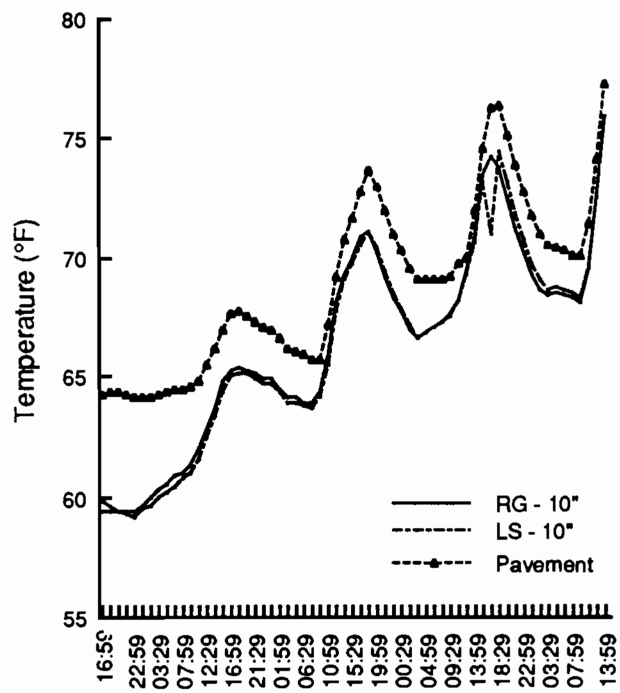

Fig A.14. Temperatures at mid-depth thermocouples, data set 2, 10-inch-thick portable slabs.

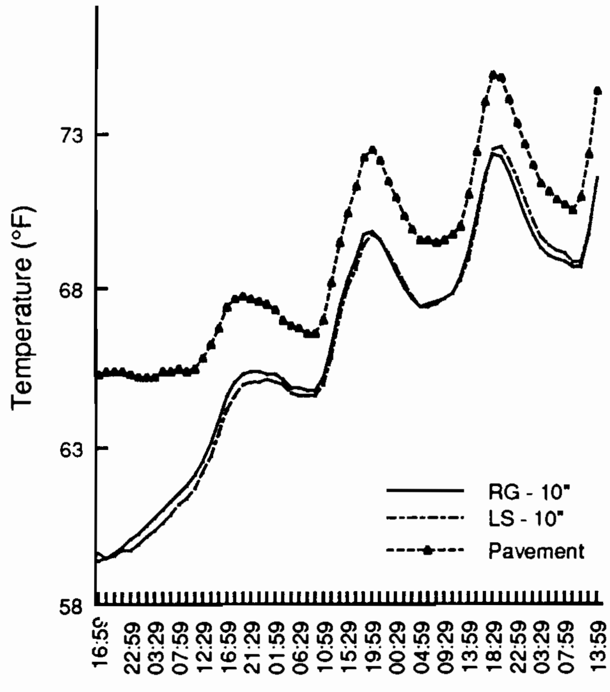

Fig A.15. Temperatures at bottom thermocouples, data set 2, 10-inch-thick portable slabs.

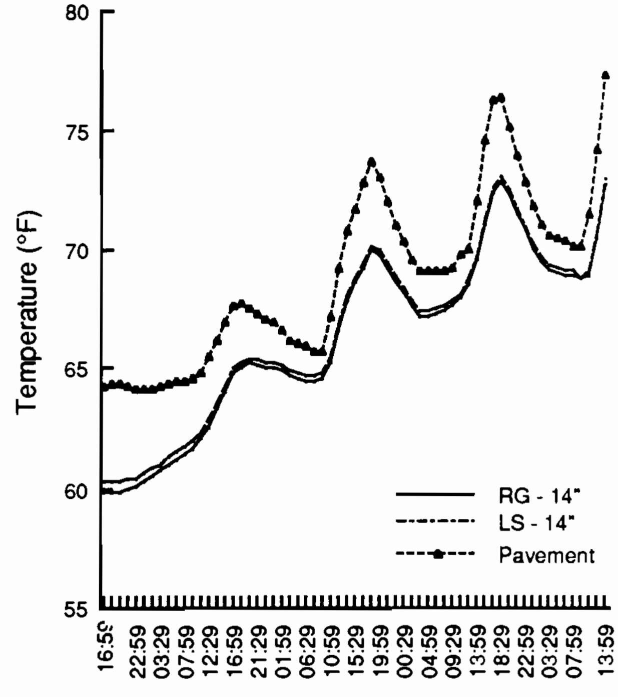

Fig A.17. Temperatures at mid-depth thermocouples, data set 2, 14-inch-thick portable slabs.

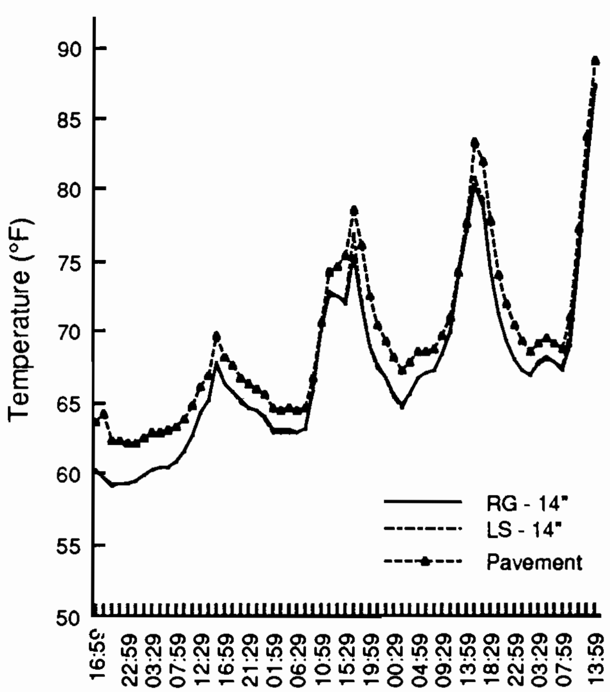

Fig A.16. Temperatures at top thermocouples, data set 2, 14-inch-thick portable slabs.

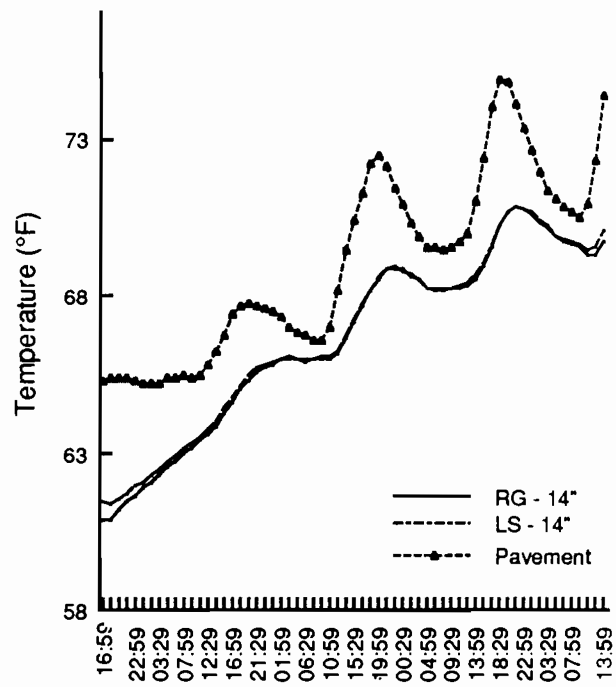

Fig A.18. Temperatures at bottom thermocouples, data set 2, 14-inch-thick portable slabs.

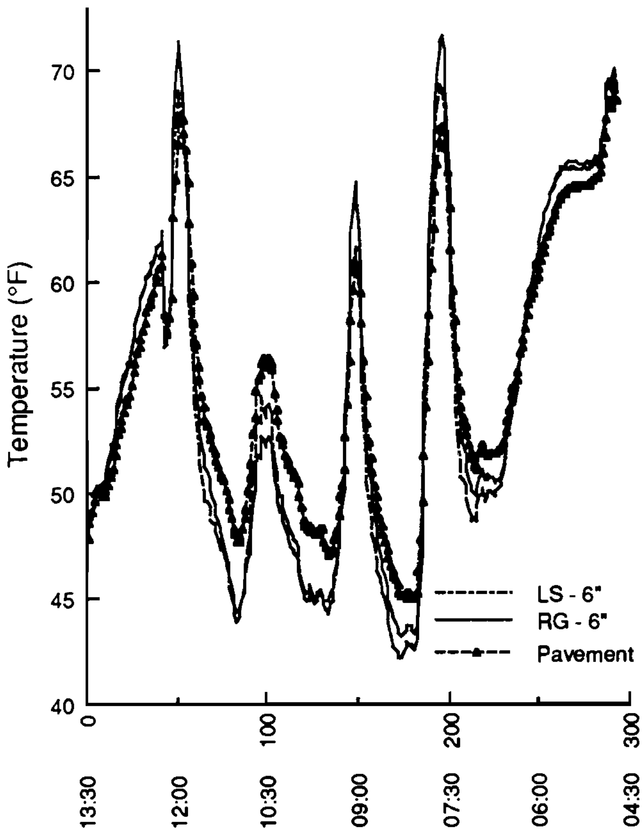

Fig A.19. Temperatures at top thermocouples, data set 3, 6-inch-thick portable slabs.

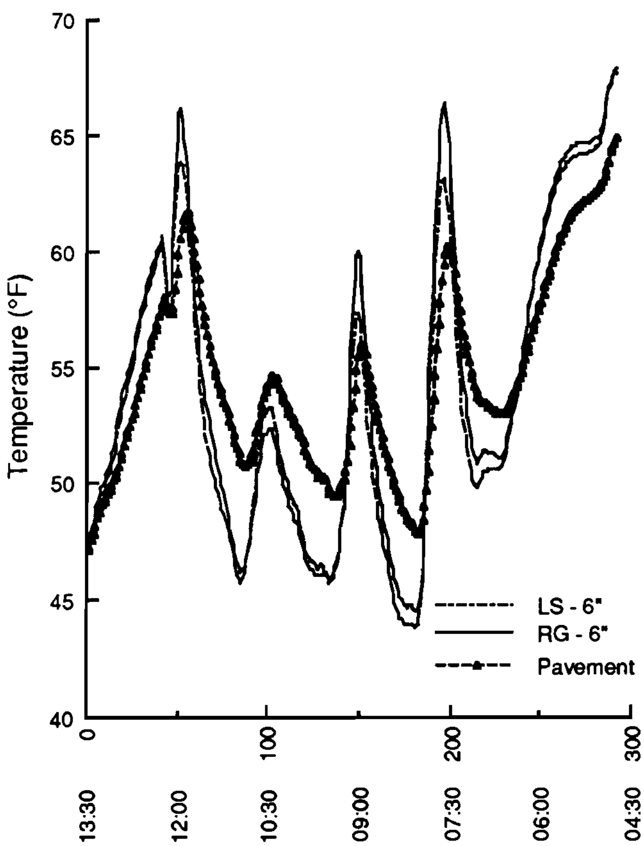

Fig A.20. Temperatures at mid-depth thermocouples, data set 3, 6-inch-thick portable slabs.

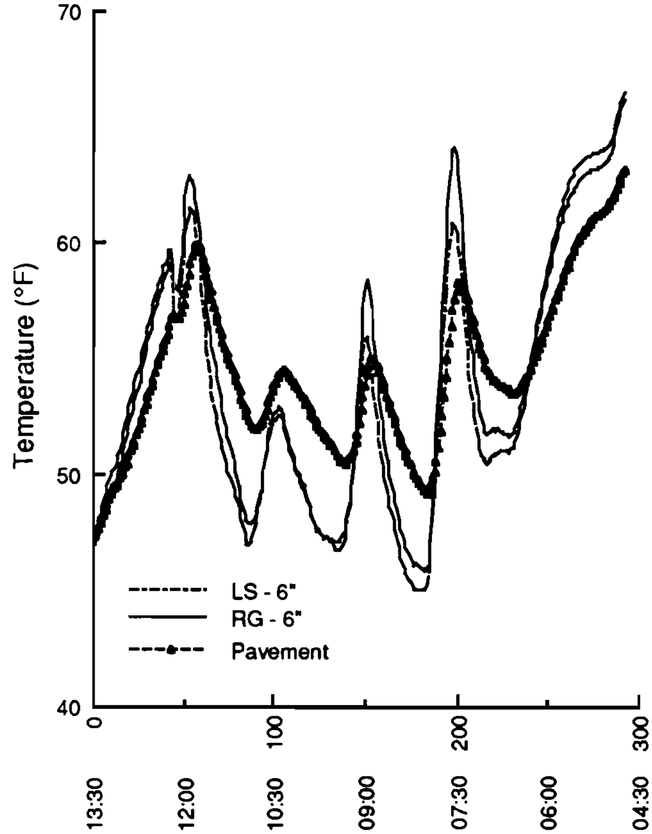

Fig A.21. Temperatures at bottom thermocouples, data set 3, 6-inch-thick portable slabs.

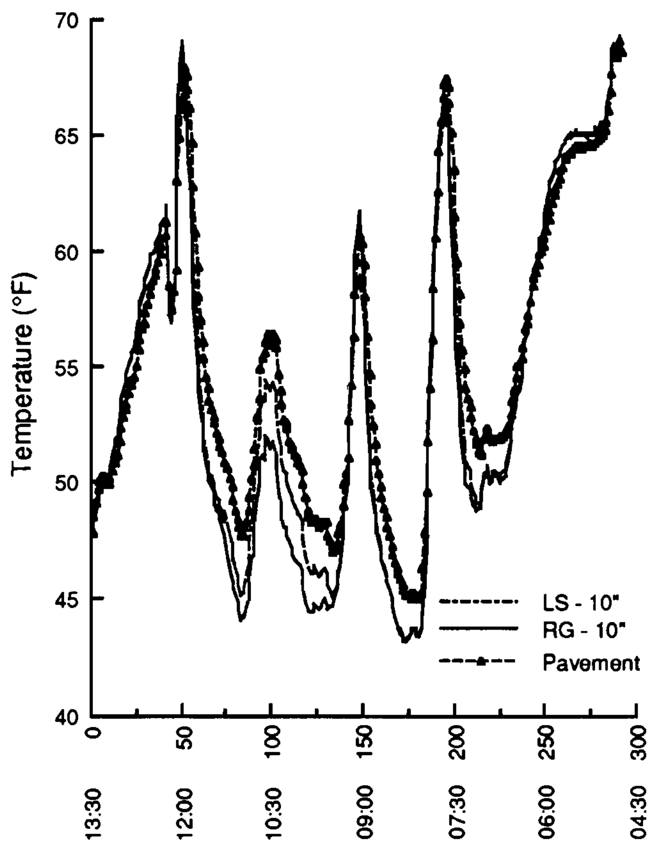

Fig A.22. Temperatures at top thermocouples, data set 3, 10-inch-thick portable slabs.

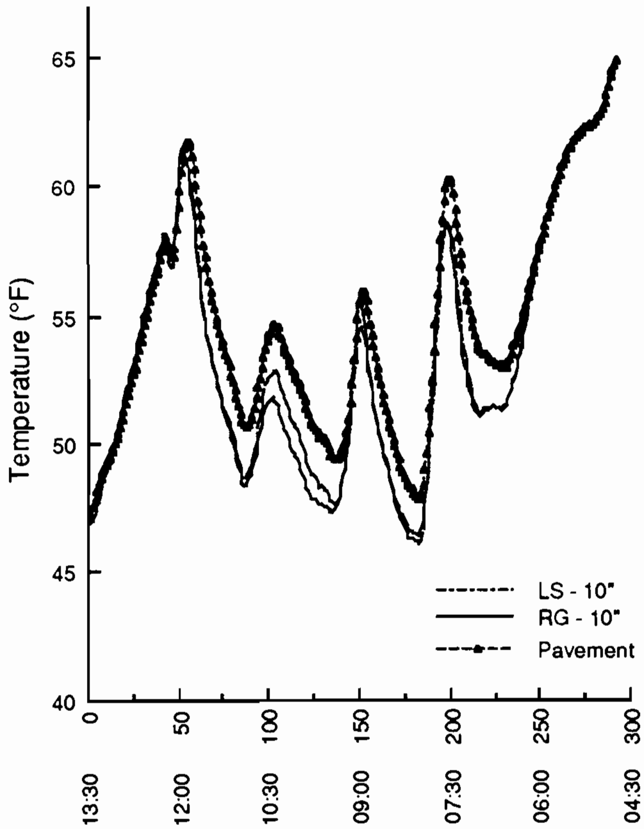

Fig A.23. Temperatures at mid-depth thermocouples, data set 3, 10-inch-thick portable slabs.

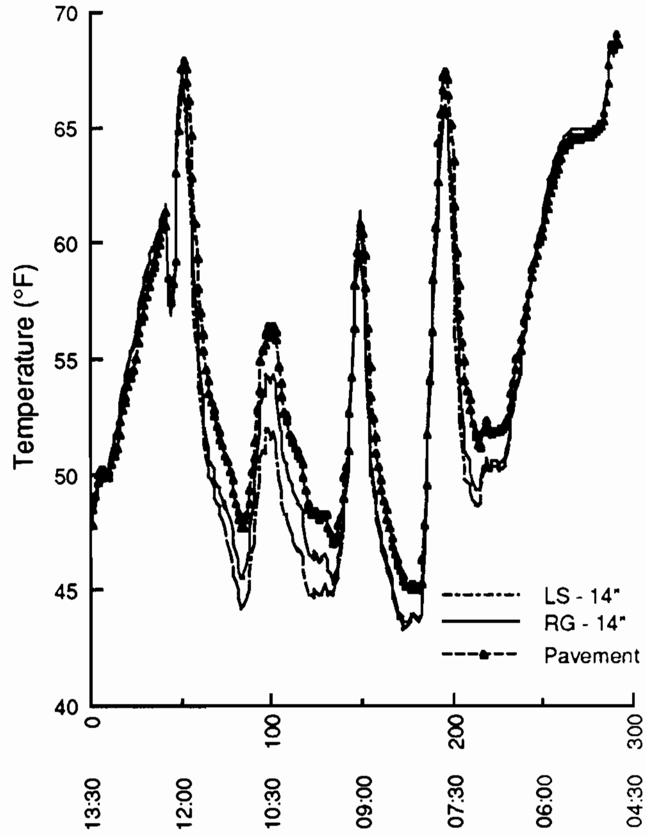

Fig A.25. Temperatures at top thermocouples, data set 3, 14-inch-thick portable slabs.

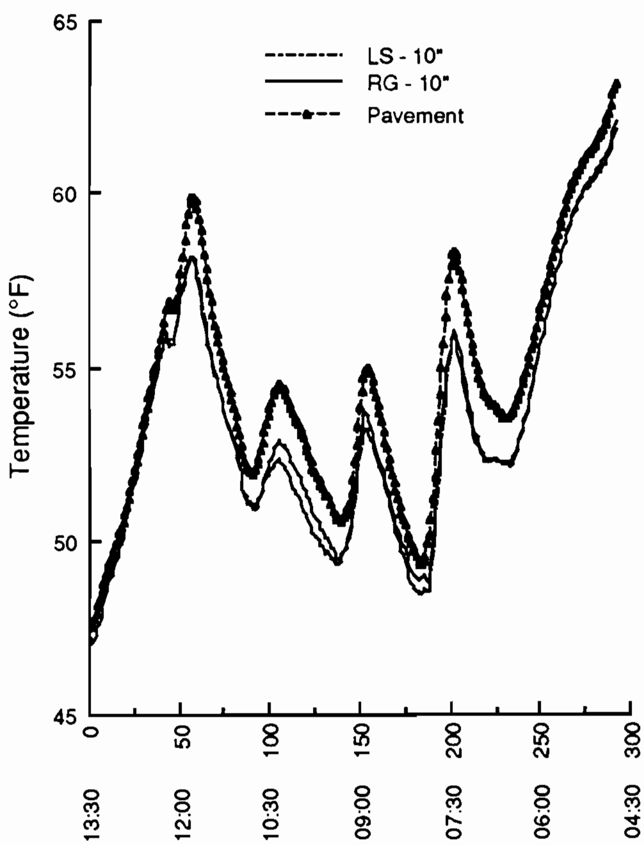

Fig A.24. Temperatures at bottom thermocouples, data set 3, 10-inch-thick portable slabs.

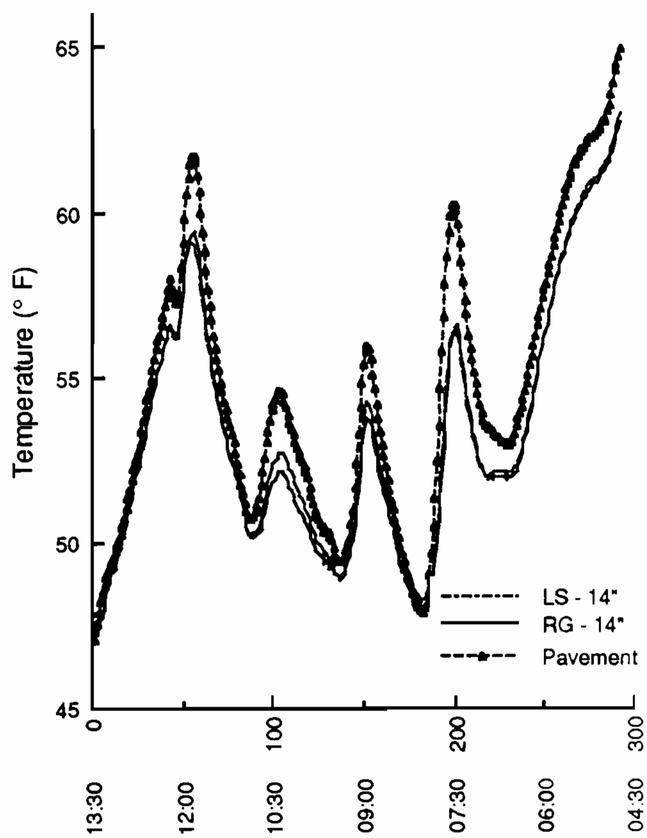

Fig A.26. Temperatures at mid-depth thermocouples, data set 3, 14-inch-thick portable slabs.

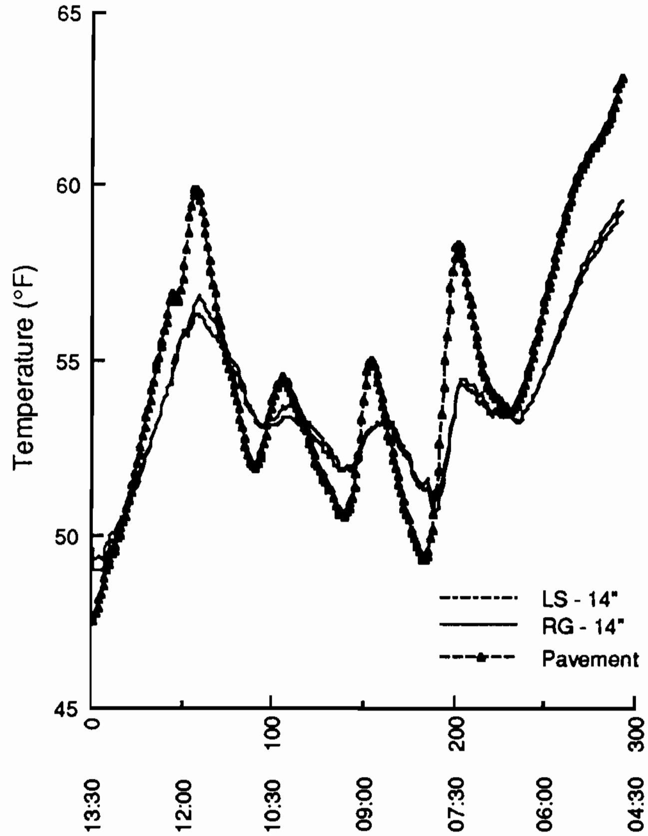

Fig A.27. Temperatures at bottom thermocouples, data set 3, 14-inch-thick portable slabs.

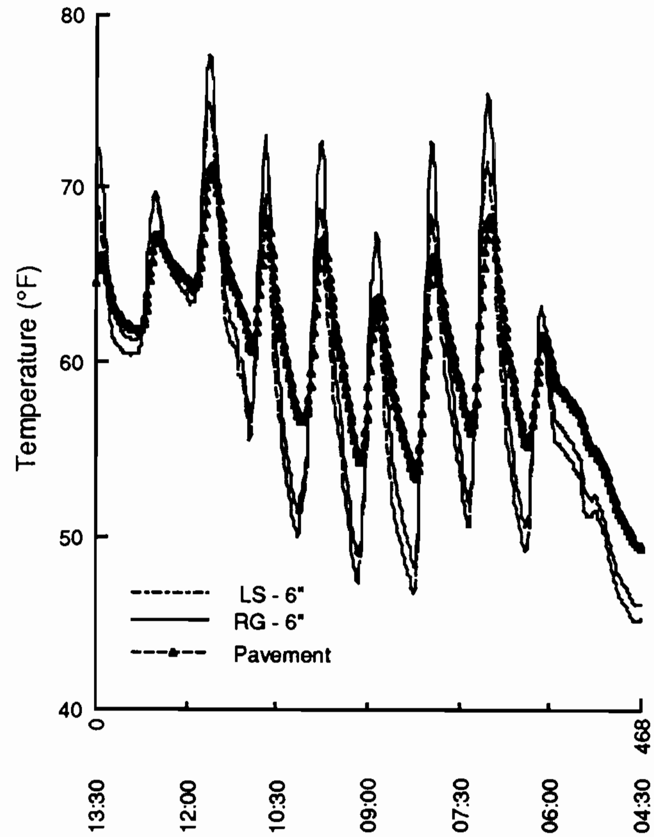

Fig A.29. Temperatures at mid-depth thermocouples, data set 4, 6-inch-thick portable slabs.

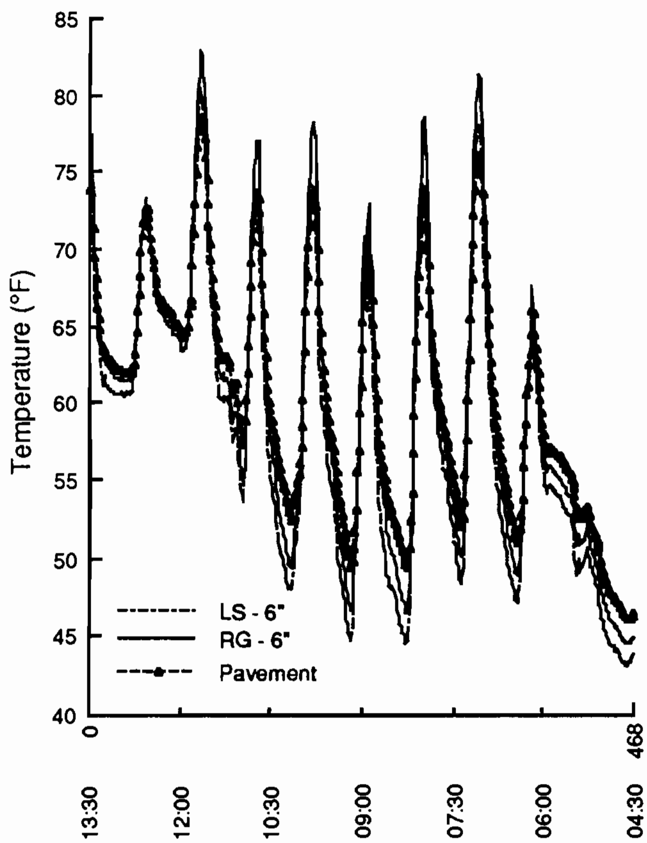

Fig A.28. Temperatures at top thermocouples, data set 4, 6-inch-thick portable slabs.

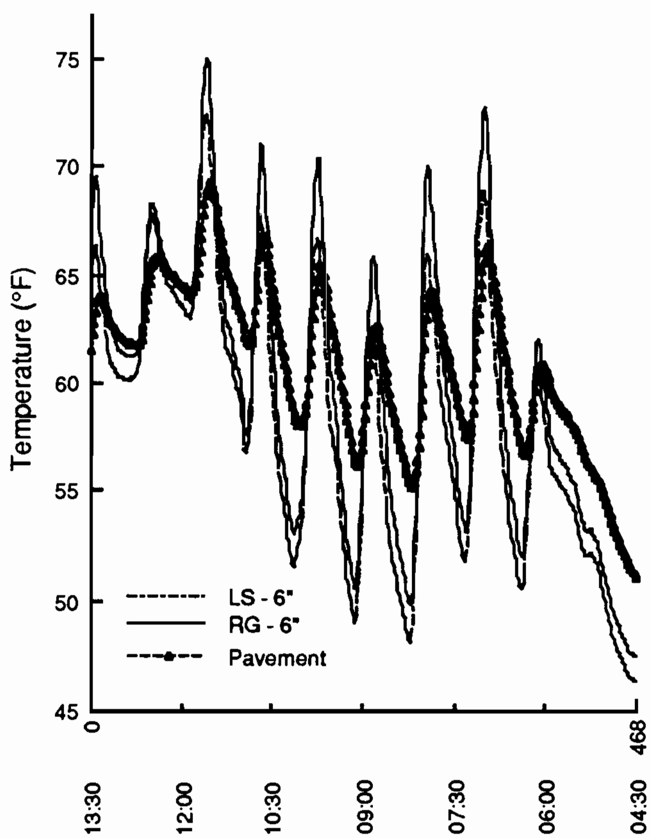

Fig A.30. Temperatures at bottom thermocouples, data set 4, 6-inch-thick portable slabs.

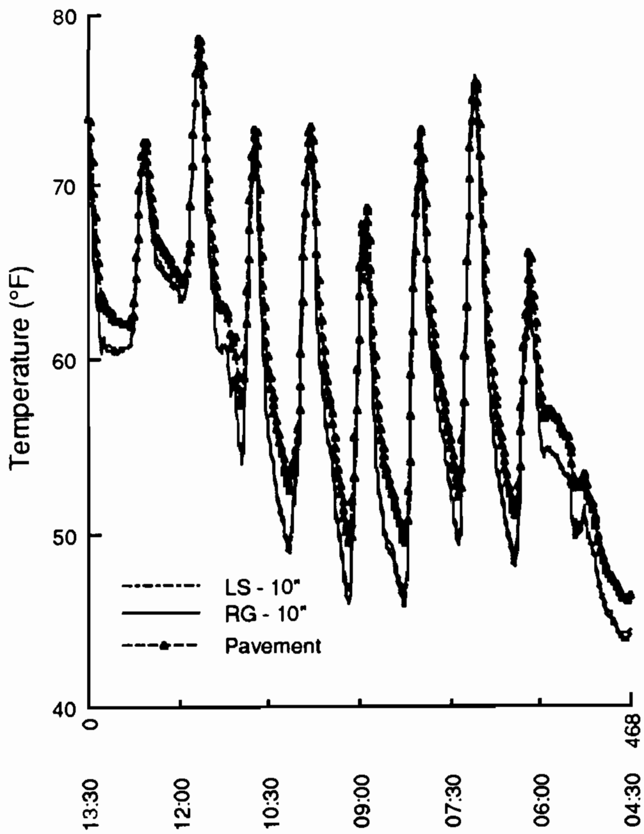

Fig A.31. Temperatures at top thermocouples, data set 4, 10-inch-thick portable slabs.

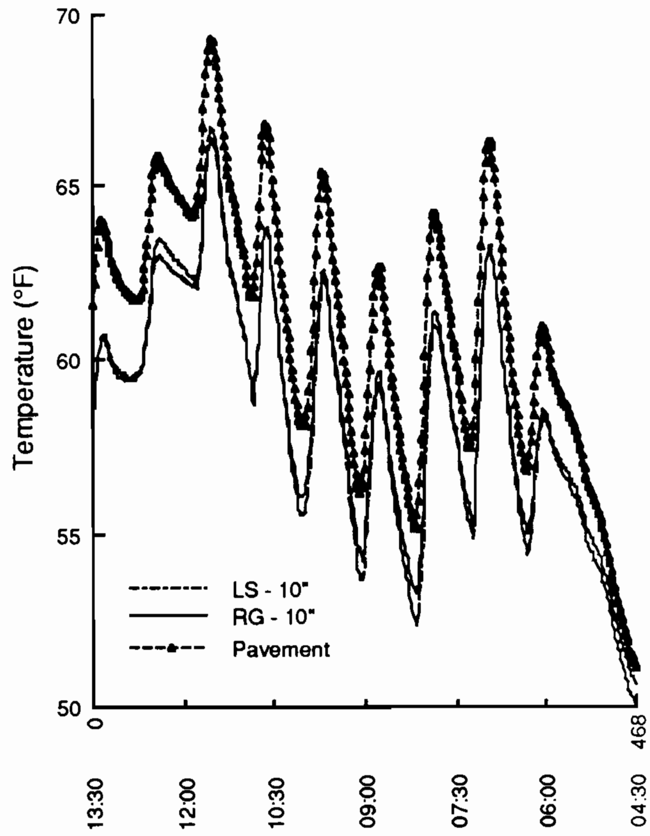

Fig A.33. Temperatures at bottom thermocouples, data set 4, 10-inch-thick portable slabs.

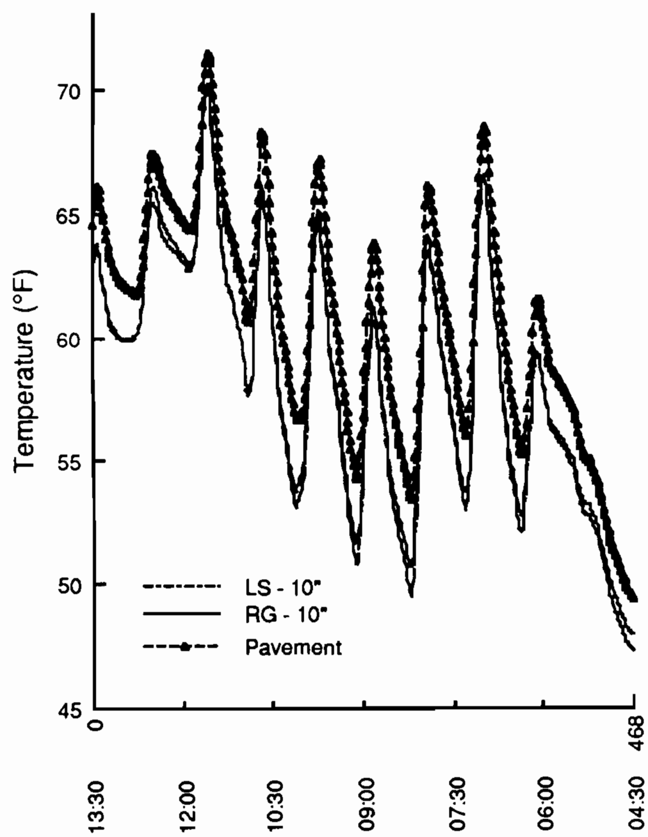

Fig A.32. Temperatures at mid-depth thermocouples, data set 4, 10-inch-thick portable slabs.

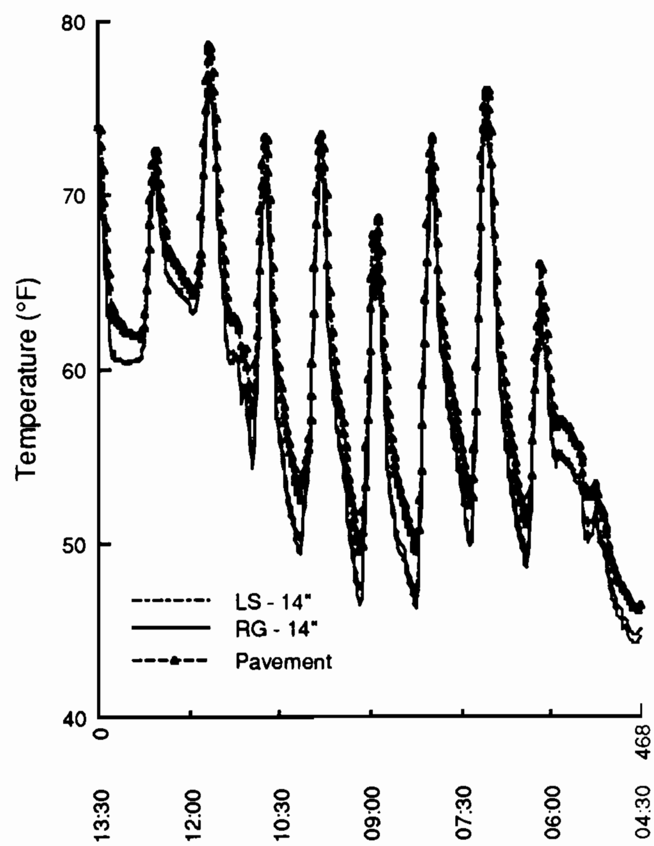

Fig A.34. Temperatures at top thermocouples, data set 4, 14-inch-thick portable slabs.

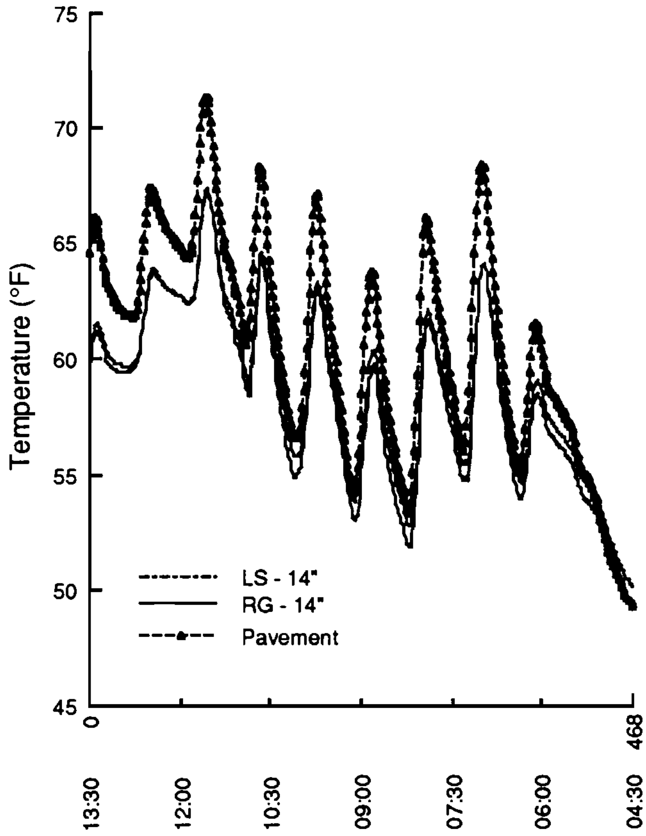

Fig A.35. Temperatures at mid-depth thermocouples, data set 4, 14-inch-thick portable slabs.